# ASSESSMENT OF MECHANICAL PROPERTIES AND TRANSFORMATION BEHAVIOR OF LOCALLY-MADE NI-TI ALLOYS USED IN ORTHODONTICS

**NATTIREE CHIRANAVANIT**

**A THESIS SUBMITTED IN PARTIAL FULFILLMENT**
**OF THE REQUIREMENTS FOR**
**THE DEGREE OF MASTER OF SCIENCE**
**(ORTHODONTICS)**
**FACULTY OF GRADUATE STUDIES**
**MAHIDOL UNIVERSITY**
**2008**

Thesis
Entitled

# ASSESSMENT OF MECHANICAL PROPERTIES AND TRANSFORMATION BEHAVIOR OF LOCALLY-MADE NI-TI ALLOYS USED IN ORTHODONTICS

Nattiree Chiranavanit

Miss Nattiree Chiranavanit,
Candidate

Surachai Dechkunakorn

Assoc.Prof.Surachai Dechkunakorn,
B.Sc., D.D.S., Dip. in Orthodontics,
Diplomate Thai Board of Orhtodontics
Major-Advisor

Niwat Anuwongnukroh

Assoc.Prof.Niwat Anuwongnukroh,
D.D.S., M.S.D. (Orthodontics),
Diplomate American Board,
Diplomate Thai Board of Orthodontics
Co-Advisor

Assist.Prof.Dr. Anak Khantachawana,
B.Eng., M.Eng., D.Eng.
(Materials Science and Engineering)
Co-Advisor

B. Mahaisavariya

Prof.Banchong Mahaisavariya,
M.D.
Dean
Faculty of Graduate Studies

Nita Viwattanatipa

Assoc.Prof.Nita Viwattanatipa,
D.D.S., M.S.(Orthodontics)
Diplomate American Board of Orthodontics
Chair
Master of Science Programme in Orthodontics
Faculty of Dentistry

Thesis
Entitled

# ASSESSMENT OF MECHANICAL PROPERTIES AND TRANSFORMATION BEHAVIOR OF LOCALLY-MADE NI-TI ALLOYS USED IN ORTHODONTICS

was submitted to the Faculty of Graduate Studies, Mahidol University
For the degree of Master of Science (Orthodontics)
on
24 March, 2008

Nattiree Chiranavanit
Miss Nattiree Chiranavanit
Candidate

Dr.Julathep Kajornchaiyakul,
Ph.D.
Chair

Surachai Dechkunakorn
Assoc.Prof.Surachai Dechkunakorn,
B.Sc., D.D.S., Dip. in Orthodontics,
Diplomate Thai Board of Orthodontics
Member

Assist.Prof.Dr. Anak Khantachawana,
B.Eng., M.Eng., D.Eng.
(Materials Science and Engineering)
Member

Niwat Anuwongnukroh
Assoc.Prof.Niwat Anuwongnukroh,
D.D.S., M.S.D. (Orthodontics),
Diplomate American Board,
Diplomate Thai Board of Orthodontics
Member

B. Mahaisavariya
Prof.Banchong Mahaisavariya,
M.D.
Dean
Faculty of Graduate Studies
Mahidol University

Theeralaksna Suddhasthira
Assoc. Prof. Theeralaksna Suddhasthira
B.Sc., D.D.S., Diplomate, American
Board of Oral and Maxillofacial Surgery,
Ph.D. (Biomedical Science)
Dean
Faculty of Dentistry, Mahidol University

# ACKNOWLEDGEMENT

I wish to express my gratitude to my major advisor, Associate Professor Surachai Dechkunakorn, and all my co-advisors: Associate Professor Niwat Anuwongnukroh and Assistant Professor Dr. Anak Khantachawana for their guidance, advice and encouragement.

I would like to express my appreciation to Dr. Julathep Kajornchaiyakul for his kindness of serving as an external examiner for my thesis defense.

I wish to express my thankfulness to Mr. Jirasak Srirat, Mr. Panupong Rattanarojjanathom and Mr. Aphinan Phukaoluan, the postgraduate students in the Department of Mechanical Engineering, Faculty of Engineering, King Mongkut's University of Technology Thonburi, for their invaluable willingness to help strengthen many laboratory procedures and give morale support.

I am grateful to every staff in the Research Unit, Faculty of Dentistry, Mahidol University, especially Dr. Pornkiat Churnjitapirom, Mr. Apiwat Riddhabhaya and Ms. Chayada Teanchai, for their advice and assistance in facilitating the use of many laboratory equipment.

In addition, I would like to acknowledge the National Metal and Materials Technology Center of Thailand or MTEC for allowing me to use the Universal testing machine for tensile strength test and reducing testing fees.

I appreciate all of my teachers for giving me invaluable background knowledge to conduct this research project. I also wish to thank all of my classmates in the Department of Orthodontics, Mahidol University for all of their help and friendship during my studies. Furthermore, I am particularly indebted to the Faculty of Dentistry, Mahidol University for funding part of this study.

Finally, I would like to express my grateful appreciation to my beloved family for their unconditional support, invaluable assistance, and constant encouragement in every way. I was able to achieve success with their help.

Nattiree Chiranavanit

ASSESSMENT OF MECHANICAL PROPERTIES AND TRANSFORMATION BEHAVIOR OF LOCALLY-MADE NI-TI ALLOYS USED IN ORTHODONTICS

NATTIREE CHIRANAVANIT 4937190 DTOD/M

M.Sc.(ORTHODONTICS)

THESIS ADVISORS: SURACHAI DECHKUNAKORN, Dip. in Ortho., NIWAT ANUWONGNUKROH, Dip. in Ortho., ANAK KHANTACHAWANA, D.Eng.

## ABSTRACT

Ni-Ti alloy wires have been widely used in clinical orthodontics because of their properties of superelasticity (SE) and shape memory effect (SME).

The purpose of this study was to assess the mechanical properties and phase transformation of 50.7Ni-49.3 Ti (at%) alloy (NT) and 45.2Ni-49.8Ti-5.0Cu (at%) alloy (NTC), both of which underwent different degrees of reduction (10%, 20% and 30 %) and then received heat treatment at 400°C or 600°C respectively. The Ni, Ti and Cu (purity 99.99%) were prepared and melted by Argon atmosphere arc furnace with a non-consumable tungsten electrode. After being sliced with wire cutting machine, the specimens were cold-rolled with a reduction ratio ranging from 10% to 30%. In order to investigate SE and SME, heat-treatment was performed for 1 h at 400°C or 600°C respectively. The specimens were examined using Energy-Dispersive X-ray Spectroscope (EDS), Differential Scanning Calorimeter (DSC), Universal Testing Machine (Instron), Vickers hardness tester, Optical Microscope (OM) and X-ray Diffractometer (XRD).

The chemical compositions were Ni 47.65at%, Ti 52.01at%, Si 0.24at% for NT, and Ni 41.94at%, Ti 50.21at%, Cu 7.56at%, Si 0.29at% for NTC. On the three-point bending test, superelastic load-deflection curve was seen in NTC heat-treated at 400°C. NT heat-treated at 400°C with 30% reduction produced a partially superelastic curve. For SME, NTC heat-treated at 600°C tended to be superelastic at the oral temperature if the $A_f$ was set slightly lower than 26°C-30°C. For tensile test, the ultimate tensile strength increased when increasing the percentage reduction. On the other hand, the percentage elongation decreased when increasing the percentage reduction. Micro-harness value increased when increasing the percentage reduction. The average grain size was typically 50-80 μm. In order to improve the superelasticity and shape memory effect, the transformation temperature range should be lower than the oral temperature, either by increasing cold-working over 30% reduction, or adding more Ni/Cu.

The results showed that locally-made Ni-Ti alloys have various transformation behaviors and mechanical properties depending on three principal factors: chemical composition, work-hardening (% reduction) and heat-treatment temperature. In order to fabricate Ni-Ti alloy used in orthodontics, these three factors should be carefully monitored. This information was valuable as a baseline data for further development of locally-made Ni-Ti alloyed used in orthodontics.

KEY WORDS: MECHANICAL PROPERTIES/ PHASE TRANSFORMATION/ LOCALLY-MADE NI-TI ALLOYS / ORTHODONTICS

117 pp.

การประเมินสมบัติทางกลและการเปลี่ยนแปลงเฟสของโลหะผสมนิกเกิลไทเทเนียมที่ผลิตขึ้นเอง สำหรับใช้งานทางทันตกรรมจัดฟัน (ASSESSMENT OF MECHANICAL PROPERTIES AND TRANSFORMATION BEHAVIOR OF LOCALLY-MADE NI-TI ALLOYS USED IN ORTHODONTICS

ณัฐฐิรีย์ ชีรณวาณิช 4937190 DTOD/M

วท.ม. (ทันตกรรมจัดฟัน)

คณะกรรมการควบคุมวิทยานิพนธ์: สุรชัย เดชคุณากร, Dip. In Ortho., นิวัต อนุวงศ์นุเคราะห์, Dip. In Ortho., อนรรฆ ขันธะชวนะ, D. Eng.

**บทคัดย่อ**

วัตถุประสงค์ของการศึกษานี้เพื่อประเมินคุณสมบัติทางกลและการเปลี่ยนเฟสของโลหะผสมนิกเกิล-ไทเทเนียม 50.7Ni-49.3Ti (at%) (NT) และ 45.2Ni-49.8Ti-5.0Cu (at%) (NTC) ที่ได้รับการขึ้นรูปด้วยการรีดเย็นที่ระดับการรีดลดความหนาที่ 10, 20 และ 30 เปอร์เซ็นต์ แล้วอบภายใต้บรรยากาศแก๊สอาร์กอนที่อุณหภูมิ 400 และ 600 องศาเซลเซียสเป็นเวลาหนึ่งชั่วโมง ตามลำดับ จากนั้นทำการวิเคราะห์องค์ประกอบทางเคมีด้วย Energy-dispersive X-ray sectroscope วิเคราะห์อุณหภูมิการเปลี่ยนเฟสด้วย Differential Scanning Calorimeter (DSC) วิเคราะห์คุณสมบัติเชิงกลด้วยการทดสอบแรงดึงและแรงกดแบบสามจุดด้วย Universal Testing Machine (Instron) และทดสอบความแข็งแรงผิวด้วย Vickers hardness tester ศึกษาลักษณะโครงสร้างเกรนด้วยกล้องจุลทรรศน์แบบแสงและศึกษาโครงสร้างผลึกด้วยX-ray Diffractometer (XRD) และใช้ค่าสถิติเชิงพรรณนาในการวิเคราะห์ข้อมูล

ผลการศึกษาพบว่า NT ประกอบด้วย Ni 47.65 at%, Ti 52.01 at% และ Si 0.20 at% ส่วน NTC ประกอบด้วย Ni 41.94 at%, Ti50.21 at%, Cu 7.56 at% และ Si 0.29 at% จากการทดสอบแรงกดสามจุด พบว่า NTC ที่ได้รับการอบที่อุณหภูมิ 400 องศาเซลเซียสมีการคืนกลับแบบยืดหยุ่นยิ่งยวด ส่วน NT ที่ได้รับการรีดลดความหนา 30 เปอร์เซ็นต์ก่อนนำไปอบที่อุณหภูมิ 400 องศาเซลเซียสมีการคืนกลับแบบยืดหยุ่นยิ่งยวดบางส่วน สำหรับการจำรูป NTC ที่ได้รับการอบที่อุณหภูมิ 600 องศาเซลเซียส มีแนวโน้มแสดงความยืดหยุ่นยิ่งยวดที่อุณหภูมิช่องปาก ถ้าสามารถกำหนดให้อุณหภูมิออสเตไนท์สิ้นสุดที่ระดับต่ำกว่า 26-30 องศาเซลเซียสเล็กน้อย ค่าความต้านทานแรงดึงสูงสุดและค่าความแข็งแรงผิวจะเพิ่มขึ้นตามระดับการรีดลดความหนาที่เพิ่มขึ้น ส่วนอัตราส่วนการยืดตัวจะลดลง เกรนของชิ้นงานมีขนาดเฉลี่ย 50-80 ไมโครเมตร ในการปรับปรุงคุณสมบัติความยืดหยุ่นยิ่งยวดและการจำรูปให้ดีขึ้น สามารถทำได้โดยการลดอุณหภูมิในการเปลี่ยนเฟสให้ต่ำกว่าอุณหภูมิช่องปาก ซึ่งอาจทำได้โดยการเพิ่มระดับการรีดลดความหนาให้มากกว่า 30 เปอร์เซ็นต์ หรือเพิ่มนิกเกิลหรือทองแดงในส่วนผสมอีกเล็กน้อย

จากการศึกษาพบว่าโลหะผสมนิกเกิล-ไทเทเนียมทั้งสองชนิดมีความแตกต่างกันทั้งการเปลี่ยนเฟสและคุณสมบัติทางกล ขึ้นกับองค์ประกอบทางเคมี ระดับการขึ้นรูป และอุณหภูมิการอบ ข้อมูลที่ได้จากการศึกษานี้สามารถใช้เป็นข้อมูลพื้นฐานในการพัฒนาการผลิตโลหะผสมนิเกิล-ไทเทเนียมสำหรับใช้ในทางทันตกรรมจัดฟันต่อไป

117 หน้า

# CONTENTS

# LIST OF TABLES

## LIST OF FIGURES

FIGURE PAGE

# LIST OF FIGURES (Cont.)

FIGURE PAGE

# LIST OF FIGURES (Cont.)

# LIST OF FIGURES (Cont.)

# LIST OF FIGURES (Cont.)

# LIST OF FIGURES (Cont.)

# CHAPTER I
# INTRODUCTION

In orthodontics, ideally arch wire used to create tooth movement should provide light , continuous forces.[1] Such forces may reduce the potential discomfort, tissue hyalinization, and undermining resorption.[2]

There are many types of arch wires available now: Stainless steel, Cobalt-Chromium, Nickel-Titanium and Beta-Titanium. Orthodontists should select, from all the available wire types, one that best meets the demands of a particular clinical situation. For Nickel-Titanium alloy wires, they have extraordinary properties: shape memory effect and superelasticity with excellent corrosion resistance, and good mechanical properties and biocompatibility. Ni-Ti alloy wire are wildly used in clinical orthodontics since their superelasticity produces light and continuous forces transmitted to the dentition over a long activation period resulting in a desirable biological response.[3] Furthermore, superelasticity is manifested by a considerable range of deflection without permanent deformation. This phenomenon means that an arch wire would exert constant force whether it were deflected a relatively small or a large distance, which is a unique and extremely desirable characteristic especially for leveling and aligning severely mal-positioned teeth.[1]

There are many companies in Thailand marketing Ni-Ti alloy wires, which are imported from foreign countries. Within the last few years, many new nickel-titanium orthodontic wire alloys have been introduced in Thailand with the large variety of the prices and manufactures. The cost of these materials is a factor in using the newer ones since the nickel-titanium orthodontic arch wire costs 5 to 40 times as much as stainless steel wire. In addition, there is still no nickel-titanium orthodontic arch wire producer in Thailand.

Therefore, this study will be a preliminary work to fabricate samples of Ni-Ti alloy specimens. Two systems of Ni-Ti alloy composition are chosen from the study of Ijima et al.[4] in order to obtain superelasticity and/or shape memory effect. The purpose of this study is to evaluate the chemical composition, metallurgical

structure, mechanical properties and phase transformation of the fabricated near equiatomic Ni-Ti alloy samples with different degrees of cold-rolling and heat treatment temperatures. This experiment will be the first step for the project of local-made Ni-Ti alloy wire in Thailand.

# CHAPTER II
# OBJECTIVES

This study is designed as an in vitro study to assess the mechanical properties and phase transformation of nickel-titanium alloys which were locally-made by electrolytic arc furnace with different degrees of cold-rolling and heat treatment temperatures.

**The purposes are:**

1. To assess the phase transformation of locally-made nickel-titanium alloys.
2. To assess the mechanical properties of locally-made nickel-titanium alloys.

**Thesis questions:**

1. What are the phase transformations of locally-made nickel-titanium alloys?
2. What are the mechanical properties of locally-made nickel-titanium alloys?

**Limitations of the Study are:**

1. This is an initial study which the fabrication process of nickel-titanium alloys were not finished as a wire product. The specimens of nickel-titanium alloys were made in bar shaped by wire-cut machine. The specimens were not further drawn into specific wire shaped dimension.

2. The assessment of nickel-titanium alloys was done in vitro, which may not correspond to the results found under intra-oral conditions. However, the results may give information in further development of locally-made nickel-titanium alloy wires used in orthodontics.

**The expected benefits of this study are:**

This study is a preliminary work to fabricate the nickel-titanium alloys and assess the phase transformation and mechanical properties for further development of locally-made nickel-titanium alloy wires used in orthodontics.

# CHAPTER III
# LITERATURE REVIEW

In light of the present stable of knowledge, bone biology research may be interpreted to imply that the light continuous forces may be best suited for optimal orthodontic movement. This conclusion is based on two important factors:[5]

1. Light forces create minimal hyalinized tissue and therefore avoid undermining resorption thus allowing quick tooth movements.

2. Continuous forces create a constant system for continued effect. Periods of rest are required for the tissues to recover and, therefore intermittent application of forces is preferred.

In the rational selection of wires for a particular treatment, the orthodontist should consider a variety of factors, including the amount of the force delivery, the elastic (working) range or springback, formability or ease of manipulation and the need for soldering or welding to assemble an appliance, corrosion resistance and biocompatibility.[6]

Profitt and Fields [1], Kusy R.P.[2] explained that an ideal arch wire material for orthodontic purposes should possess high strength, low stiffness, high range, high formability, weldability or solderability, resilience, biocompatibility, low friction, good springback, poor biohost, reasonability in cost and esthetic. In contemporary practice, there is no one of the arch wire material meets all these requirements, so that the best results are obtained by using specific arch wire materials for specific purposes. During the initial leveling and alignment are desired, great range and light forces are needed. By referencing elastic property ratios of strength, stiffness, and range, two principal types of wires are suggested: a multistranded stainless steel wire or a Ni-Ti wire. As treatment progresses into intermediate stage, beta-titanium alloys are favorable as their formability, springback, range, and modest forces per unit deactivation. As the final stage of treatment wherein more arch stability and small tooth movements are required, wires having substantial stiffness but limited ranges are

acceptable. Large gauges of beta-titanium or stainless steel wires may be used to maintain arch form while making minor tooth movement or adjustment.[2, 7, 8]

**Nickel titanium alloy**

A Ni-Ti alloy was developed in the early 1960s by Buehler W.F., a metallurgist investigating non-magnetic, salt resisting, waterproof alloys for the space programme at the Naval Ordnance Laboratory in Maryland, USA.[9] This intermetallic alloy has thermodynamic properties which can be producing a shape memory effect to specific heat treatment. The name "Nitinol" given to a family of intermetallic alloys of Ni and Ti is an acronym for the elemental composition; ni for nickel, ti for titanium and nol from the Naval Ordnance Laboratory.

In near equiatomic Ni-Ti shape memory alloys, there are three different phases.[10, 11]

1. *The austenite phase or parent phase* ($B_2$ phase) is a face-centered cubic lattice of CsCl structure at higher temperature ranges.

2. *The R phase* is a rhombohedral or trigonal lattice.

3. *The martensite phase or daughter phase* (B19' phase) exists at lower temperatures in a closely packed hexagonal lattice.

Among these phases, three transformations are possible, The B2 ↔ B 19', B2 ↔ R and R ↔ B 19'. All three transformations involve lattice distortions and are martensite in nature. Consequently, the transformations are sensitive to variations in metallurgical and mechanical conditions as well as chemical composition.

B2 ↔ B 19' and R ↔ B 19' are characterized by large lattice distortions and large transformation hysteresis. Due to the large lattice distortions, these transformations introduce structural defects to the microstructure during the processes and, at the same time, are sensitive to influences of structural defects. Therefore, these transformations have relatively low thermal and mechanical stability for their functional properties.

In contrast, the B2 ↔ R transformation is characterized by a small lattice distortion and a small temperature hysteresis. The small lattice distortion implies less damage to the microstructure during transformation and lower sensitivity to structural modification, hence higher reversibility and higher property stability. The small

thermal Hysteresis implies high response rate and high reversibility. Owing to these unique advantages, the R-phase transformation is of particular importance for many applications, such as actuators and sensors.[11]

***R-Phase***

The R-phase transformation gives rise to shape memory effect and pseudoelasticity. Shape memory effect due to R-phase transformation has low thermal hysteresis and exhibits excellent fatigue properties. In fully annealed binary near-equiatomic Ti-Ni alloys, usually only the B2 ⟷ M transformation is observed.

The B2 ⟷ R transformation can be introduced by many different ways.

- Addition of third elements, such as Fe and Al is effective in suppressing the B2 ⟷ M transformation to lower temperatures to reveal the B2 ⟷ R transformation.
- Thermo-mechanically treated near-equiatomic Ni-Ti alloys: cold working, partially annealing after cold work and thermal cycling have been found to cause the appearance of the B2 ⟷ R transformation. Su and Wu [12] have obtained a complex 4-stage multi-stage martensitic transformation (MST) in a 20% cold-rolled and annealed Ti49Ni51 alloy and they suggested that the MST is the result of the combined effect of severe cold-working and long-time annealing. Kim et al. [11] reported a low temperature aging-induced two-stage R-phase transformation in Ti49.1Ni50.9 alloy.
- Nickel rich Ni-Ti alloys (Ni > 50.5at%) aged after solution treatment at an appropriate low temperature. Khalil-Allafi et al.[13] found two distinct steps of B2 ⟶ R and R ⟶ B’19 in the DSC cooling curves of aged Ni-rich NiTi alloys. They proposed that the MST comes from the inhomogeneous distribution of $Ti_3Ni_4$ precipitates.[14]

Proffit et al.[1] has described two remarkable properties of nickel-titanium alloy wires that are unique in dentistry; **shape memory effect** and **superelasticity**.

**Shape memory effect**

In the thermoelastic effect, the inherent temperature of the oral cavity raises the martensitic active alloy through the critical temperature range thereby creating a restoring force as the arch wire transforms to austenite and returns to its prior form. By lowering the temperature, the alloy is transformed into martensite and becomes pliable and easily deformed. When the temperature rises above austenitic finished temperature, the wire will remember and recover the ideal arch form. For clinical application of this property, the $A_f$ has to be set slightly below oral temperature so that the wire will be primarily austenitic intra-orally and almost completely martensitic extra-orally.

Andresen and Morrow [15] described a unique properties of Nitinol shape memory that the characteristic of being able to return to a previously manufactured shape when it is heated through a transition temperature range. To use this property, the wire must first be set into the desired shape and held while undergoing a high-temperature heat treatment. After the wire has cooled to room temperature, it may be deformed with in certain strain limits. When heated to its unique transition temperature range, it will remember its shape and return to the original configuration.

The stabilized alloy denoted that a predetermined amount of wire deformation has occurred during processing (for Nitinol, this amount is about 8% to 10% deformation). In stabilized products the shape memory effect is suppressed by the wire drawing or working process, although in principle the shape memory effect could be restored by an appropriate heat treatment.

**Pseudoelasticity or superelasticity**

The deflection generates a local martensitic transformation and produces stress-induced martensite (SIM). The SIM is unstable and if the wire is maintained at oral temperature, it undergoes reverse transformation to the austenitic phase as soon as the stress is relieved.[16] In orthodontic clinical applications, SIM forms where the wire is tied to brackets on malaligned teeth so that the wire becomes noticeably pliable in the deflected areas. Therefore, delivery forces will be superelastic until, after tooth movement, a self-controlled reduction of the deflection will restore the stiffer austenitic phase.

The pseudoelastic effect is the mechanical analogue of the thermoelastic shape memory effect. In alloy whose austenitic transformation temperature is close to but allow ambient oral cavity temperature, a stress-induced martensitic (SIM) transformation may be induced by gross deformation. In nickel-titanium alloys the transformation of austenite to martensite on activation and the reverse transformation of martensite to austenite in deactivation account for the favorable, constant force over a wide working range. Because of the flat, plastic appearance of the force-deactivation curve, the phenomenon has been denoted in the metallurgic literature as *pseudoplasticity.* The more common name for the phenomenon, that of pseudoelasticity, is derived its plastic appearance, has high springback. This apparent rubber like elasticity, which exceeds that found in other conventional alloys by at least 10 times, has also been denoted as superelasticity.

The superelastic alloy wires require a deflection of at least 2 mm over a span of 13 mm before superelastic behavior is detected. Therefore, austenitic alloy wires are superelastic mainly when used for the correction of gross malaligned teeth.[17, 18]

**Transition Temperature Range (TTR)**

Andresen et. al. [19] explained that transition temperature range (TTR) is a range of temperature below which the material can be deformed in a plastic state, when the wire is heated by thermal energy from below to above the transition temperature range the alloy will return to its original shape. Transition temperature range can be controlled by composition of alloy.

Water [20] explained that martensitic active alloys have transformation temperature between room temperature and body temperature while austenitic active alloys have transformation temperature below room temperature. The austenitic produces higher force than the martensitic but both have a large elastic range and produce a nearly constant force over part of this range during unloading.

The shape memory characteristics of the nickel-titanium alloys are associated with a reversible transformation between the austenitic and martensitic nickel-titanium phases, which occurs by a twinning process. The martensitic phase forms from the austenitic phase over a certain transformation temperature range or when the stress is increased above some appropriate level. The austenitic phase forms from the

martensitic phase over a different transformation temperature or when the stress is decreased below the appropriate level.

The difference in the temperature ranges for the forward transformation from the martensitic phase to the austenitic phase and for the reverse transformation from the austenitic phase to the martensitic phase is termed ***hysteresis***. Frequently, an intermediate phase, termed R-phase because of its rhombohedral structure, forms during the forward and reverse transformations between martensitic nickel-titanium and austenitic nickel-titanium. In order for a nickel-titanium arch wire to posses shape memory in vivo, the transformation from the martensitic nickel-titanium structure to the austenitic nickel-titanium structure must be completed at the temperature of the oral environment.[21]

In summary, there are two basically properties should be taken into consideration to make an appropriate selection of a NiTi wire:[22]

1. A proper stress-related TTR, corresponding to or slightly below oral temperature.
2. A low deactivation force released to the dento-alveolar structures to prevent deleterious side effects, such as pain after bone hyalinization and root resorption.

In today's practice three types of nickel titanium wires are available:

**1. Conventional nitinol (Martensitic stabilized alloy)**

The conventional wire was first introduced to the orthodontic profession by Dr. George Andreason in the early 1970s as Nitinol$^{TM}$.[2] This wire was marketed by the Unitex Corporation [1] The name *nitinol* was derived from the elements that make up these alloys-"ni" for nickel, "ti" for titanium, and "nol" for Naval Ordinance Laboratory, its place of origin. This first 50:50 composition of Ni and Ti was a shape memory alloy in composition only. Indeed, this alloy was passive or lack of superelasticity, as the shape memory effect had been suppressed by cold working the wire during drawing to more than 8-10%. [2] One important property of nitinol wires is that they are not very stiff. (low force per unit of deactivation). Therefore the force applied with large deflections is extremely low when compared with stainless steel wires. This wire was quite springy- delivering only 1/5 to 1/6 the force per unit of deactivation. Unfortunately, its lack of formability (brittleness) is a limitation especially when wires broke.

**2. Pseudoelastic nitinol (Austenitic active alloy)**

In 1985 Burstone et al.[23] developed a new superelastic Ni-Ti alloy named "Chinese NiTi" for orthodontic appliances. Concurrently, the Japanese introduced their version by Miura et al, 1986.[24] In vitro-studies by several authors [17, 23, 24, 25, 26, 27, 28] have demonstrated that these alloys possess excellent springback and provide constant force delivery at increasing wire deflection.

The pseudoelastic wires have the capability of phase transformation on applied stress to maintain the same force of activation. The wire undergoes a transformation from the active austenitic phase to martensitic phase and then back to austenitic based on the stress applied. This feature gives these wires the property of longer periods of light continuous forces compared with the conventional nickel titanium wires. For clinical purposes "active" austenitic archwires are not intended to undergo phase transformation at mouth temperature, so their superelasticity results from a phase transformation under stress induction, as in archwire ligation.

This type of Ni-Ti alloy can be described by the stress-strain diagram. The superelastic stress-strain curve may demonstrate 3 distinct phases (figure 1). The initial and final slopes are given by the Young's modulus of the austenitic and martensitic phases, respectively. The stress-induced transformation from austenite to martensite manifests itself in the almost flat section or plateau of the load-deflection curve. At the plateau, a superelastic alloy does not follow Hooke's law because there is little change in stress with increasing strain. Thus, superelastic arch wires may exert the same amount of force independent of the degree of activation within a wide range. [20, 23, 24]

Superelastic arch wires also exhibit hysteresis (i.e., the activation and deactivation plateaus have different stress magnitudes). As a result, the wire does not deliver the same force as that applied to activate it (figure 1). Hysteresis can be thought of as the friction associated with the movement of twin-related martensite boundaries. The magnitude of the hysteresis depends on the alloy composition.

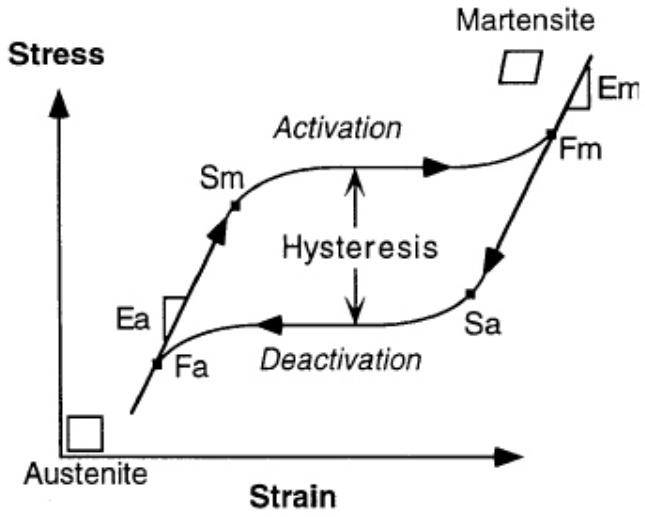


**Figure 1** Stress-strain diagram of nickel-titanium alloy with superelastic behavior application of stress leads to linear increase in strain up to point where martensitic transformation starts to occur [29], i.e., minimum stress at which transformation to martensitic phase starts to occur during activation. Slope is equal to austenitic modulus of elasticity (Ea). Between martensitic transformation start and point where martensite transformation is completed [30], there is remarkable increase in strain without concomitant increase in stress. This plateau-phase is due to formation of stress-induced martensitic transformation (SIM). When test piece is completely martensitic (right of point Fm), relationship between stress and strain is linear again. Slope is now equal to martensitic modulus of elasticity (Em). In deactivation, there will be a linear relationship between stress and strain down to point where austenitic transformation starts to occur (Sa). Thereafter, there is deactivation plateau between Sa and point where restoration of austenitic structure is complete (Fa) and a linear relationship between stress and strain down from point Fa. Note that there is hysteresis (activation and deactivation plateaus have different stress magnitudes) associated with martensitic transformations [31]

**3.Thermoelastic nitinol (Martensitic active alloy)**

The third type of nickel titanium wire undergoes phase transformation at oral temperature to produce the active austenitic phase. This wire can be distorted at lower temperatures and undergoes a thermally induced shape memory effect to return to an active austenitic phase.[2] By using exacting various heat treatment procedures under

inert atmospheric or vacuum conditions, manufacturers can vary the percent of austenite present at room temperature which result in different stress levels to initiate the phase transformations and different degrees of force delivery in the same diameter of NiTi wires.

Otsubo K. 1994 [32] has introduced a technique of double heat treatment (600°C for 5 min and 280°C for 180 min) in order to reduce the stress hysteresis through extremes of temperature likely in the oral environment (Low Hysteresis Sentalloy).

Transition temperature range (TTR) of Ni-Ti alloys can now be set around the clinical temperature due to improvements in processing refinement. The compositions of NiTi alloys can be controlled in an ingot to within parts per million. In addition, one manufacturer claims the incorporation of copper substituted the Ni content can increased sensitivity to changes in mouth temperature, by allowing greater precision in the setting of transformation temperatures.[33]

An ideal thermodynamic NiTi wire would have the characteristics as follows: [19, 34, 35]

- Dead soft at room temperature so that it can be tied easily.
- Instantaneously activated by the heat of the mouth temperature.
- Able to apply clinically acceptable orthodontic forces that would result in tooth movement.
- Once fully activated, would not be affected by increased heat in the mouth.
- Fairly narrow TTR which it should be completely active at mouth temperatures and completely passive at lower temperatures. This property would allow the clinician sufficient time to tie the archwire into the bracket slots before the heat of the mouth activates the wire.

This type of Ni-Ti alloy can be described by the strain-temperature diagram. The shape-memory phenomenon is related to the ability of nickel-titanium arch wires to undergo temperature-induced martensitic transformation (figure 2). There is a temperature range specific for the wire alloy during which this transformation takes place. Below the martensite final (Mf) temperature, the test piece is completely martensitic. By raising the temperature above the austenitic start temperature, the

material undergoes a transformation to austenite structure. At the austenite final temperature, the process is complete, and the test piece is austenitic. With cooling, the reverse process takes place. At the martensite start temperature, the process is completed.

Hysteresis is also associated with thermally induced martensitic transformations; that is, the transformation temperatures differ on heating and cooling. In some nickel-titanium alloys, an intervening stage can occur between the martensitic and austenitic phases, known at the R-phase. [36] The R-phase transformation is analogous to the austenite-martensite transformation and has its corresponding R-phase start (Rs) temperature and R-phase final (Rf) temperature. Thus, both shape memory and superelasticity are associated with the R-phase transition.

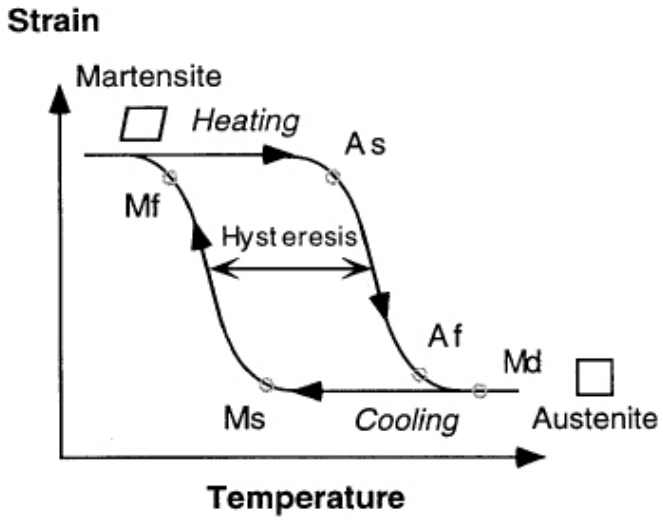


**Figure 2** Strain-temperature diagram of alloy with shape-memory effect. Below martensite final temperature, test piece is completely martensitic. By raising temperature above austenitic start (As) temperature, material undergoes transformation to austenite structure. At austenite final temperature, process is complete, and test piece is austenitic. By cooling, reverse process takes place. At martensite start temperature, martensitic structure starts to form; at martensite final temperature, process is complete [31].

Kusy [37] has suggested that the NiTi orthodontic wire products can alternatively be classified into the following 3 categories:

1. The martensitic-stabilized alloy (e.g. Nitinol SE, Unitex/3M Corp., USA) do not possess shape memory or superelasticity (Nonsuperelastic wire)
2. The martensitic-active alloy (e.g. Sentaloy, GAC Corp., USA) employ the thermoelastic effect to achieve shape memory.
3. The austenitic-active alloy (e.g. NiTi, Ormco Corp., USA) undergo a stress-induced martensitic transformation when activated. These alloys display superelastic behavior.

**Shape Memory Alloys**

Shape memory alloys (SMAs) are a unique class of metal alloys which can recover the original shape when heated over the certain temperature, Af. Currently most of the applications of superelastic NiTi alloy are related to the human body. The first was orthodontic archwires. The use of superelastic wire reduces the need to tighten and adjust the wire due to the increased elastic range compared to conventional material such as stainless steel. In addition, the constant force during unloading adds to patient comfort. Superelastic coil springs are also used for opening or closing extraction spaces, and provide greater efficiency in tooth movement.[38]

For the medical application, the Hammalok $^{TM}$ needle wire localizer is used to locate and mark breast tumors so that surgical procedures can be more exact and less invasive. Another application of NiTi in medicine is an invasive endovascular medical application as the guide wire, which is passed through blood vessels and used as a guide for catheters. Recently a suture anchor has been developed is used to reattach ligaments to a bone.

Other applications include Autoflex $^{TM}$ eyeglass frames made by Marchon and brassiere under-wire which helps retain shape.

Nickel-Titanium alloys are generally preferred over copper-based alloys for superelastic applications because of superior corrosion resistance and biocompatibility, larger superelastic strains and a longer fatigue life.

**Martensitic Transformation**

Shape memory effect and superelasticity are closely associated with the martensitic transformation which is basically characterized by a lattice transformation without atomic diffusion. The atomic arrangement in the parent lattice changes to the martensitic lattice while the ordered structure of the parent phase is inherited to the martensitic phase called a "lattice correspondence".

The transformation induced in the alloy occurs by a shear type of process to a phase called the "martensitic phase", which gives rise to *twinned martensite*. Almost no macroscopic shape change is detectable on the transformation, unless there is application of an external force. The martensite shape can be deformed easily to a single orientation by a process known as de-twinning to *de-twinned martensite,* when there is a flipping over type of shear. The NiTi alloy is more ductile in the martensitic phase than the austenite phase. (Figure 3)

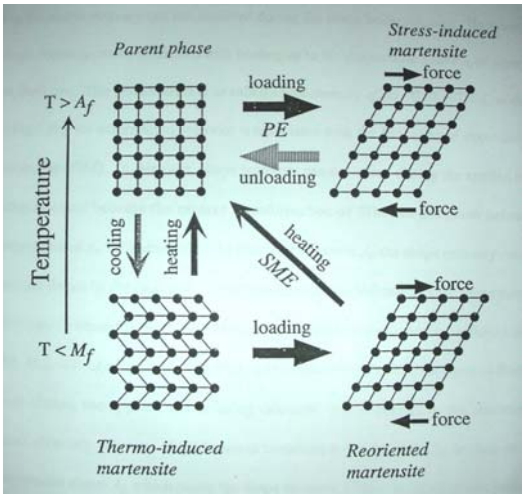


**Figure 3** The mechanism of shape memory effect and pseudoelasticity

The deformation can be reversed by heating the alloy above the TTR. The total atomic movement between adjacent planes of atoms is less than a full inter-atomic distance when based on normal atomic lattice arrangements. This phenomenon is termed *shape memory* and allows the alloy to return to its previous shape, by forming strong, directional and energetic electron bonds to pull back displaced atoms to their previous position.[39]

**Deformation characteristics**

The deformation behavior of shape memory alloys is strongly sensitive to temperature, because the deformation is associated with the martensitic transformation. In the temperature range of $T < M_s$ (Figure 4), the alloy is in stabilized martensitic phase and the deformation behavior is associated with the reorientation of the preferred variants of the martensite under an applied stress (twinned martensite). In this situation, the shape recovery is not occurred during the stress being released. However, the shape recovery can be obtained by heating up to the temperature above $A_f$ as shown by the dash line. This phenomenon if called *shape memory effect.*

In the temperature range of $M_s < T < A_s$, the parent phase elastically deforms at first and yielding occurs due to the stress-induced martensitic transformation. Therefore, the yield stress linearly increases with increasing temperature satisfying the Clausius-Clapeyron relationship. The stress-induced martensite phase remains after unloading because the temperature is below As.

In the temperature range of $A_s < T < A_f$, the deformation induced by the stress-induced martensitic transformation recovers partially upon unloading, resulting in partial superelasticity and partial shape memory effect by the following heating. In the temperature range of $A_f < T < T_s$, perfect superelasticity appears, where Ts stands for the critical temperature above which the martensitic transformation dose not take place and deformation occurs by slip. If $T > T_s$, plastic deformation occurs as in conventional metals and alloys.[40]

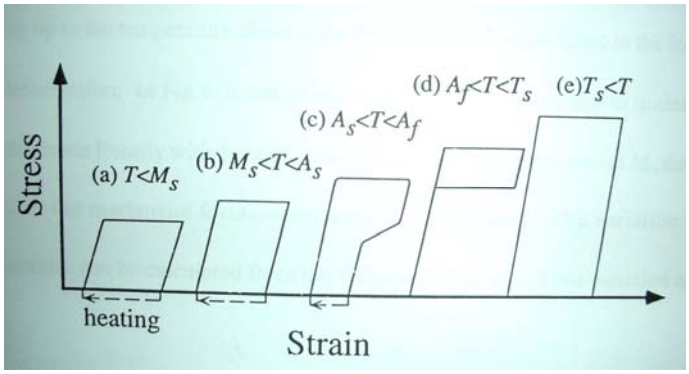


**Figure 4** The temperature dependence of stress-strain curves

## Structure and Properties of Metal and Alloys

### The crystal structure of metals

The arrangement of the atoms in the crystal is called “crystalline structure”. The smallest group of atoms showing the characteristic “lattice structure” of a particular metal is known as a unit cell. [41] It was discovered that there are 14 unique space lattices. The unit cell of each crystalline material, no meter how complex, corresponds with one of these 14 space lattice unit cells. [21]

There are three basic atomic arrangements of the metals:

1. Body-centered cubic
2. Faced-centered cubic
3. Hexagonal close-packed

The appearance of more than one type of crystal structure is known as *allotropism* or *polymorphism*. Because the properties and behavior of a metal depend greatly on its crystal structure, allotropism is an important factor in the heat treatment of metals and in metal working and welding operations.[41]

### Nucleation and grain structure

When a mass of molten metal begins to solidify, crystals begin to form independently of each other at various locations within the liquid mass; they have random and unrelated orientations. Each of these crystals grows into a *crystalline structure* or *grain.* A grain boundary is formed where the grains grow into contact. The number and size of the grains developed in a unit volume of the metal depends on the rate at which nucleation takes place.

If the crystal nucleation rate is high, the number of grains in a unit volume of metal will be large; consequently, grain size will be small. On the other hand, if the crystal nucleation rate is low, there will be fewer grains per unit volume, and their size will be larger. Generally, rapid cooling produces smaller grains, where as slow cooling produces larger grains.

### Grain size and properties

Grain size significantly influences the mechanical properties of metals. At room temperature, a large grain size is generally associated with low strength, low

hardness, and low ductility. Large grains, particularly is sheet metals, also cause a rough surface appearance after the material has been stretched.

The finer grain size can raise the yield stress, increase the ductility (percent of elongation), and raise the ultimate strength.

There are two basic mechanisms by which plastic deformation may take place in crystal structures:

1. The slipping under a shear stress
2. The twinning, a portion of the crystal forms a mirror image of itself across the plane of twinning. It usually occurs in hexagonal close-packed metals.

**Deformation in Metals**

There are two types of deformation that can occur in metals:

1. Elastic deformation

The strain is directly proportional to the applied stress up to the proportional limit stress. When the stress is removed, the atoms return to equilibrium atomic spacing. Compared with most polymeric materials, metals generally have strong metallic bonds and resist elastic stretching. This stiffness is indicated by the high elastic modulus of metals.

2. Plastic deformation

Plastic deformation is a permanent deformation that begins when the elastic limit stress or its approximation, yield stress, is reached. This mode of deformation requires that atoms be shifted to new atomic sites on the lattice which should be identical to the old sites and not far away.

The mechanism of plastic deformation is called *dislocation motion.* A dislocation is the line of atoms that denotes the edge of an additional half-plane of atoms that appears to be wedged into the lattice. The lattice is distorted by the presence of the dislocation line of atoms. Dislocation motion shifts atoms from one lattice site to the next, rather than moving all the atoms of the plane at one time.

**Plastic deformation of polycrystalline metals**

If a piece of polycrystalline metal with uniform equiaxed grains is subjected to plastic deformation at room temperature (cold-working), the grains become

deformed and elongated. The deformation process may be carried out either by compressing the metal, as is done in forging, or by subjecting it to tension, as is done in stretching sheet metal.

During plastic deformation, the grain boundaries remain intact, and mass continuity is maintained. The deformed metal exhibits greater strength, because of the entanglement of dislocations with grain boundaries. The increase in strength depends on the amount of deformation (strain) to which the metal is subjected; the greater the deformation, the stronger the metal becomes. Furthermore, the increase in strength is higher for metal with smaller grains, because they have a larger grain-boundary surface area per unit volume of metal.

**Fabrication processes of Nickel-Titanium alloy**

NiTi alloy properties are extremely sensitive to the initial chemical compositions and fabrication processes such as work-hardening rates and heat-treatment procedures. It is necessary to understand various manufacturing processes and theirs effects on product performance in order to receive successful process controls. There are plenty methods of NiTi fabrication used in the industry. For the conventional method, there are consist of 5 stages as follows: (10)

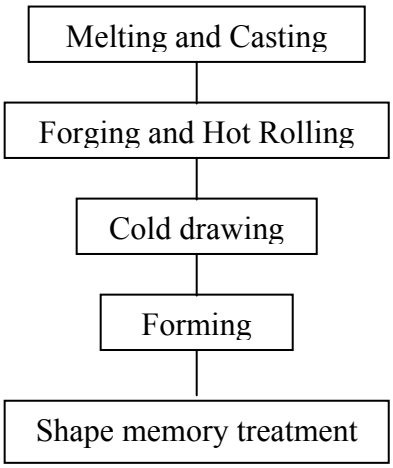


**Figure 5** Fabrication processes of nickel-titanium shape memory alloys (10).

***Melting and casting processes of nickel-titanium alloy***

Casting is a solidification process in which molten metal is poured into a mold and allowed to cool. Solidification of pure metals takes place at a constant

temperature; solidification of alloys occurs over a range of temperatures, depending on composition. Phase diagrams are important tools for identifying the solidification point.

Composition and cooling rates of the melt affect the size and shape of grains and dendrites in the solidifying alloy. In turn, the size and structure of grains and dendrites influence properties of the solidified casting. Solidification time is a function of the volume of a casting and its surface area.[41]

According to ASTM standard, F2063-00[42], there are general requirements on Nitinol chemistry and trace elements. The NiTi alloys are extremely sensitive to a small variation in the Ni or Ti concentration especially increasing of Ni content. For NiTi alloys having greater than 55.0 wt%Ni, a 1% deviation in Ni or Ti concentration will result in approximately a 100°C shift in transformation temperatures.

Since molten titanium is very reactive to oxygen, nickel-titanium alloy is recommended to be melted in high vacuum or an inert gas atmosphere. Both vacuum induction melting (VIM) and vacuum consumable arc melting (VAR) processes are commonly employed. Other melting processes such as non-consumable arc melting, electron beam melting and plasma melting are also used in experimental scales.[43]

Vacuum induction melting method (VIM) The first advantage of induction melting is the homogeneity of chemical composition throughout the ingot, since alternating current induction has a mixing effect on the molten alloy. The recommended crucible material is graphite of calcia [44]. Alumina or magnesia is not suitable because the oxygen contained in the crucible contaminates the molten alloy. In the case of a graphite crucible, oxygen contamination is negligible, but carbon must be considered. By keeping the melting temperature below 1450°C, the carbon contamination can be controlled between 200 to 500 ppm. Such a small amount of carbon does not affect the shape memory characteristics of the alloy. The other advantage of induction melting is the controllability of the chemical composition.[43]

Vaccuum consumable arc melting method (VAR) consumable electrodes of NiTi are melted and solidify in a water-cooled copper mold. The NiTi alloys are contained less than 200 ppm of carbon because there is no contamination from the crucible. However, the molten pool is limited to a small zone so that the entire ingot is not completely mixed. This leads to less homogeneous chemistry and the distribution

in transformation temperature when compared to the VIM ingot. Multiple re-melted are required to achieve acceptable homogeneity.

Sczerzenie F., 1995 employed double melting process using VIM primary melting followed by VAR re-melt routinely to produce NiTi ingots of 1,000 kg and 14 inch diameter.

***Forming of nickel-titanium alloy (Hot and cold working)***

Ingots are converted to wrought (worked) structures by the deformation processes as follows.

Rolling process

Rolling is the process of reducing the thickness of a long work piece by compressive forces applied through a set of rolls. Traditionally, the initial material form for rolling is an ingot. Rolling may be carried out at room temperature (cold rolling) or at elevated temperatures (hot rolling). During hot rolling process, the coarse-grained, brittle, and porous structure of the ingot or the continuously cast metal is broken down into a wrought structure having finer grain size and enhanced properties.

The rolling process involves several material and process variables, including roll diameter (relative to material thickness), reduction per pass, speed, lubrication, and temperature. Spreading, bending, and flattening are important considerations for controlling the dimensional accuracy of the rolled stock.

This practice is now being rapidly replaced by that of continuous casting and rolling, at much higher efficiency and a lower cost.

Drawing process

In drawing, the cross-section of a round rod or wire is typically reduced or changed by pulling it through a die. As reduction increases, the drawing force increases. However, there has to be a limit to the magnitude of the force, because when the tensile stress due to the drawing force reaches the yield stress of the metal being drawn, the work piece will simply yield and, eventually, break.

Successful drawing operations require careful selection of process parameters and consideration of many factors. Drawing speeds depend on the material

and on the reduction in cross-sectional area; they may range from 1 m/s to 2.5 m/s for heavy sections, to as much as 50 m/s for very fine wire.

Reductions in cross-sectional area per pass range from near zero to about 45%. The smaller the initial cross-section, the smaller the reduction per pass. Fine wires are usually drawn at 15% to 25% reduction per pass, larger sizes at 20% to 45%. Reductions of more than 45% may result in lubricant breakdown and resultant surface-finish deterioration. [41]

After melting, the ingot is usually forged and rolled into a bar or a slab with appropriate size at elevated temperature. Such hot working process breakdown the cast structure and improve mechanical properties. Figure 4 shows the tensile strength and elongation of nickel-titanium alloy at high temperature. [43]

The tensile strength begins to decrease at 600 K and the decline accelerates above 650 K. The elongation rises at 800 K and exceeds 100% at 900 K. Thus the alloy is easily worked if the temperature is above 800 K. The optimum heating temperature for hot-working is around 1,073 K. Although the workability of the nickel-titanium alloy is improved at higher temperatures, the alloy surface is more roughened by oxidation. [10]

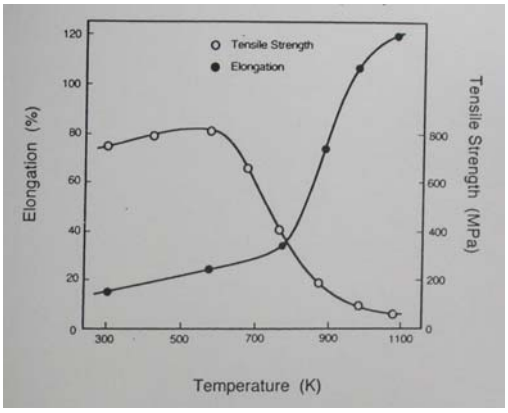


**Figure 6** Tensile strength and elongation of a 50.0 at% nickel-titanium alloy at high temperature (10).

Following hot working, NiTi alloys are cold worked and heat-treated to obtain final dimensions with desired physical and mechanical properties. Compared to the hot working, cold working of NiTi alloy is far more difficult because the alloys are

work-harden rapidly. It requires multiple reductions and frequent *inter-pass annealing* at 600-800°C until the final dimension is obtained.

Round wires are produced by die drawing processes which need to use lubricants such as sodium stearate soap, molybdenum disulfide, graphite-containing water based lubricant [45] and oil based lubricant. Following a similar reduction schedule, rectangular wires can be manufactured by drawing round wires while flat wires are typically produced by cold rolling. Furthermore, rolled NiTi alloy sheets can be made with thickness down to 0.010 inch and width up to 5 inches.

The workability strongly depends on the alloy composition. It becomes harder with increasing nickel content. Especially, working becomes difficult when the nickel content exceed 51 at%. [10]

It is necessary to check tensile strength of the cold-drawn wire before starting forming process. If the wire has tensile strength less than 1000 MPa, sufficient shape memory effect dose not appear after the heat treatment.[10]

Annealing

After the deformation at room temperature (cold rolling) has occurred, strength of the metals generally increases but decreases in ductility. These effects can be reversed by heating the metals in a specific temperature range for a proper period of time. This process is called “annealing”. The temperature range and the amount of time depend on the material and on other factors. Three events take place consecutively during the heating process:

1. *Recovery*:

Recovery occurs at a certain temperature range below the recrystallization temperature of the alloy. The stresses in the highly deformed regions are relieved. Sub-grain boundaries begin to form.

*2. Recrystallization*:

New equiaxed and strain-free grains are formed and replace the older grains. The temperature for recrystallization ranges between approximately 0.3 $T_m$ and 0.5 $T_m$, where $T_m$ is the melting point of the metal on the absolute scale. Recrystallization depends on the degree of prior cold work (work hardening): the more cold work, the lower the temperature required for recrystallization to occur. It can be explained that, as the amount of cold work increases, the number of dislocations and the amount of

energy stored in dislocations (stored energy) also increase. This energy supplies the work required for recrystallization.

3. Grain growth:

If we continue to raise the temperature of the metal, the grains begin to grow, and their size may eventually exceed the original grain size. This phenomenon is known as "grain growth", and it affects mechanical properties.

Annealing is a general term used to describe the restoration of a cold-worked or heat-treated alloy to its original properties – for instance, so as to increase ductility (hence formability) and reduce hardness and strength, or so as to modify the microstructure. Annealing is also used to relieve residual stresses in a manufactured part for the sake of improved machinability and of dimensional stability.

The annealing process consists of the following steps:

- Heating the work piece to a specific range of temperature in a furnace
- Holding it at that temperature for a period of time (soaking); and
- Air or furnace cooling.[41]

***Forming and shape memory treatment of nickel-titanium alloy***

The cold drawn nickel-titanium wire is formed to the final product shape. Like shape memory NiTi alloys, if the part is not constrained during heat treatment, the shape wills recovery partly back to the original configuration. Prototype NiTi components are normally fabricated by holding the part in a fixture during heat treatment. This process can be scaled up to production quantities by increasing the number of fixture and heat treatment capacity. Semi-automation of this process is also possible by cold forming the part using automatic forming machine. The formed part is then placed and constrained in a fixture and subsequently heat treated to a desired shape with final properties.

The final process of nickel-titanium shape memory alloy fabrication is shape memory treatment. The most widely used treatment is the so-called *medium temperature treatment*. The actual procedure of this treatment is quite simple. The formed wire is fastened on a jig and then heated at 623-723 K (350-450$^{o}$C) to memorize the shape. Fastening is necessary not to change the wire shape during the

heat treatment. The holding time ranges from 10 to 100 minutes depending on the product size.

For NiTi alloys with greater than 55.5 wt%Ni, good superelasticity and shape memory effect can be achieved by solution treatment at high temperatures between 600°C and 900°C, then subsequent aging at a temperature around 400°C. This aging process induces precipitation hardening of Ni-rich phases.[46]

Since the treatment temperature affects the transformation temperature and other shape memory characteristics, the furnace is circulated sufficiently to homogenize the temperature distribution. The air circulation is also effective in accelerating the heating rate of the product. When heating is accomplished, the alloy products are taken out and cooled.

***Finishing process of nickel-titanium alloy***

Heat treated NiTi alloys have a typical oxide finish ranging from straw to blue color. These oxide layers can be removed by mechanical procedures such as grit blasting and polishing. Chemically etching is effective in removing oxide layer as well. Electro-polishing has also been demonstrated to produce a highly smooth finish.

The corrosion resistance of nickel-titanium alloy is superior by methods of surface preparation. Because of the preferential formation of Ti oxide on the surface which enhances passivity and corrosion resistance of the alloys, surface treatment for corrosion protection is not needed. Passivation following ASTM F86 procedure results in much improved corrosion resistance and biocompatibility.

Shabalovskaya et al., 2003 [47] etched nickel-titanium alloy samples after mechanical polishing in a 1 HF + 4 $NHO_3$ + 5 $H_2O$ solution for at least 4 min, then ultrasonically cleaned in deionized distilled water for 5 min, and aged in distilled boiling water for 20 min. This cost-effective surface treatment combining chemical etching and aging in boiling water results in porous, amorphous, Ni-depleted surface built exclusively with $TiO_2$ highly corrosion-resistant oxide. These oxide films required for shape setting and maintain their stability in physiological solution.

**Factor affecting shape memory behavior of Nickel-Titanium alloy**

Factors such as variation in the chemical composition, material processing, and thermo-mechanical treatment and addition of alloying elements, which affect the structure, are important for controlling the memory behavior of Nickel-Titanium shape memory alloy. [10, 48]

***Alloy composition***

The nickel-titanium alloy is an equiatomic intermetallic compound and a composition shift from stoichiometry greatly affects the characteristics of the alloy. In particular, transformation temperature is extremely sensitive to composition. One percent shift in nickel content results in a 100 K change in the martensitic started and austenitic finished temperature point.[10]

The transitional temperature range (TTR) of a 1:1 ratio of nickel and titanium is in the range of -50 to +100°C. In the manufacturing process both cold working and thermal heat treatment can significantly affect TTR. In addition, altering chemical composition by changing the Ni-Ti ratio in favor of excess Ni or by substituting cobalt for Ni can reduce TTR. [39]

Kusy R.P., 1997 has reported that for every 150 parts per million (ppm) variations in composition, the transition temperature changes 1°C. [2]

Many investigations have been made on the equilibrium phase diagram of the nickel-titanium system and the parent phase region is very narrow at temperature below 923 K (650$^{o}$C). Figure 5 is the equilibrium nickel-titanium phase diagram in the vicinity of nickel-titanium. Although in this phase diagram, the parent phase region below 923 K (650$^{o}$C) is not specifically shown, it is generally accepted that the parent region is only between 50.0-50.5% of nickel.

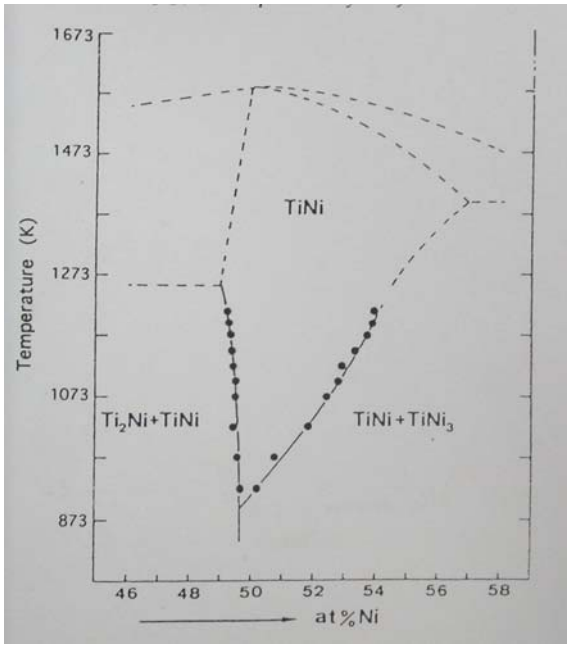


**Figure 7** Equilibrium phase diagram for nickel-titanium in the vicinity of nickel-titanium.[10]

Nickel-titanium alloys with nickel contents exceeding 50.5 at % decompose on cooling slowly from a high temperature or on aging at a temperature below 973 K (700$^{o}$C) after quenching from a high temperature. There are the following three temperature ranges, in each of which the decomposition scheme is unique.

1. aging at temperature below 953 K (680$^{o}$C)
   TiNi→ TiNi + $Ti_3Ni_4$→ TiNi + $Ti_2Ni_3$→ TiNi + $TiNi_3$
2. aging at temperature between 953 K (680$^{o}$C) and 1023 K (750$^{o}$C)
   TiNi→ TiNi + $Ti_2Ni_3$→ TiNi + $TiNi_3$
3. aging at temperature between 1023 K (750$^{o}$C) and 1073 K (800$^{o}$C)
   TiNi→ TiNi + $TiNi_3$

In any of the three temperature ranges, the final product of decomposition is a mixture of $TiNi_3$ and TiNi. The $Ti_3Ni_4$ phase from in the early stages of aging at low temperature as fine platelets with coherency to the matrix and affects the properties of the nickel-titanium alloys. The $Ti_3Ni_4$ phase has a rhombohedral structure. Precipitation of $Ti_3Ni_4$ strengthens the matrix of parent phase and thus improves the recoverability of the shape memory effect.

Gall et al, 2005 [49] studied the tensile stress-strain response of Ti-50.1at%Ni and Ti-50.9at%Ni wires related to the wire structure and deformation mechanisms. They concluded that the more Ni rich wires contained fine second phase precipitates, while the wires with lower Ni content were relatively free of precipitates. Increasing Ni concentration caused the formation of $Ti_3Ni_4$ precipitates and leaded to material strengthening, a decrease in the primary martensitic transformation temperature, and an increase in the critical transformation stresses at a given test temperature. In addition, the $Ti_3Ni_4$ precipitates decreased the strain observed during stage II deformation which indicated that increased difficulty of martensitic deformation.

The alloy of nickel contents exceeding at 50.5% are sensitive to heat treatment at temperature between 573 K (300$^o$C) and 773 K (500$^o$C) due to the resulting precipitation of $Ti_3Ni_4$, those of the alloys of nickel contents between 50.0-50.5% are insensitive to heat treatment because no precipitation of the $Ti_3Ni_4$ occurs in this alloy. However, thermo-mechanical treatments by annealing at a temperature below 773 K (500$^o$C) after cold-working affect their properties very much.

The workability strongly depends on the alloy composition. It becomes harder with increasing Ni content, especially when exceeding 51 at%. Near-equiatomic Ni-Ti alloys of Ni content less than approximately 50.5 at% Ni behave pseudoelastically only partially when fully annealed.

***Ternary alloying***

Ternary alloying additions affect the transitional temperatures and thus shape recovery temperatures of nickel-titanium alloys.

- Substitution of vanadium, chromium, manganese or aluminum for titanium lowers the transformation temperatures.
- Substitution of cobalt or iron for nickel also lowers the martensitic transformation temperature ranges.
- Palladium and gold are the only alloying elements which are known to be effective for raising the transformation temperatures.
- Substitution of cobalt or iron for nickel also lowers the martensitic transformation temperatures.

- Substitution of iron for nickel separates the transformation temperature ranges of the B2 → R and the R → B19' effectively. This reveals R-phase transformation which can reduce thermal hysteresis.

Ternary titanium-nickel-copper alloys have been investigated extensively in view of improving the shape memory and pseudoelasticity characteristics. Copper addition reduces the stress-hysteresis in the pseudoelastic effect and avoids aging effects [50]; it prevent $Ti_3Ni_4$ precipitation and thus it is effective for avoiding martensitic started temperature change due to differences in cooling step. Composition sensitivity of martensitic started temperature is also very much reduced by copper addition. However, copper addition exceeding 10 at% embrittles the alloy and spoils the formability.

Some superelastic wires contain copper 5-6 at% to increase strength and reduce energy loss (hysteresis). Unfortunately, these benefits are accompanied with an increase in the phase transformation temperature above that of the ambient value in the mouth; 0.5 at% of chromium is added to the alloy in order to reduce the stress transformation temperature to 27°C. [2, 51]

Gill F.J. et al [3, 52] studied the effect of copper addition on the superelastic behavior of Ni-Ti shape memory alloys for orthodontic application. They conclude that copper was effective in narrowing the stress hysteresis and in stabilizing the superelasticity characteristics against cyclic deformation. In their experiment, Ni-Ti with copper 5.7 wt% has a narrowest hysteresis. Moreover, it produced greater stability of both the transformation temperature and the force applied to the teeth for a determined design and wire cross-section. In addition, copper alloying in Ni-Ti arch wires can reduce the ageing effect because the substitution of Ni atoms by copper atoms produce a decrease of the Ni content down to 50.4% which is the chemical content that limit needed for the precipitation process.

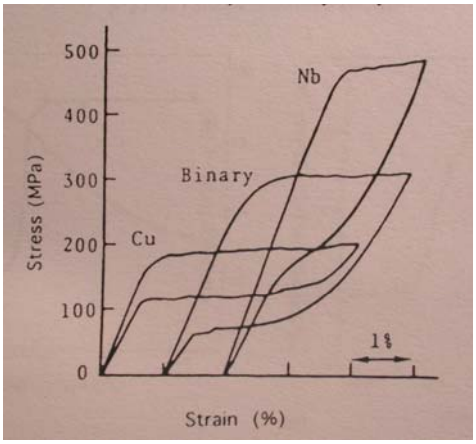


**Figure 8** Effect of ternary alloying addition on stress-hysteresis of pseudoelasticity.
Binary: Ti-50.2at%Ni annealed at 673 (400$^{o}$C) after cold rolling 30%.
Cu: Ti-40.0Ni-10.0Cu (at %) annealed at 1073 (800$^{o}$C).
Nb: 48Ti-50Ni-2Nb (at %) annealed at 1123 K (850$^{o}$C). [10]

***Thermo-mechanical Treatment***

In shape memory alloys generally, transformation pseudoelasticity should appear in a certain temperature range above austenitic finished temperature. In this way, for the fully annealed near-equiatomic nickel-titanium alloys, pseudoelasticity is incomplete at any temperature above austenitic finished temperature and shape memory also is not good. However, the pseudoelastic strain increases substantially by thermo-mechanical treatment which effectively increased the resistance for slip deformation and prevents plastic deformation by slip.

When the alloy is cold-rolled more than 20% and then annealed at 673 K (400$^{o}$C), it shows complete pseudoelasticity. Figure 7 shows the effect of thermo-mechanical treatment. There, the specimens were cold-rolled as much as 6 to 25% and then annealed at 673 (400$^{o}$C), for 1 hour. Degree of cold-rolling is shown above each stress-strain curve. The tensile test was made at 323 K (50$^{o}$C), which is about 40 K above the martensitic started temperature. It is clearly seen in the figure that the strain recoverable on unloading increases with increasing degree of cold-rolling prior to annealing.

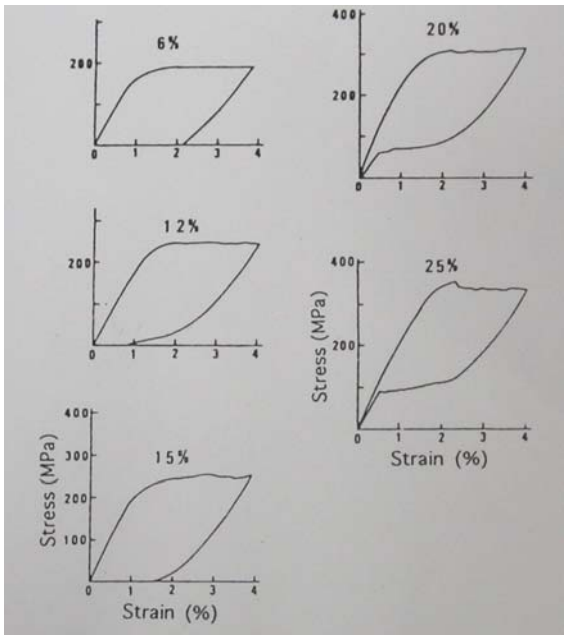


**Figure 9** Improvement of pseudoelasticity achieved by cold-rolling followed by annealing at 313 K (400°C). Degree of cold-rolling is shown above each stress-strain curve. Tensile tests were made at 323 K (50°C). [10]

Specimens cold-rolled 25% and annealed at 873 K (600°C), which is nearly the recrystallization temperature, behave like those annealed at 1123 K (850°C) and pseudoelastic strain recovery is only partial. This indicates that annealing in the thermo-mechanical treatment has to be done at an appropriate temperature below the recrystallization temperature to maintain the high dislocation-density introduced by cold-working.

Kurita et al, 2004 [53] studied the transformation behavior of the equiatomic rolled NiTi alloy by using a differential scanning calorimeter (DSC) in order to reveal the effects of inner stress and defects. They concluded that the temperature region of the transformation of cold-worked NiTi alloys was expanded and the DSC peak was small. The broadening of the peak is enhanced by increasing the cold-working reduction percent. The intermediate phase appeared after cold-working and subsequent annealing at a temperature of 500°C. Furthermore, the thermal hysteresis of the phase transformation between high and intermediate phases is narrow.

The reduction of grain size is very effective for improving the pseudoelasticity. Figure 10 illustrated the grain size dependence of recoverability of a

Ti-50.5% Ni alloy which was annealed at 1073 K (800°C) for 1 hour and quenched. The stress-strain curves in the figure were obtained by tensile testing the specimens with three different grain sizes: (a) 50μm, (b) 1 mm. and (c) single crystal. The tests were made at 313 K (40°C) which is 10 K above the austenitic finished temperature (303 K or 30°C).

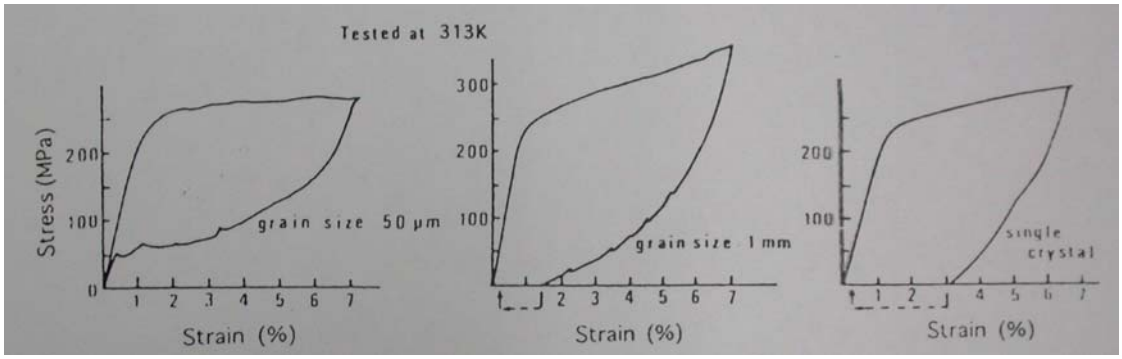


**Figure 10** Grain size dependence of pseudoelasticity in Ti-50.5% Ni alloy. [10]

**Standard Specification for Nickel-Titanium Shape Memory Alloys for Medical Devices and Surgical Implants**

According to ASTM: F 2063-00, the chemical , physical , mechanical and metallurgical requirements for wrought nickel-titanium bar, wire, flat rolled products and tubing containing nominally 54.4% to 57.0% nickel and used for the manufacture of medical devices are mentioned.

1. Chemical composition

Major elements shall be analyzed by direct current plasma spectrometry according to Guide E 1097; atomic absorption, inductively coupled plasma spectrometry according to Practice E 1497; X-ray spectrometer according to Practice E 1172 or an equivalent method.

X-ray Fluorescence (XRF) Spectrometry is used for elemental analysis. Elemental identification is accomplished by spectrometers that resolve the spectral lines emitted into separate components. There are two types of spectrometers that are available in:

- Wavelength-dispersive spectrometry (WDS): The X-rays emitted are dispersed into specific wavelengths by the mechanical movement of

analyzing crystals attached to a goniometer and detected by proportional or scintillation counters.

- Energy-dispersive spectrometry (EDS): Semiconductors are used to create signals proportional to the X-ray energy.

The WDS systems demonstrate higher resolution, higher-sensitivity detection, and higher counting rates than the EDS system. However, owing to single-channel detection they are slow, and because of the goniometer arrangement they are very sensitive to topographic features. EDS is very fast due to multichannel detection and provides simultaneous multi-element analysis capability, although not all elements can be determined in every sample under the same conditions. The voltage of the X-ray tube is critical for the excitation of the elements in both WDS and EDS, and should be set higher than the absorption edge of the elements probed.

The range of acceleration voltage for WDS is 0-100 keV, while for EDS the range is 0-40 keV. The tube current affects only the X-ray photon flux and thus the count rate. XRF spectrometers can operate with the sample chamber kept at atmospheric conditions, under vacuum or under helium. Generally, for detection of X-rays below 5 keV, vacuum or helium purging is required.

XRF spectrometry can be applied non-destructively to the analysis of solid samples of various forms (bulk, powders and briquette), liquids, thin films, and filtered aerosol samples. The technique can detect elements with atomic number $Z > 11$. Oxygen and fluorine can be semi-quantitatively measured using special crystal or detectors. Detection limits for bulk determinations are typically from a few ppm up to a few tens of ppm, dependent on the energy used and the sample composition. For thin films, detection limits may reach 100 $ng/cm^2$.

Bulk materials may be analyzed as received since the typical sample size is 32 mm, placed in special cups or holders. For smaller samples (up to 1 mm) beam collimators are required. For quantitative determinations, precise positioning of the sample in the spectrometer is of paramount importance, especially in WDS. Samples for analysis should have a surface roughness less than 100 μm when X-ray above 4 keV is used. Care should be taken when polishing samples to avoid surface contamination, as surface smears remaining may affect the intensities of the emitted X-rays.

The depth of analysis in XRF varies from few micrometers to a millimeter or more, depending on the X-ray energy used and the nature of the target.

2. Transformation Temperature

Differential scanning calorimetry is used to assure the alloy formulation in terms of transformation temperature parameters: $M_f$, $M_p$, $M_s$, $A_s$, $A_p$, $A_f$. The ASTM international F 2005-05 [54] gives definition of differential scanning calorimetry that is a technique in which the difference in heat flow into or out of a substance and an inert reference is measured as a function of temperature while the substance and the reference material are subjected to a controlled temperature program. It is a highly important member of the general class of thermal analysis methods that includes thermomechanical analysis, thermogravimetric analysis, and differential thermal analysis. Differential scanning calorimetry is employed extensively to characterize industrial polymers and over the past decade has been increasingly used for study of orthodontic materials, particularly nickel-titanium arch wire alloys and polyurethane elastomers. Differential scanning calorimetry is particularly useful for studying phase transformations in the nickel-titanium arch wire alloys, where there is substantial supporting engineering materials science literature about the differential scanning calorimetry peaks for the nickel-titanium phases. [6]

According to ASTM international F 2004-05 [54], differential scanning calorimetry involves heating and cooling a test specimen at a controlled rate in a controlled environment through the temperature interval of the phase transformation. The difference in heat flow between the test material and a reference material due to energy change is continuously monitored and recorded. Absorption of energy due to a phase transformation in the specimen results in an endothermic peak on heating. Release of energy due to a phase transformation in the specimen results in an exothermic peak on cooling. This test method uses small, stress-free, annealed samples (typically much less than 50 mg) to determine whether a sample of Ni-Ti alloy is austenitic or martensitic at a particular temperature. Since chemical analysis of these alloys does not have sufficient precision to determine the transformation temperature by measuring the Ni to Ti ratio of the alloy.

In conventional DSC, two small pans, one containing the material to be analyzed and the other containing an inert reference material such as indium, are heating at the same rate, typically 5°C or 10°C per min (termed the ramp rate or scanning rate). The difference in thermal energy (power) supplied to each pan to maintain equal heating rates is plotted as a function of temperature over the scanning range to yield the DSC curve or thermogram. The changes in the thermal power difference for the two pans are related to changes in the heat capacity (specific heat, Cp) of the material under study.[6]

Bradley, et al, 1996 [55] reported that the superelastic wires were austenitic nickel-titanium and underwent a reversible stress-induced transformation to martensitic nickel-titanium during activation, whereas the non-superelastic wires, such as Nitinol, had stable work-hardened martensitic structures. Differential scanning calorimetry show the phase transformations in the superelastic nickel-titanium wires were more complex and involved an immediate rhombohedral structure. However, recent research has suggested that these concepts for the metallurgical structures and phase transformation in orthodontic nickel-titanium alloys may require some revision. To reconcile these conflicting results, differential scanning calorimetry used to analyze the superelastic and non-superelastic nickel-titanium orthodontic wires. They found that the superelastic nickel-titanium alloys undergo austenitic transformations involving the rhombohedral structure which begin below $0^{o}$C. The differential scanning calorimeter analyses indicated that in the oral environment nickel-titanium is almost entirely austenite, whereas Nitinol superelastic is a mixture of austenite and rhombohedral structure. The non-superelastic alloy Nitinol is entirely or almost entirely martensite at room temperature, and contains small additional amounts of austenite in the oral environment.

3. Phase analysis

The X-ray diffraction (XRD) is a valuable tool for the determination of the crystallographic structure of materials. In the customary XRD methodology for orthodontic materials, nearly monochromatic characteristic X-rays, such as Cu Kα radiation, are used. Characteristic X-ray are generated when the accelerating voltage in the X-ray tube is sufficiently high (typically > 10 kV) that the electrons, created by

passing a current through a filament, have the necessary energy to knock out core electrons from the K level (innermost shell) of the target metal. The most likely transitions are for electrons from the L shell to fill the vacancies in the K shell, with the creation of Kα X-ray. An appropriate filter material or a crystal monochromator is used to greatly reduce the intensity of the Kβ X-rays, so that nearly monochromatic Kα X-rays are used for XRD analyses. In the usual experiments, a polycrystalline specimen in flat plate from or a polycrystalline powder specimen is analyzed. In XRD studies of archwires, a series of parallel wire segments may be placed in contact to obtain an acceptable specimen for the diffractometer. Plate-shaped archwire specimens used with the diffractometer will not have randomly oriented crystals because of the preferred crystallographic orientation resulting from the wire drawing process.[6]

Typical XRD equipment includes: x-ray tube or source, sample holder, goniometer for angle measurement, x-ray detector for intensity measurement, and optics for beam filtering and columnation. The wavelength of rays is similar to the spacing between planes of atoms in materials. As a result, planes of atoms constructively interfere with roentgen rays and diffraction occurs. Roentgen rays of a known wavelength, λ, are used. The wavelength of the Cu Kα radiation which is usually used is 1.5418 °A or 0.15418 mm.[54]

For materials containing more than one phase, such as 40°C Copper NiTi in Figure 11, the XRD pattern will contain the series of peaks for each phase.[6]

X-ray diffraction is inherently a near-surface analytical technique, since the depth of penetration of the x-ray beam is typically no greater than 50 μm and frequently much less for the metals of usual interest. Consequently, caution is necessary when interpreting the results of XRD experiments, since the near-surface structure of a material may differ significantly from the bulk structure. While such an experiment is generally very difficult to conduct, the safest procedure is to perform a series of XRD analyses on specimens from which known thicknesses of surface layers have been removed.[6]

Thayer et al, 1995 [54]used XRD to identify phases of superelastic arch wires before and after samples were strained. They found that the transformation occurs at different stress levels and to different degrees in different Ni-Ti alloy wire

products. Moreover, they concluded that the XRD peak width showed the effect of cold work to superelasticity.

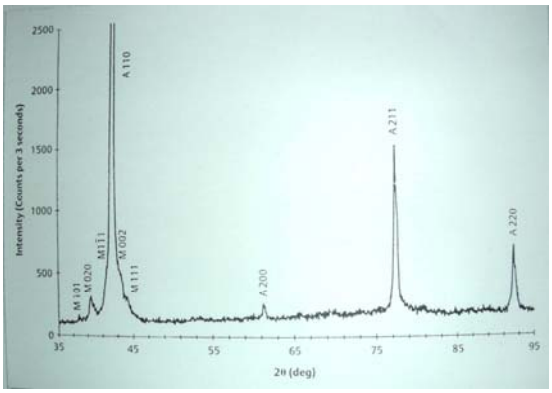


**Figure 11** X-ray diffraction pattern for 40°C Copper Ni-Ti obtained at room temperature. (An abstract describing this study is found in Brantley et al, 1998) [6]

4. Metallurgical structure

4.1 Grain structure

According to Guide E 3-01, the specimens are subjected to metallographic examination to reveal the constituents and structure of alloys by means of a light optical or scanning electron microscope. The metallographic specimens of hot-worked or cold-worked alloys should be studied in both transverse and longitudinal sections. Special investigations may require specimens with surfaces prepared parallel to the original surface of the product. Specimens to be polished are generally not more than about 12 to 25 mm square or in diameter. If the specimens are fragile, oddly shaped or too small to be handled readily during polishing, they should be mounted to ensure a surface satisfactory for microscopic study. Cleanliness of the specimens from all greases, oils, coolants and residue from cutoff blades is acquired by dissolving in suitable organic solvent. Failure to clean thoroughly can prevent cold mounting resins from adhering to the specimen surface. Grinding can be done in a number of ways, ranging from rubbing the specimen on a stationary piece of abrasive paper to the use of automatic devices. After grinding, the specimen must be cleaned thoroughly with ultrasonic cleaning in a water/soap solution containing a corrosion inhibitor. After that, polishing with loose abrasive (≤ 6μm) embedded in an appropriately lubricated supporting surface.

According to Practice E 407-99, Electrolytic etchants for Ni-Ti alloy are as follows;

| Etchant composition | Procedure |
|---|---|
| 5 mL acetic acid<br>10 mL $HNO_3$<br>85 mL water | Use hood. Do not store. Electrical at 1.5 V for 20-60 s. Use platinum wires. |
| 50 mL $HNO_3$<br>50 mL acetic acid | Use hood. Do not store. Mix fresh. immerse or swab 5-30 s. Will chemically polish with longer times. Sulfidized grain boundaries etched before normal grain boundaries. |
| 10 mL HF<br>25 mL $HNO_3$<br>150 mL water | Swab 5-30 s. |

5. Mechanical Properties

5.1 Tensile test

Tension test is a common test for determining such mechanical properties of materials as strength, ductility, toughness, elastic modulus and strain hardening. The test first requires the preparation of a test specimen. In the United States, the specimen is prepared according to ASTM specification. Typically, the specimen has an original gage length, generally 50 mm (2 in.), and a cross-sectional area, usually with a diameter of 12.5 mm (0.5 in.). The specimen is mounted between the jaws of a tension-testing machine. These machines are equipped with various controls so that the specimen can be tested at different rates of deformation and temperature.(44)

The force application causes an internal resisting force in the material or stress ($\sigma$) due to the displacement of the atoms. In the metric or System International (SI) system, the usual unit of stress is the mega Pascal [56].

$$\sigma = F/A_0$$

Where; F = applied force,

$A_0$ = the original cross-sectional area

The force application concurrently causes strain (ε), i.e., a change in dimension of the material specimen.

$$\varepsilon = \Delta l/l_0$$

Where; $\Delta l$ = the change in length,

$l_0$ = the original length

The slope of the initial linear region is the modulus of elasticity (E), which corresponds to the elastic stiffness or rigidity of the material.

$$E = \sigma/\varepsilon$$

Where σ dose not exceed the proportional limit

An important mechanical property for orthodontic alloys is the modulus of resilience which is the area of the stress-strain plot up to the proportional limit (PL). The modulus of resilience represents the energy per unit volume required to load a specimen of the alloy to the end of the elastic range and is equivalent to the biomechanical spring energy of the alloy. Since this area on the stress-strain plot is a right triangle, it follows that the modulus of resilience is given by;

$$\text{Resilience} = (PL)^2/2E$$

Corne et al, 2001 [57] used tensile test for characterizing the mechanical properties of the cold rolled NiTi samples with an Instron 5566 testing machine. Tension samples were machined by electrical discharge machining [58] to 1.8 mm in width and 6 mm in gauge length. Loading was conducted at a displacement rate of 0.05 mm/min to 6% strain, immediately followed by unloading until the stress

returned to zero. Between cycles, the deformed sample was allowed to full recovery in 15 minutes while the Instron software actively held the displacement at zero.

According to ASTM E8-04, describes the procedures for tension testing as follows:

1. Preparation of the test machine
    - To warm up the machine to normal operating temperatures and minimize errors that may result from transient conditions.
2. Gage length marking of test specimens
    - Gage marks shall be stamped lightly with a punch, scribed lightly with dividers or drawn with ink as preferred.
3. Zeroing of the testing machine
    - The testing machine shall be set up to zero force on the specimen. Preloads imparted by the gripping of the specimen may be the result of such things as grip design, malfunction of gripping apparatus (sticking, binding, etc.), excessive gripping force or the sensitivity of the control loop.
4. Gripping of the test specimen
5. Speed of testing
    - Speed of testing can be defined in term of rate of straining of the specimen, rate of stressing of the specimen, rate of separation of the two heads of the testing machine during a test or free-running crosshead speed.
    - Free-running crosshead speed is specified in inches per inch of distance between grips for specimens not having reduced section.
    - When performing a test to determine yield properties, the rate of stress application shall be between 10,000 and 100,000 psi/min.
    - When determining only the tensile strength, or after the yield behavior has been recorded, the speed of the testing machine shall be set between 0.05 and 0.5 in./in. of the distance between the grips per minute. Alternatively, an extensometer and strain rate indicator may be used to set the strain rate between 0.05 and 0.5 in./in./min.
6. Determination of yield strength

- Offset method: It is necessary to secure data (autographic or numerical) from which a stress-strain diagram may be drawn. On the stress-strain diagram, lay off straight line equal to the specified value of the offset is drawn parallel to straight line of the diagram. The intersection of this lay off line with the stress-strain diagram is located as yield point. In reporting values of yield strength obtained by this method, the specified value of offset used should be stated in parentheses after the term yield strength.
- Extension-Under-Load method: This method determines the stress value at the specified value of extension, or uses devices that indicate when the specified extension occurs. The stress at the specified extension shall be reported as follows:

  Yield strength (Extension under load = 0.5%) = 52,000 psi.

7. Yield point elongation
   - Calculate the yield point from the stress-strain diagram of data by determining the difference in strain between the upper yield strength and the onset of uniform strain hardening.
8. Tensile strength
   - Calculate the tensile strength by dividing the maximum force carried by the specimen during the tension test by the original cross-sectional area of the specimen.
9. Elongation
   - In reporting values of elongation, give both the original gage length and the percentage increase. For example: elongation = 30% increase (2-in. gage length)
   - When the specified elongation is greater than 3%, fit ends of the fractured specimen together carefully and measure the distance between the gage marks to the nearest 0.01 in. for gage lengths of 2 in. and under, and to at leas the nearest 0.5% of the gage length for gage lengths over 2 in.
   - When the specified elongation is 3% or less, determine the elongation of the specimen using the following procedure. Prior to testing, measure the original gage length of the specimen to the nearest 0.002 in. Remove

partly torn fragments that will interfere with fitting together the ends of the fractured specimen or with making the final measurement. Fit the fractured ends together with matched surfaces and apply a force along the axis of the specimen sufficient to close the fractured ends together. If desired, this force may then be removed carefully, provided the specimen remains intact. Measure the final gage length to the nearest 0.002 in. and report the elongation to the nearest 0.2%.

According to ASTM F 2516-06, Standard Test Method for Tension Testing of Nickel-Titanium Superelastic Materials, the material is pulled to 6% strain, then unloaded to less than 7 MPa, then pulled to failure. The procedure shall be per Test Method E8 with the following additions:

- Temperature of the test shall be 22.0°C. Tolerance shall be ± 2.0°C.
- If the diameter or thickness of the specimen is between 0.5 to 2.5 mm., the maximum crosshead speed in mm./min. per mm. of initial distance between grips for specimens not having reduced sections is 0.02 for first cycle (load to 6% strain and unload) and 0.2 for second cycle (load to failure)
- Test shall consist of zeroing the force transducer, gripping the specimen, pulling the specimen to 6% strain, reversing the motion to unload the specimen to less than 7 MPa, and then pulling the specimen to failure.
- For materials with diameter greater than 0.2 mm., strain shall be determined by use of a calibrated extensometer.
- Upper plateau strength shall be determined by the stress at a strain of 3.0% during the initial loading of the specimen.
- Lower plateau strength shall be determined by the stress at a strain of 2.5% during the unloading of the specimen.
- Residual elongation shall be determined by the difference between the strain at a stress of 7.0 MPa during unloading and the strain at a stress of 7.0 MPa during loading.
- The uniform elongation shall be determined by elongation when the maximum load is reached just prior to necking or fracture, or both.

5.2 Micro-indentation hardness test

The micro-indentation hardness test method according to ASTM E 384-05a [9] is a hardness test using a calibrated machine to force a diamond indenter of specific geometry into the surface of the material being evaluated, in which the test forces range from $9.8x10^{-3}$ to 9.8 N (1 to 1000gf), and the indentation diagonal, or diagonals are measured with a light microscope after load removal (Figure 12); for any indentation hardness test, it is assumed that the indentation does not undergo elastic recovery after force removal. The test should be performed on the flat specimen with a polished or otherwise suitably prepared surface. Furthermore, the test specimen surface should not be etched before making an indentation. This test method covers micro-indentation tests made with Knoop and Vickers indenters. For the Vickers hardness test, in practice, test loads are in grams-force and indentation diagonal are in micrometers. The Vickers hardness number is calculated as follows:

$$HV = \frac{1854.4 \times P}{M^2}$$

Where: P = force, gf

M = mean diagonal length of the indentation, μm

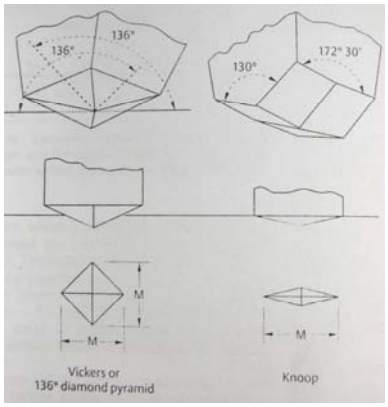


**Figure 12** Geometry of diamond indenters and schematic appearance of surface indentations for the Vickers and Knoop microhardness tests. The lengths of the diagonals designated by M are measured microscopically.

(Adapted from Anusavice, 1996) [6]

Hardness tests have been found to be very useful for materials evaluation, quality control of manufacturing processes and research and development efforts. Hardness can be correlated to tensile strength for many metals, and is an indicator of wear resistance and ductility.[59]

Oh K.T. et al 2006 [60] used a Vickers microhardness tester (MXT-α 7E model, Matsuzawa Seiki Co., Japan) to determine the microhardness of Ni-Ti alloys with the use of a 1000-g load. The results were distributed in the range of 205-313 $H_v$, with NiTi-0.263 Ag having the highest hardness value.

Yokoyama K. et al, 2005 [61] performed Vickers microhardness tests to evaluate the property of work-hardened NiTi wires. They embedded wire specimens in epoxy resin and polished on the transverse cross section of the wires. The tests were carried out from the periphery to the center of the wire at 0.05-mm intervals. Measurements were performed under an applied load of 0.98 N for 15 s

.

5.3 Three-point bending test

The International Organization for Standardization [62] reported the mechanical testing of metals in international standard ISO 7438: Metallic materials-Bend test. The principle of bend test consists in submitting a test piece of round, square, rectangular, or polygonal cross-section to plastic deformation by bending, without changing the direction of loading, until a specified angle of bend is reached.

The ASTM International has reported about the three-point bending test in the standard test methods for bend testing of metallic flat materials for spring applications involving static loading: E 855-90 [63]. The three-point bending test methods cover the determination of the modulus of elasticity in bending and the bending proof strength of flat metallic strips or sheets for spring applications. The test methods consist of deflection tests of a simple beam configuration subjected to three-point symmetrical loading. The thickness range covered is 0.010 to 0.050 in. (0.25 to 1.3 mm). The modulus of elasticity in bending is obtained by load-deflection measurements at stresses below the elastic limit. Rectangular test specimens shall be used. Specimen orientation relative to the rolling direction must be identified. The recommended minimum specimen thickness shall be 0.25 mm. The thickness should be measures at the four corners and at the center of the specimen's gage section. The

span length shall be 150 times the nominal thickness in the range 0.25 to 0.51 mm, inclusive, and 100 times the nominal thickness in the range exceeding 0.51 mm. Specimen width shall be 3.81 mm in the thickness range 0.25 to 0.51 mm, inclusive, and 12.7 mm in the thickness range exceeding 0.51 mm. The total specimen length shall be 250 times the nominal thickness in the range of 0.25 to 0.51 mm and 165 times the nominal thickness in the range exceeding 0.51 mm. A minimum of 6 specimens shall be tested.

This test method is useful for obtaining values of proof strength in bending and modulus of elasticity in bending. These values are useful to spring designers to determine spring constants and maximum permissible deflection of flat springs. Furthermore, it can also serve for research and development to study the effects of metallurgical variables such as composition, heat treatment, fabrication operations and alloy development.

Miura et. al. [64] introduced a three-point bending test, which designed to clarify the relationship between the loading and deflection by determining the nature of the force being delivery during orthodontic treatment. They explained that the approved American Dental Association standard method is a cantilever type of test. This method is an acceptable one to demonstrate the springback properties. Wires of good springback property increase the length and the angle of the specimen so that super-elastic-like property appears even if the wires do not possess this feature. Instead, a three-point bending test was designed because this would accurately differentiate the wires that do not possess superelastic features. At the same time the three-point bending test actually simulates the application of wire pressure on the teeth in the oral cavity. From that time, three-point bending test was the most favorite method, with many investigators used to test the mechanical properties of orthodontic wires. [22, 23-30]

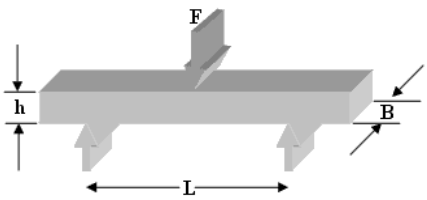


**Figure 13** Model representing three-point bending test method.

# CHAPTER IV
# MATERIALS & METHODS

## Materials

1. Titanium (purity 99.9%)

**Figure 14** Titanium

2. Nickel (purity 99.9%)

**Figure 15** Nickel

3. Copper (purity 99.9%)

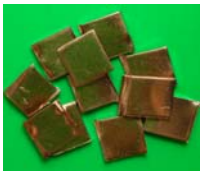

**Figure 16** Copper

4. Silicon-carbide (SiC) papers 200-2000 grit
5. Alumina paste 1.0, 0.3 μm
6. Acrylic resin
7. Polyvinyl chloride pipes
8. Acetone
9. Methyl alcohol solution
10. Nitric acid
11. Hydrofluoric acid
12. Distilled water

## Apparatus

1. Electric balance

**Figure 17** Electric balance

2. Electrolytic arc furnace


**Figure 18** Electrolytic arc furnace

3. CNC wire cut machine

**Figure 19** CNC wire cut machine (Sodick: Linear Servo Controller LN1W)

4. Bar rolling machine

**Figure 20** Bar rolling machine

5. Heat treatment furnace
6. Universal polisher


**Figure 21** Universal polisher

7. Micrometer

**Figure 22** Micrometer

8. Ultrasonic cleanser

**Figure 23** Ultrasonic cleanser

9. Differential scanning calorimeter

**Figure 24** Differential scanning calorimeter (Metter Toledo DSC 822 $^{e}$)

10. Energy-Dispersive Spectrometer with Scanning Electron Microscope:

**Figure 25** EDS-SEM: JSM-5410LV JEOL LTD, Tokyo, Japan

11. X-ray diffractometer

**Figure 26** X-ray diffractometer

12. Optical microscope

13. Instron Universal testing machine

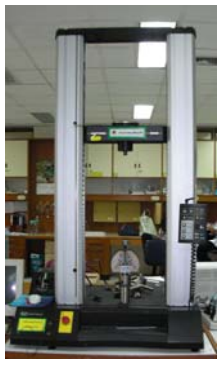

**Figure 27** Instron Universal testing machine

14. Micro-hardness tester

**Figure 28** Vickers-hardness tester

**Methods:**

NiTi Samples Fabrication and Surface Preparation

There are two steps as follows:

*Step I: Fabrication of two systems of Ni-Ti alloy samples*

1. The alloy compositions used in this experiment are shown in table 1.

**Table 1** Compositions of the alloys

| System | At%Ti (wt%) | At%Ni (wt%) | at%Cu (wt%) |
|---|---|---|---|
| **Ti:Ni** | 49.3 (44.238) | 50.7 (55.762) | - |
| **Ti:Ni:Cu** | 49.8 (44.515) | 45.2 (49.549) | 5.0 (5.936) |

2. Ingot preparation

A conventional vacuum arc re-melting technique was employed to prepare the equiatomic Ni-Ti alloy. After received exact amounts of each element: titanium (purity, 99.9%), nickel (purity, 99.9%) and copper (purity, 99.9%), they were cleaned in acidic solution (Hydrofluoric and nitric solution) in order to remove surface grease and oxide. Then the elements were melted together in an electrolytic arc furnace in argon atmosphere. The alloy was turned over and was re-melted five times to ensure chemical homogeneity.

3. Specimens preparation

The as-melted ingots were sliced into small plates (1.5 mm. in thickness) in distilled water using a CNC wire cut machine (Sodick: Linear Servo Controller LN1W). After the specimens were cleaned ultrasonically in acetone to remove surface grease, they were followed by repeating cold-rolling. No annealing process was conducted during the cold-rolling to avoid the occurrence of recrystalization. The final thicknesses of the cold-rolled plates were 1.35, 1.20 and 1.05 mm. with a cold-rolling reduction of 10, 20 and 30 % respectively. Then the cold-rolled plates were cut into specific shaped specimens by a CNC wire cut machine (Sodick: Linear Servo Controller LN1W) for various test methods as described below.

- 3.0 X 3.0 mm. Rectangular shaped specimens for Phase-transformation temperature analysis by Differential Scanning Calorimetry (DSC)
- 3.0 X 7.0 mm. Rectangular shaped specimens for Chemical composition analysis by Scanning electron microscopy with X-ray energy-dispersive spectroscopy (SEM-EDS)m Micro-indentation hardness test by Vickers

microhardness tester, Grain structure analysis by optical microscope after etching

- 15.0 X10.0 mm. Rectangular shaped specimens for Crystallographic structure analysis by X-ray Diffraction (XRD)
- 45.0 X 5.0 mm. Rectangular shaped specimens for Tensile test by Instron universal testing machine
- 30.0 X 1.0 mm. Rectangular shaped specimens for Three-point bending test by Instron universal testing machine

Surfaces of all specimens were polished with Silicon Carbide papers 240-1,200 grit size in order to remove any oxide layers and surface contaminants. Subsequently each test specimen in every condition of % cold working was annealed in the rate of 10°C/min at 400°C (below the recrystalization temperature) and 600°C (over the recrystalization temperature) in a heat treatment furnace for 1 hour (Table 2). After the heat treatment procedure, the surfaces of all specimens were re-polished.

**Table 2** All groups of the test specimens in various conditions

| **Nominal composition (at%)** | **Cold rolling (% of reduction)** | **Heat treatment temperature (°C)** |
|---|---|---|
| **Ti:Ni (49.3:50.7)** | 10 | 400 |
| | | 600 |
| | 20 | 400 |
| | | 600 |
| | 30 | 400 |
| | | 600 |
| **Ti:Ni:Cu (49.8:45.2:5.0)** | 10 | 400 |
| | | 600 |
| | 20 | 400 |
| | | 600 |
| | 30 | 400 |
| | | 600 |

*Step II: Analysis of the Ni-Ti alloy specimens*

1. Chemical composition

Scanning electron microscopy with X-ray energy-dispersive spectroscopic (SEM-EDS: JSM-5410LV JEOL LTD, Tokyo, Japan) was used to assess the elemental composition of the specimens. For this purpose, specimens were bonded to aluminum stabs, vacuum coated with a thin layer of conductive carbon, and examined under an SEM unit. Spectra were obtained under the following conditions: 20 kV accelerating voltage, 50 μA beam current, 500x original magnification and 120 seconds acquisition time.

The test specimens in both alloy systems (Ni-Ti and Ni-Ti-Cu) were analyzed for chemical composition. Means and standard deviations (n=6) of the chemical composition of each alloy were calculated.

2. Transformation temperature range

The transformation behavior was measured in a differential scanning calorimeter with a liquid nitrogen cooling accessory (Mettler Toledo DSC822$^e$). Measurements were carried out at a thermal cycling rate of 10°C/min. First heating cycle began from 30°C to 120°C and then cooled down from 120°C to -50°C. The machine was programmed to settle at -50°C for 5 minutes before beginning second heating cycle from -50°C to 120°C.

The transformation peaks on heating and the reverse martensite peaks on cooling from thermogram were determined. The data was presented as transformation temperatures ($M_f$, $M_s$, $A_s$, $A_f$) and enthalpy changes or thermal hysteresis ($\Delta H$) in each condition of the test specimens.

3. Mechanical properties

3.1 Three-point bending test

The specimen length was 30 mm in straight condition. The width of the specimens was 1 mm. The thickness of the specimens was depended on the degrees of reduction (10%, 20% and 30%) or 1.35, 1.20 and 1.05 mm. respectively. The apparatus used for the three-point bending test was a further development of the device described by ISO/CD 15841. The specimens were subjected to a symmetrical

three-point bending test. A 10 mm. span of the specimens between supports was used. Deflection was carried out with a centrally placed indenter. The supports and indenter had an edge curvature between 0.05 mm. and 0.13 mm. The mid-span deflection rate was 1.0 mm/min. with 1 KN load cell. The samples were tested in the direction of the thickness of the specimen. The three-point bending test was carried out under constant temperature range 36.0±1.0$^{o}$C (The oral temperature) by using water bath. The samples were deflected to 1.5 mm. and then were unloaded to 0 mm. for 1 cycle. Each specimen was tested for 3 cycles.

Before testing, the specimens were dipped into hot water (85°C) for 3 minutes in order to change alloy specimens to austenitic phase completely. This method reduces error of the data. The load cells registered the force placed on the specimen and transmitted this value to a computer.

Six samples of the test specimen in both alloy systems (Ni-Ti and Ni-Ti-Cu) were tested (n=6). The best load-deflection curve was selected to represent the bending property of the alloys.

3.2. Tensile test

Tensile specimens were prepared in specific shape as followed:

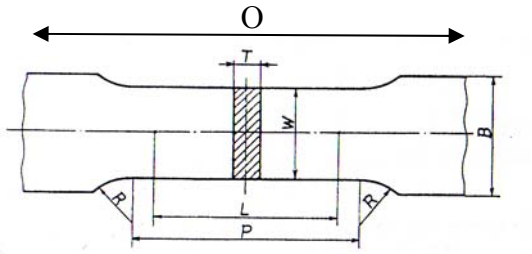


**Figure 29** Tensile specimen

| Width / W (mm.) | Grip width / B (mm.) | Gauge length / P (mm.) | Over-all length / O (mm.) | Radius of fillet / R (mm.) |
|---|---|---|---|---|
| 3 | 5 | 23 | 45 | 1 |

Tension properties were measured with a universal testing machine under the controlled atmospheric temperature at 36±1°C. The 1 KN load cell worked in the tensile mode with a cross-head speed of 5.0 mm/min. The specimens for tensile test were 3.0 mm in width and 23.0 mm in gauge length.

Before testing, the specimens were dipped into hot water (85°C) for 3 minutes in order to change specimen structures to austenitic phase completely. This method reduces error of the data. Properties of uniform elongation (Elu%) and ultimate tensile strength were obtained from the stress-strain diagrams.

Three specimens in all conditions were tested. (n = 3) Means and standard deviations of uniform elongation (Elu%) and ultimate tensile strength were calculated.

### 3.3. Micro-hardness test

The specimens were cold-mounted with acrylic resin by using Polyvinyl chloride pipes as a mold. After that, the specimens were polished by SiC papers 600-1,200 grid size followed by alumina paste 1.0 and 0.3 micrometer respectively. The polished surfaces of the specimens were cleaned by ethanol and dried before testing. According to ASTM E384-05a [59], a test specimen should have flat surface and free of any defects that could affect the indentation or the subsequent measurement of the diagonals. The specimens should be placed on the stage so that the specimen surfaces were perpendicular to the indenter axis. The measuring microscope was focused with a low power objective so that the specimen surface could be observed and selected the area desired for hardness determination. Before applying the force, the indenter was adjusted to the proper place for force application. For this test, a 500-g load was used. The indenter was automatically lowered and made contact with the specimen for the normally required time period or dwell time was set at 15 seconds. After the force was removed, the machine was automatically switched to the measuring mode. The image was examined and measured both diagonals of a Vickers indentation and determine within 0.1 μm. The programme was automatically calculated Vickers Hardness Number (HV).

For each specimen in both longitudinal and cross sections, 5 different locations were randomly tested. Means and standard deviations (n = 5) of Vicker Hardness Number (Hv) were calculated.

4. Grain structure

The specimens were subjected to metallurgical analysis after polishing and etching to evaluate the morphology and structure of alloy surfaces. Both longitudinal and cross-sectional surfaces of the specimens were embedded in epoxy resin using Polyvinyl chloride pipes as a mold and were polished with 600-1,200 grit size SiC papers followed by 1.0 and 0.3 mm alumina paste. Specimens were further etched with an etching solution of concentrated hydrofluoric acid: nitric acid: and distilled water at 1:4:5 volume ratios to reveal the grain structure of alloys. All specimens were studied under an optical microscope for analysis of the average grain size.

Ten cross-sectional grain structures were randomly measured. Means and standard deviations (n = 10) of the grain sizes were calculated.

5. Crystallographic structure

X-ray diffraction (XRD) studies were performed with X-ray diffractometer with Cu Kα radiation at 40 kV and 40 mA. The diffractometer was equipped with a diffracted monochromatic beam, 1°divergent slit and a 0.6 mm receiving slit. The scans started at 25° 2θ and ended at 95° 2θ with a step size of 0.02° and count time at each step of 0.2 second. The data was received as a graph called diffractogram representing the relationship between the intensities of diffracted X-ray beams on the vertical axis and the diffraction angles of X-ray beams (2θ) for each phase on the horizontal axis. In order to identify crystallographic structure of the alloys, the XRD peaks were indexed by comparing their positions to those in the polycrystalline powder standards for austenitic (18-899) and martensite (35-1281) NiTi, published by the International Center for Diffraction Data (ICDD) of Swartmore, PA, USA.

# CHAPTER V
# RESULTS

The results of this study were divided into five parts.

1. Chemical composition
2. Transitional temperature ranges
3. Mechanical properties
    - 3.1 Three-point bending test
    - 3.2 Tensile strength test
    - 3.3 Micro-hardness test
4. Grain structure
5. Crystallographic structure

**Chemical Composition**

The chemical composition of the experimental alloys used in this experiment was determined by Scanning Electron Microscopy with an X-ray Energy-Dispersive Spectroscope (SEM-EDS: JSM-5410LV JEOL LTD). Means and standard deviations (n=6) of the chemical compositions of each alloy were calculated and listed in Table 3.

**Table 3** Means and standard deviations of the chemical compositions of the Ni-Ti alloys

| Nominal composition (at%) | Chemical compositions by EDS | | | |
|---|---|---|---|---|
| | Ni (at%) | Ti (at%) | Cu (at%) | Si (at%) |
| 49.3Ni:50.7Ti | 47.65 ± 0.22 | 52.01 ± 0.28 | - | 0.24 ± 0.15 |
| 45.2Ni:49.8Ti:5.0Cu | 41.94 ± 0.12 | 50.21 ± 0.27 | 7.56 ± 0.38 | 0.29 ± 0.17 |

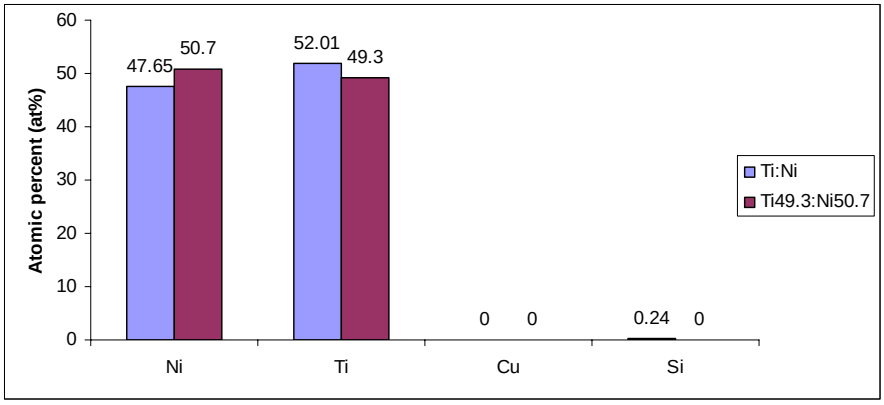


**Figure 30** Chemical composition of Ti-Ni alloys (Ti:Ni = 49.3:50.7 at%)

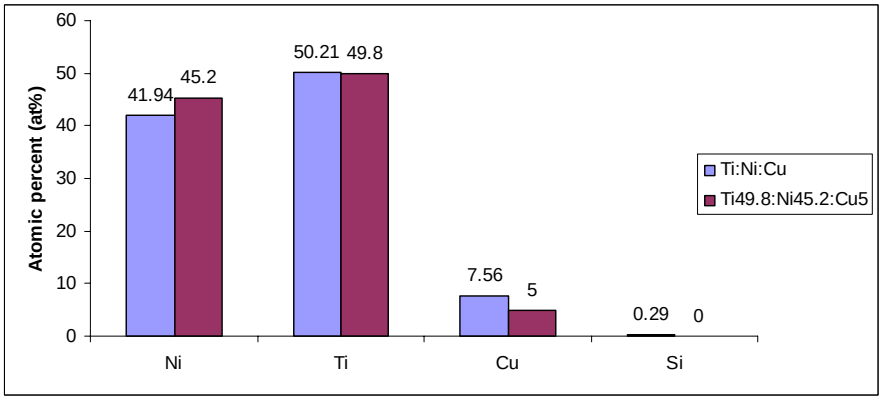


**Figure 31** Chemical composition of Ti-Ni-Cu alloys (Ti:Ni:Cu = 45.2:49.8:5 at%)

**Transformation Temperature Ranges**

Differential scanning calorimetry (DSC) was used in determining the transformation peak on heating and a reverse martensite peak on cooling.

**Table 4** Transformation temperatures and enthalpy changes (ΔH) for all conditions of nickel-titanium alloy specimens

| Ni-Ti alloy specimens (at%) | % Reduction | Heat treatment temp. (°C) | Heating (°C) | | Cooling (°C) | | Temp. hysteresis (°C) |
|---|---|---|---|---|---|---|---|
| | | | $A_s$ (°C) | $A_f$ (°C) | $M_s$ (°C) | $M_f$ (°C) | |
| Ni:Ti (50.7:49.3) | 10 | 400 | 26 | 55 | 34 | 10 | 23.17 |
| | | 600 | 54 | 70 | 48 | 34 | 24.81 |
| | 20 | 400 | 22 | 52 | 31 | 5 | 21.4 |
| | | 600 | 59 | 72 | 52 | 38 | 24.18 |
| | 30 | 400 | 18 | 49 | 29 | 0 | 19.28 |
| | | 600 | 59 | 71 | 49 | 40 | 23.01 |
| Ni:Ti:Cu (45.2:49.8:5.0) | 10 | 400 | 25 | 56 | 52* | 23** | 4.54 |
| | | 600 | -2 | 28 | 0 | -31 | 25.37 |
| | 20 | 400 | 34 | 55 | 53* | 31** | 3.71 |
| | | 600 | 11 | 30 | 3 | -16 | 20.26 |
| | 30 | 400 | 34 | 55 | 53* | 32** | 3.11 |
| | | 600 | -1 | 26 | 0 | -26 | 24.12 |

* Rs/Os, ** Rf/Of (Rhombohedral phase/ Orthorhombic phase)

For the 49.3Ni:50.7Ti (at%) specimens with 10%, 20% and 30% reductions followed by 400°C heat treatment for 1 hour presented: $A_s$ set between 18°C-26°C, $A_f$ set between 49°C-55°C, $M_s$ set between 29°C-34°C , and $M_f$ set between 0°C-10°C. This alloy could be classified as the mixture of martensite and austenite in the oral temperature (Figure 32).

Regarding the 49.3Ni:50.7Ti (at%) specimens, heat-treated at 400°C for 1 hour, the thermogram showed the different peaks of phase transformation between

10%, 20% and 30 % reductions. The transformation temperature ranges of both heating and cooling paths decreased when the percent reduction increased.

Considering the shape of the peaks, the peaks broadened when the percent reduction increased. It means that the phase transformation will occur more difficultly. By the way, the temperature hysteresis from the peak to peak tended to stabilize in all percent reductions, approximately 30°C, which is the standard value of temperature hysteresis of NiTi alloys.

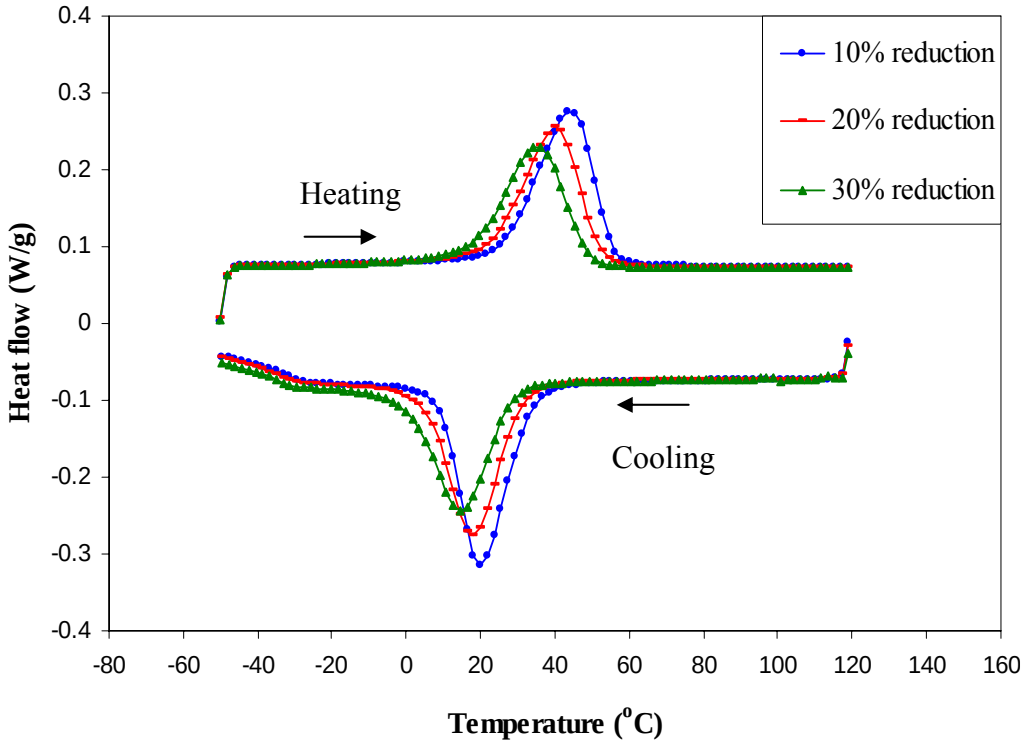


**Figure 32** Thermographs of Ni:Ti (50.7:49.3at%) with 10%, 20% and 30% reductions and heat-treated at 400°C

The 49.3Ni:50.7Ti (at%) specimens with 10%, 20% and 30% reductions followed by 600°C heat treatment presented: $A_s$ set between 54°C-59°C, $A_f$ set between 70°C-72°C, $M_s$ set between 48°C-52°C , and $M_f$ set between 34°C-40°C. This alloy could be classified as stabilized martensite in oral temperature (Figure 33).

At the 600°C heat treatment temperature, the peaks of the thermogram showed no difference between 10%, 20% and 30 % reductions or the percent

reductions had no influence on transformation temperature range. Besides, transformation temperature ranges of the specimens in all percent reductions, heat-treated at 600°C, were higher than that of the specimens in all percent reductions, heat-treated at 400°C approximately 20°C-30°C. In addition, the peaks of transformation were sharper and narrower than that of specimens heat-treated at 400°C; meaning the phase transformation can occur smoothly. For temperature hysteresis, significant difference was found between 10%, 20% and 30%reductions.

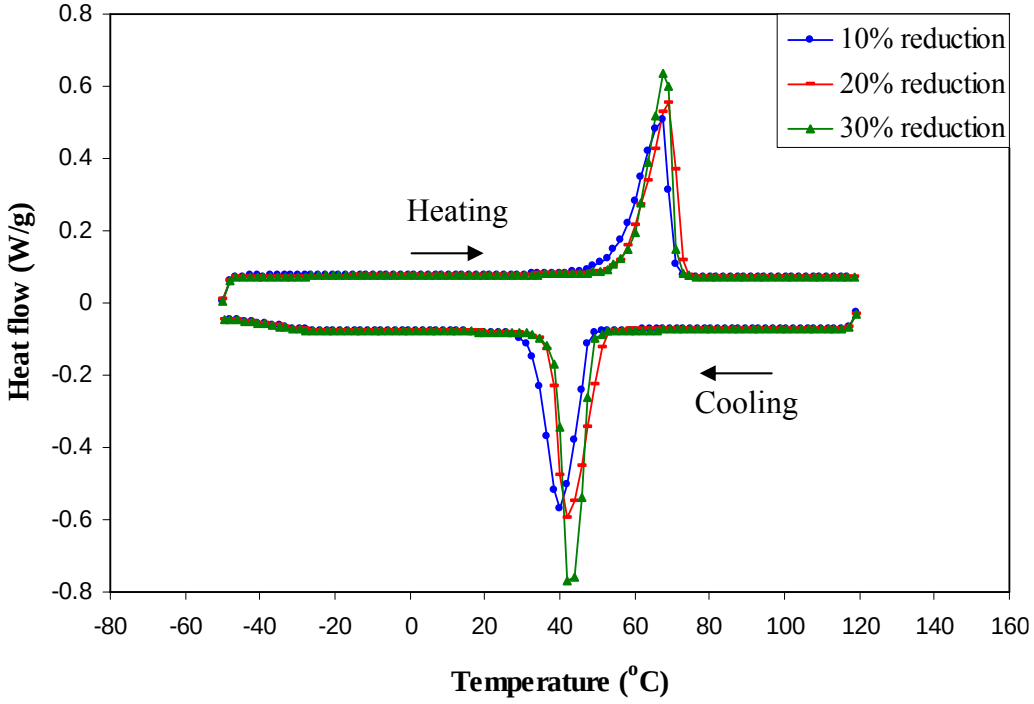


**Figure 33** Thermographs of Ni:Ti (50.7:49.3at%) with 10%, 20% and 30% reductions and heat-treated at 600°C

The 45.2Ni49.8Ti5.0Cu (at%) specimens with 10%, 20% and 30% reductions followed by 400°C heat treatment presented: $A_s$ set between 25°C-34°C, $A_f$ set between 55°C-56°C, $R_s/O_s$ set between 52°C-53°C and $R_f/O_f$ set between 23°C-32°C. This alloy could be classified as the active austenitic in oral temperature. (Figure 34)

At the treatment temperature of 400°C, no significant difference was found between the peaks of transformation temperature range of 10%, 20% and 30% reductions.

Interestingly, the heating curves of the thermogram separated into two peaks. This may have resulted from the inhomegeneity of the ingot composition. All peaks were broad and showed narrow temperature hysteresis, approximately 5°C. This phenomenon confirmed that the peak was not the martensitic transformation. The peak on cooling path was R-phase transformation or the intermediate phase occurred when the alloys were work-hardened. The other possible phase was orthorhombic phase (O-phase), which occurred by copper addition in Ni-Ti alloy. The average peak of heating and cooling curves was located approximately the same as the oral temperature. Thus, the superelastic property should be possessed in this alloy.

The martensitic transformation peak should occur below the R or O-phase. As in the graph, the martensitic transformation peak was too broad to be noticed.

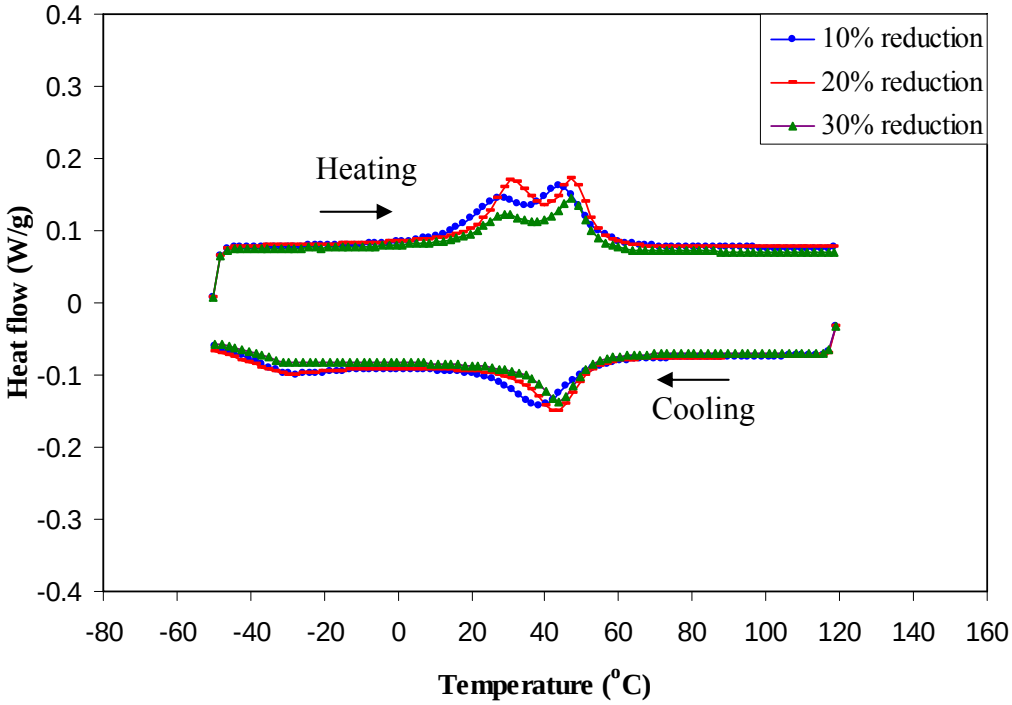


**Figure 34** Thermographs of Ni:Ti:Cu (45.2:49.8:5.0at%) with 10%, 20% and 30% reductions and heat-treated at 400°C

The 45.2Ni49.8Ti5.0Cu (at%) specimens with 10%, 20% and 30% reductions followed by 600°C heat treatment presented: $A_s$ set between -2°C-11°C, $A_f$ set between 26°C-30°C, $M_s$ set between 0°C-3°C and $M_f$ set between -31°C-(-16)°C. This alloy could be classified as active austenitic in oral temperature (Figure 35).

At the 600°C heat treatment temperature, a difference was found between 10%, 20% and 30% reductions. All in all, the peaks of the thermogram were sharper than that of NiTiCu heat-treated at 400°C. Temperature hysteresis was also broader. This characteristic revealed that the peak was the martensitic transformation, not the R or O-phase transformation. In addition, the difference between the peak position of 10%, 20% and 30% reductions indicated that the cold working had an influence on transformation temperature range. Nevertheless, heat treatment at 600°C caused the transformation temperature range of martensite to shift higher and approach the oral temperature. This means the probability of obtaining superelastic property at the oral temperature was decreased.

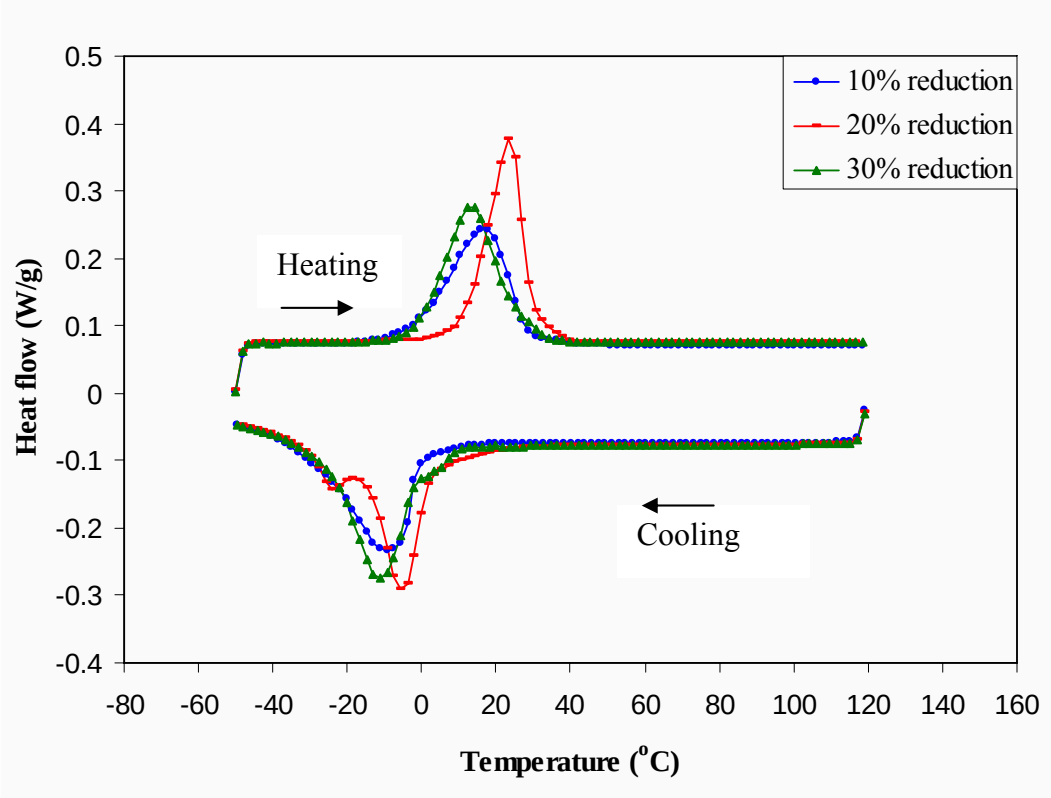


**Figure 35** Thermographs of Ni:Ti:Cu (45.2:49.8:5.0at%) with 10%, 20% and 30% reductions and heat-treated at 600°C

## Mechanical properties

### Three-point Bending Test

The bending curves for each specimen are shown in Figure 36 to 47.

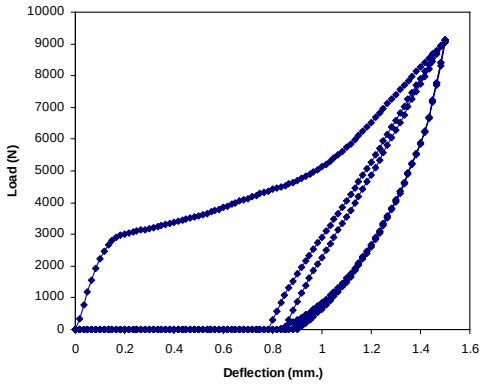


**Figure 36** Load-deflection cycles of Ni-Ti with 10% reduction and 400°C heat treatment at 37°C

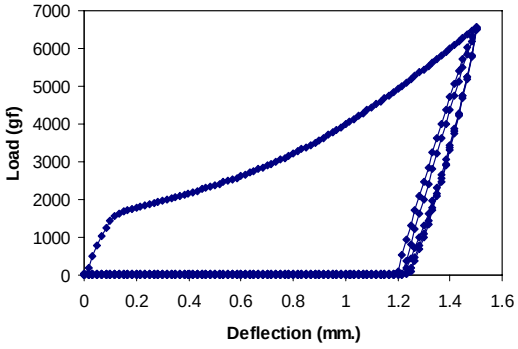


**Figure 37** Load-deflection cycles of Ni-Ti with 10% reduction and 600°C heat treatment at 37°C

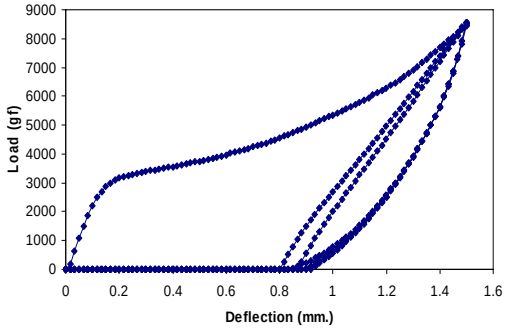


**Figure 38** Load-deflection cycles of Ni-Ti with 20% reduction and 400°C heat treatment at 37°C

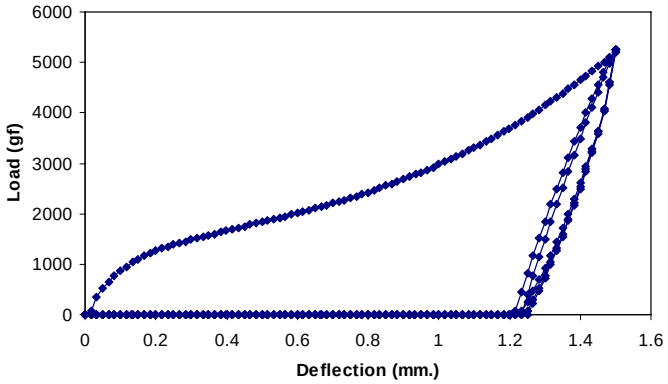


**Figure 39** Load-deflection cycles of Ni-Ti with 20% reduction and 600°C heat treatment at 37°C

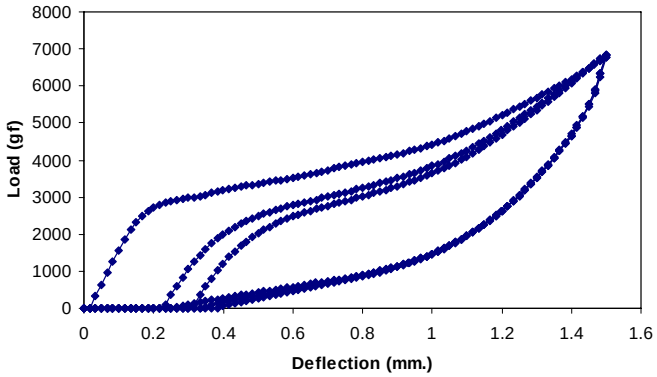


**Figure 40** Load-deflection cycles of Ni-Ti with 30% reduction and 400°C heat treatment at 37°C

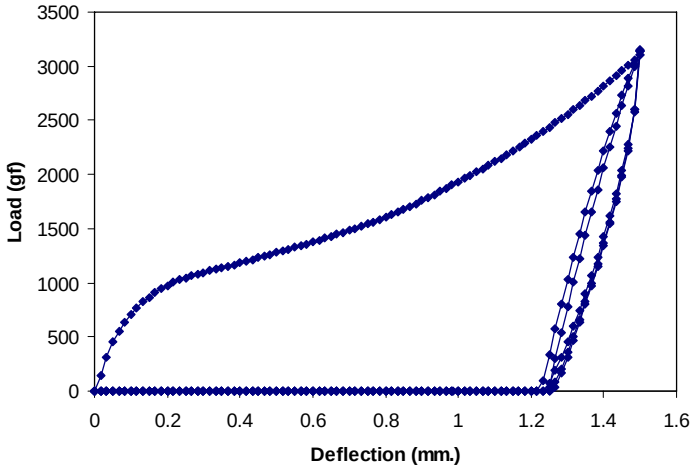


**Figure 41** Load-deflection cycles of Ni-Ti with 30% reduction and 600°C heat treatment at 37°C

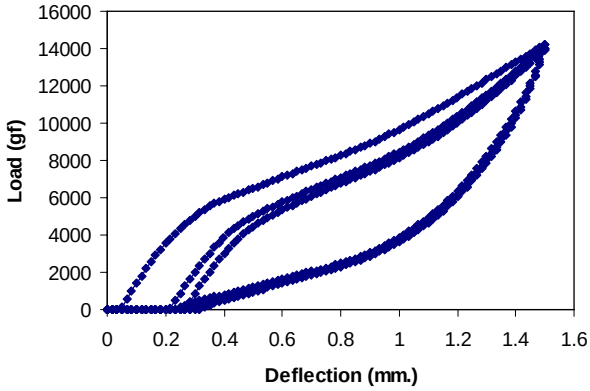


**Figure 42** Load-deflection cycles of Ni-Ti-Cu with 10% reduction and 400°C heat treatment at 37°C

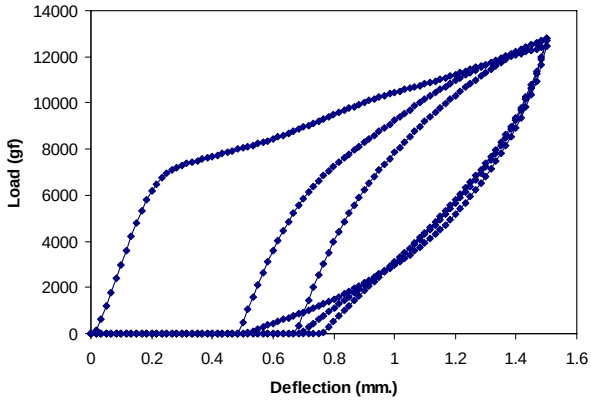


**Figure 43** Load-deflection cycles of Ni-Ti-Cu with 10% reduction and 600°C heat treatment at 37°C

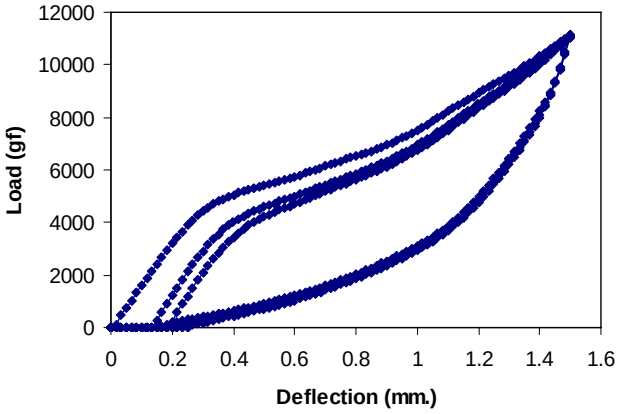


**Figure 44** Load-deflection cycles of Ni-Ti-Cu with 20% reduction and 400°C heat treatment at 37°C

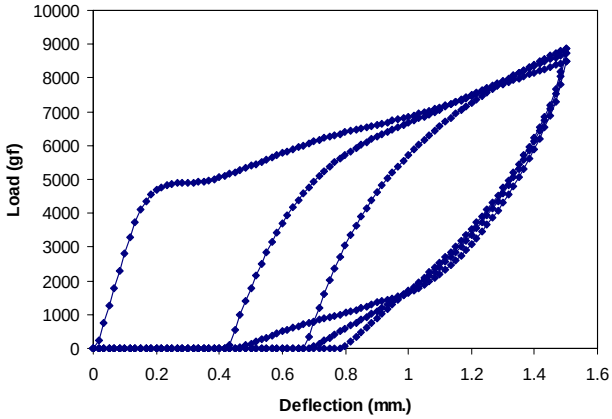


**Figure 45** Load-deflection cycles of Ni-Ti-Cu with 20% reduction and 600°C heat treatment at 37°C

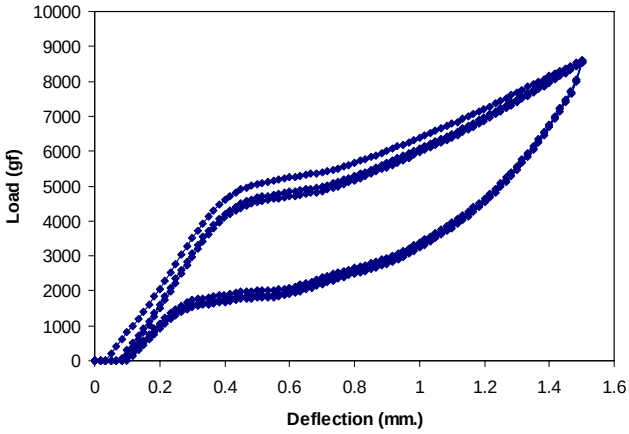


**Figure 46** Load-deflection cycles of Ni-Ti-Cu with 30% reduction and 400°C heat treatment at 37°C

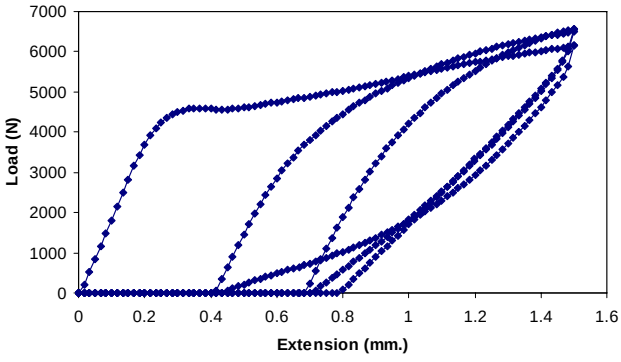


**Figure 47** Load-deflection cycles of Ni-Ti-Cu with 30% reduction and 600°C heat treatment at 37°C

Figure 48 shows the relationship between load and deflection curves of 50.7Ni:49.3Ti (at%) specimens with 10%, 20% and 30% reductions followed by heat treatment at 400°C for 1 hour. In order to investigate the cycle effect of each specimen, the first three cycles of data were plotted for each specimen.

Clear differences were seen within the three cycles of each percent reduction. For the specimens of 10% and 20% reductions, similar load-deflection curves were observed. At the first cycle, the deflection did not completely recover on the unloading path. It appeared as though the specimen had permanent deformation. On the second cycle, the point where the loading path occurs did not begin at the 0 mm. deflection. This resulted in a difference of the loading path between the first and second cycles. On the other hand, the unloading curves of each cycle nearly overlapped. On the last cycle, the loading and unloading curves were almost superelastic because they originated from the same range of deflection. Interestingly, when the percent reduction increased to 30%, the recovery stress could be noticed on the unloading curve. Moreover, the load-deflection curve showed greater superelastic property than that of 10% and 20% reductions.

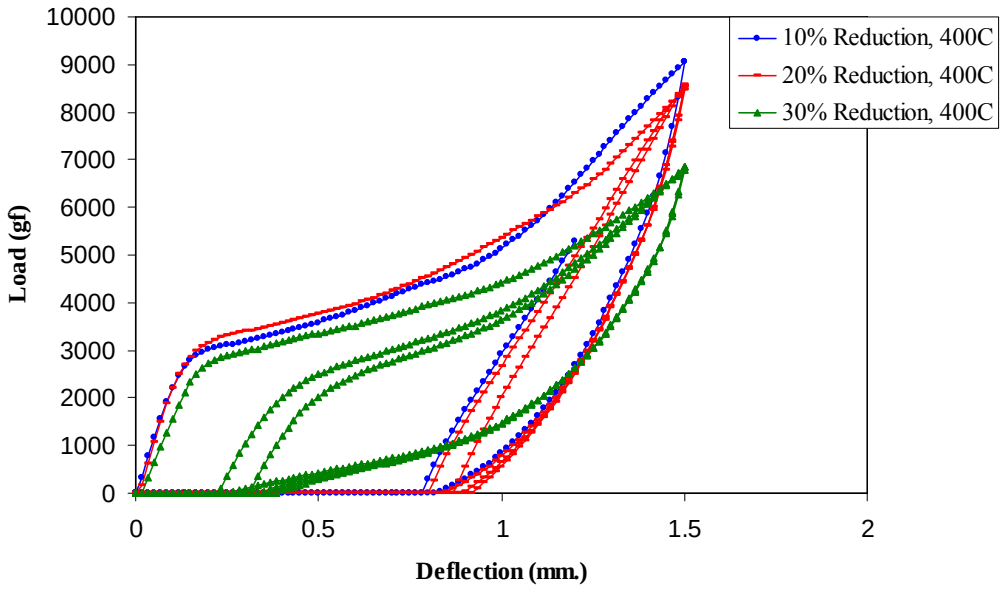


**Figure 48** Load-deflection cycles at 37°C of Ni-Ti with 10%, 20% and 30% reductions and heat-treated at 400°C

Figure 49 shows the relationship between load and deflection of 50.7Ni:49.3Ti (at%) specimens with 10%, 20% and 30% reductions, followed by heat treatment at 600°C for 1 hour. In order to investigate the cycle effect of each specimen, first three cycles of data were plotted for each specimen.

Clear differences were seen within the three cycles of each percent reduction. At the first cycle of all percent reduction, the deflection was not completely recovered on the unloading path. It appeared that the specimen had permanent deformation. On the second cycle, the point where the loading path occurred did not begin at the 0 mm. deflection. This resulted in a difference of the loading path between the first and second cycles. On the other hand, the unloading curves of each cycle nearly overlapped. On the last cycle, the loading and unloading curves were almost superelastic because they nearly originated from the same range of deflection. The stress plateaus, which determined by the slope of the loading path after the critical stress (*), tended to decrease when the percent reduction increased.

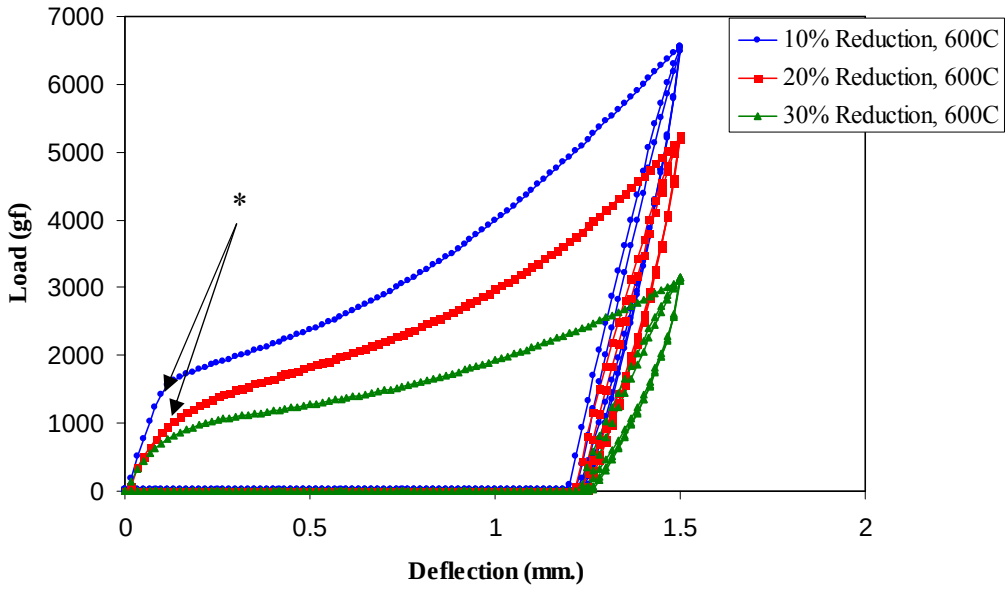


**Figure 49** Load-deflection cycles at 37°C of Ni-Ti with 10%, 20% and 30% reductions and heat-treated at 600°C

Figure 50 shows the relationship between load and deflection of Ni45.2:Ti49.8:Cu5.0 specimens with 10%, 20% and 30% reductions, followed by heat treatment at 400°C for 1 hour. In order to investigate the cycle effect of each specimen, the first three cycles of data were plotted for each specimen.

The load-deflection curves of all percent reductions were almost identical. Unloading curves in all three cycles of each specimen almost completely recovered. This characterized these alloys as superelastic at the oral temperature. Some differences were found between 10%, 20% and 30% reductions. The unloading curves of 30% reduction recovered more than that of 10% and 20% reductions. The stress plateau, determined by the slope of the loading path after the critical stress, tended to decrease when the percent reduction increased.

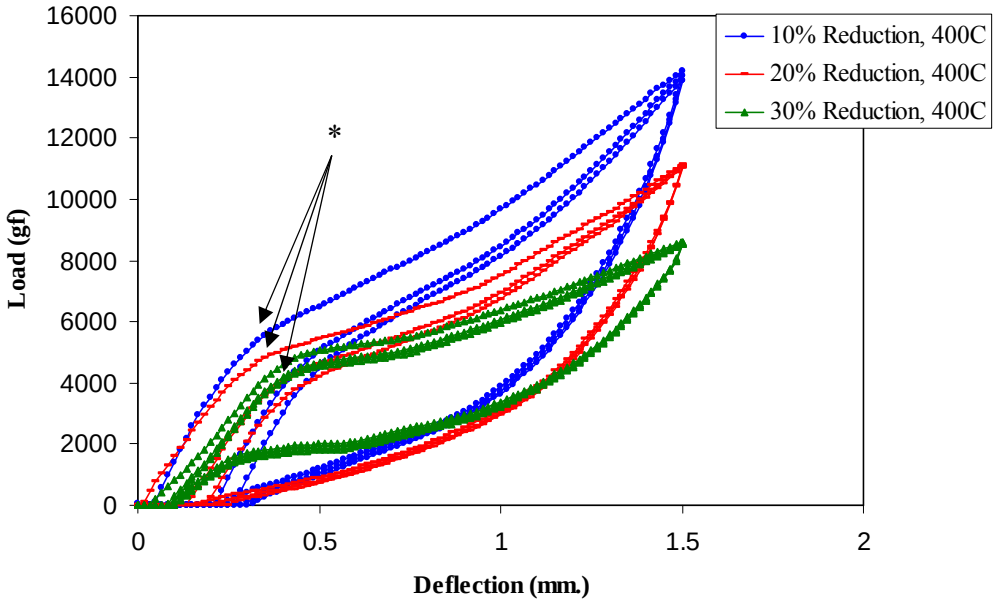


**Figure 50** Load-deflection cycles at 37°C of Ni-Ti-Cu with 10%, 20% and 30% reductions and heat-treated at 400°C

Figure 51 shows the relationship between load and deflection of Ni45.2:Ti49.8:Cu5.0 specimens with 10%, 20% and 30% reductions, followed by heat treatment at 600°C for 1 hour. In order to investigate the cycle effect of each specimen, the first three cycles of data were plotted for each specimen.

Significant differences were clearly seen within three cycles of each percent reduction. At the first cycle, the loading path revealed different critical stress (*), which decreased when the percent reduction increased. Noticeably, the deflection did not completely recover. It appeared that the specimen had permanent deformation. On the second cycle, the point where the loading path occurred did not begin at the deflection of 0 mm. This resulted in a difference of the loading path between the first and second cycles. On the other hand, the unloading curves of each cycle nearly overlapped. On the last cycle, the loading and unloading curves were shown in the same manner of the second cycle. As in the graph, the third cycles of each specimen appeared like superelastic curves.

The stress plateau, determined by the slope of the loading path after the critical stress (*), tended to decrease when the percent reduction increased.

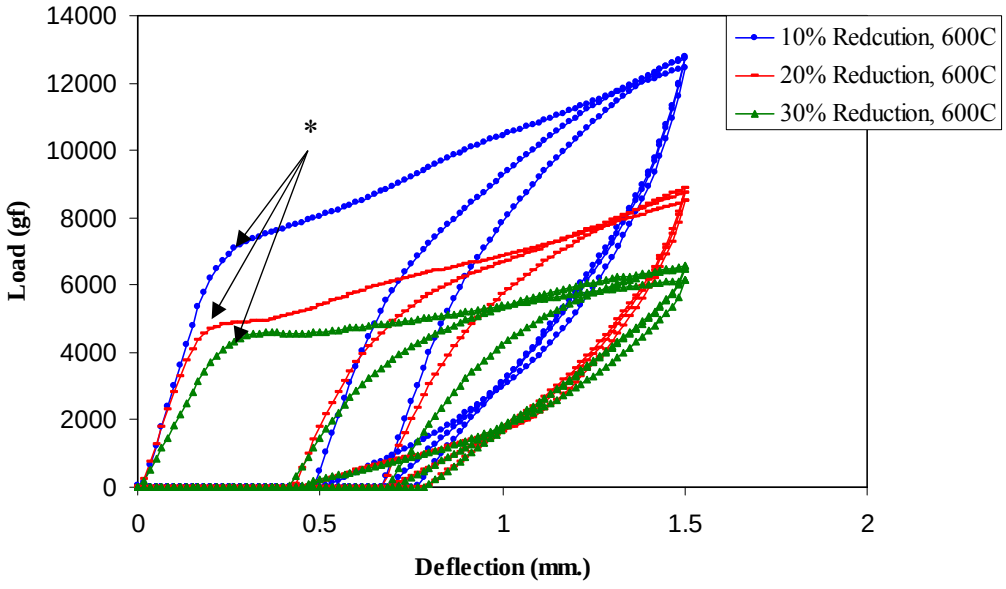


**Figure 51** Load-deflection cycles at 37°C of Ni-Ti-Cu with 10%, 20% and 30% reductions and heat-treated at 600°C

**Tensile test**

From the raw data of the tensile strength test, two columns of load (N) and extension (mm.) were used to create a stress-strain curve of each test specimen. Stress (MPa) was calculated by dividing the load (N) with the cross-sectional area of the reduced section ($mm^2$). Strain was the percentage of extension per original length ($L_0$).

**Table 5** Ultimate tensile strength (MPa) and % elongation of alloys (Average ± SD)

| % reduction / Heat treatment temperature (°C) | NiTi | | NiTiCu | |
|---|---|---|---|---|
| | UTS (Mpa) | % elongation | UTS (Mpa) | % elongation |
| 10/400 | 684.1± 115.77 | 18.19 ± 3.85 | 571.57 ± 2.11 | 9.9 ± 0.51 |
| 10/600 | 563.35 ± 66.52 | 17.54 ± 2.09 | 624.27 ± 36.45 | 13.87 ± 0.9 |
| 20/400 | 809.63 ± 136.84 | 18.55 ± 1.98 | 607.43 ± 70.71 | 11.16 ± 2.15 |
| 20/600 | 731.5 ± 35.75 | 27.76 ± 6.14 | 671.82 ± 40.88 | 19.35 ± 4.7 |
| 30/400 | 740.73 ± 292.23 | 14.47 ± 4.64 | 610.86 ± 20.35 | 10 ± 0.21 |
| 30/600 | 818.76 ± 15.25 | 35.98 ± 0.46 | 682.45 ± 7.98 | 26.27 ± 1.28 |

Figure 52 shows the relationship between the percent reduction, heat treatment temperature and ultimate tensile strength (MPa) of the 50.7Ni:49.3Ti (at%).

Considering the effect of the percent reduction, the ultimate tensile strength of the alloys tended to increase when the percent reduction increased. The only exception was the ultimate tensile strength of the 50.7Ni:49.Ti (at%) with 30% reduction and heat-treated at 400°C, which was lower than that of 20% reduction.

Considering the effect of heat treatment temperature, the ultimate tensile strength of 50.7Ni:49.3Ti (at%) heat-treated at 400°C was over the ultimate tensile strength of this alloy heat-treated at 600°C in all percent reductions except for 30% reduction.

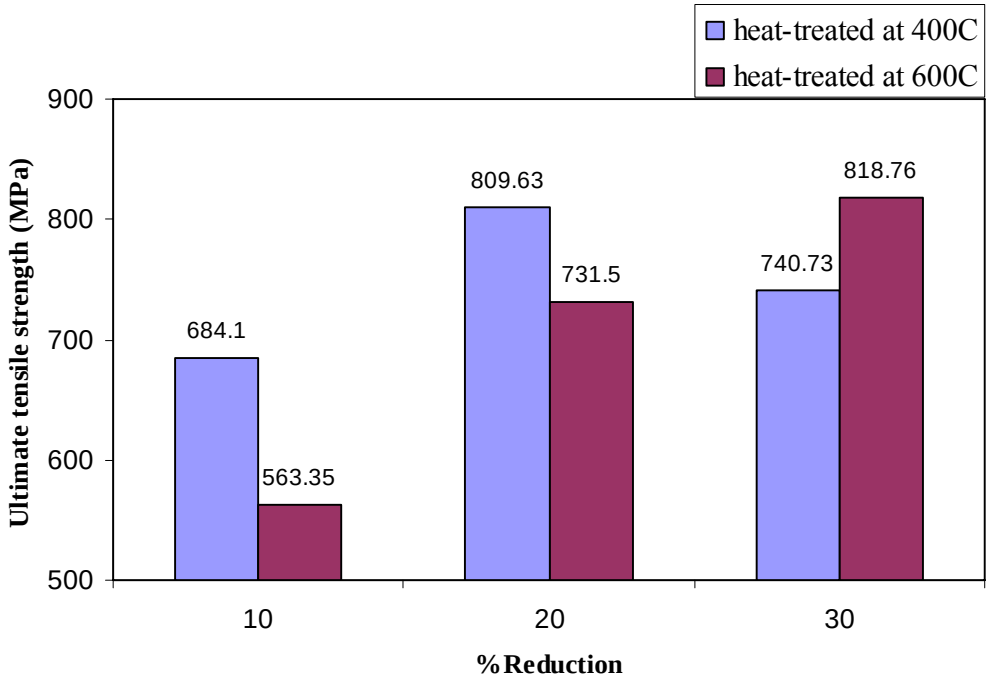


**Figure 52** Ultimate tensile strength (MPa) of Ni50.7:Ti49.3

Figure 53 shows the relationship between the percent reduction, heat treatment temperature and percent elongation of the 50.7Ni:49.3Ti (at%).

Considering the effect of percent reduction, the percent elongation of the alloys hea-treated at 400°C tended to stabilize or decrease when the percent reduction increased. For 600°C heat treatment, the percent elongation increased when the percent reduction increased.

Considering the effect of heat treatment temperature, the percent elongation of 50.7Ni:49.3Ti (at%) heat-treated at 400°C was lower than the percent elongation of this alloy heat-treated at 600°C in all percent reductions except for 10% reduction. At 10% reduction, the percent elongation of this alloy in both heat treatment temperatures (400°C and 600°C) was in the same range.

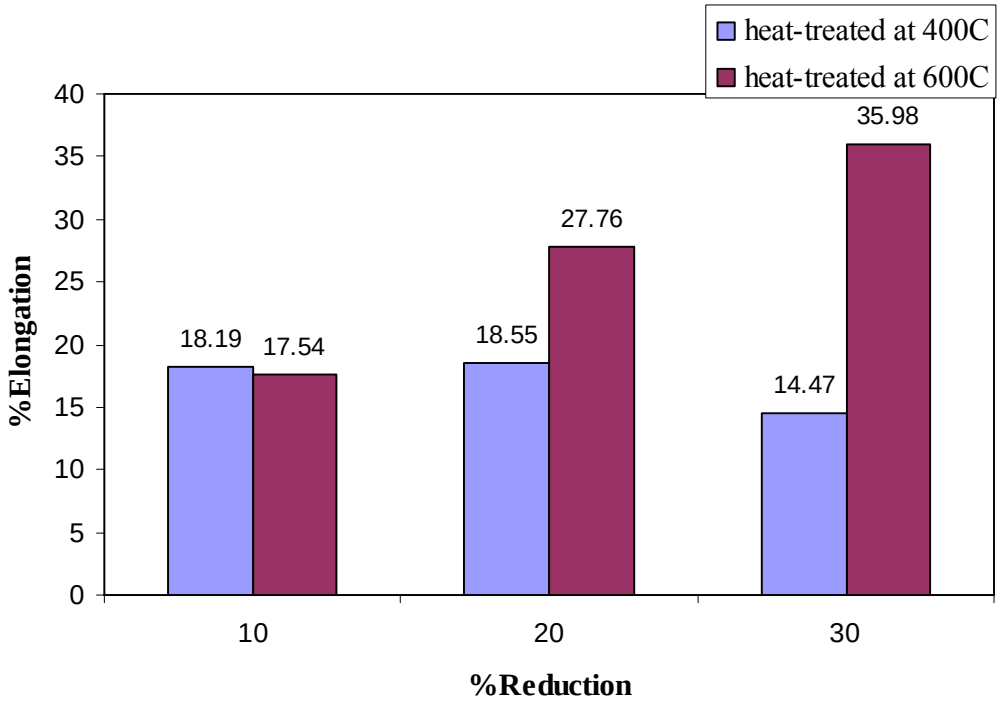


**Figure 53** % elongation of Ni50.7:Ti49.3

Figure 54 shows the relationship between the percent reduction, heat treatment temperature and ultimate tensile strength (MPa) of the 45.2Ni:49.8Ti:5.0Cu (at%).

Considering the effect of percent reduction, the ultimate tensile strength of the alloys tended to increase when the percent reduction increased.

Considering the effect of heat treatment temperature, the ultimate tensile strength of 45.2Ni:49.8Ti:5.0Cu (at%) heat-treated at 400°C was lower than the ultimate tensile strength of this alloy heat-treated at 600°C in all percent reduction.

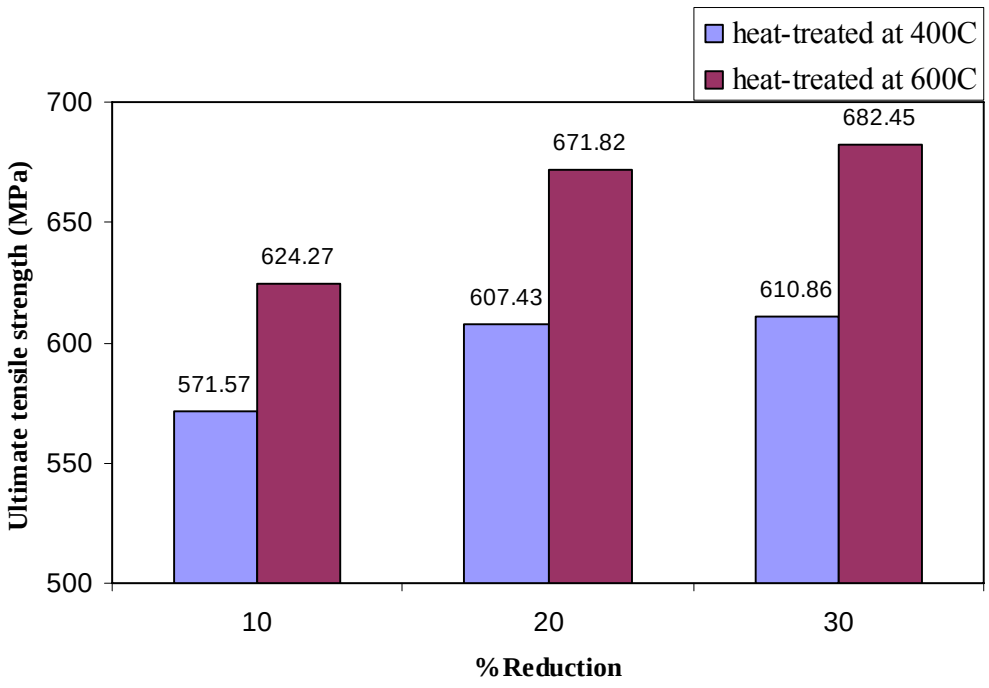


**Figure 54** Ultimate tensile strength (MPa) of Ni45.2:Ti49.8:Cu5.0

Figure 55 shows the relationship between the percent reduction, heat treatment temperature and % elongation of the 45.2Ni:49.8Ti:5.0Cu (at%).

Considering the effect of percent reduction, the percent elongation of the alloys heat- treated at 400°C tended to stabilize or decrease when the percent reduction increased. For 600°C heat treatment, the percent elongation increased when the percent reduction increased.

Considering the effect of heat treatment temperature, the percent elongation of 45.2Ni:49.8Ti:5.0Cu (at%) heat-treated at 400°C was lower than the percent elongation of this alloy heat treated at 600°C in all percent reduction.

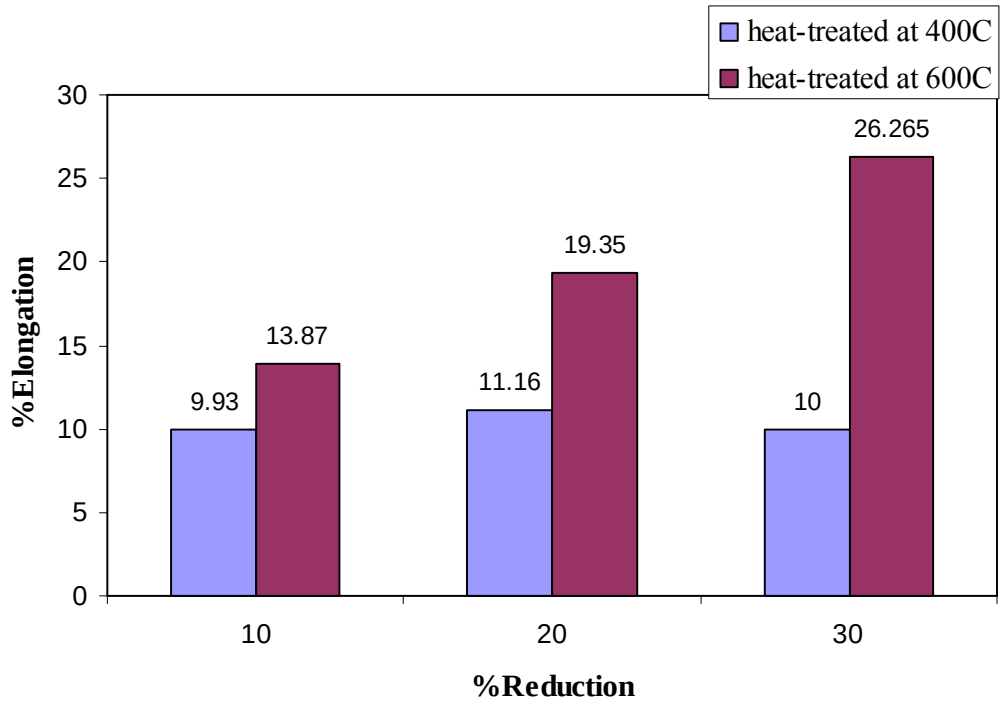


**Figure 55** % Elongation of Ni45.2:Ti49.8:Cu5.0

**Micro-indentation hardnest test (Vickers Haredness Test)**

The micro-indentation hardness was determined in both longitudinal and cross-sectional areas of each alloy specimen. The average Vickers Hardness Numbers were listed in Table 6.

**Table 6** The average Vickers Hardness Numbers (HV) of all alloy specimens from both longitudinal and cross-sectional areas (Average ± SD)

| % reduction / Heat Tx temperature (°C) | NiTi | | NiTiCu | |
|---|---|---|---|---|
| | Longitudinal | Cross-sectional | Longitudinal | Cross-sectional |
| 10/400 | 232.02 ± 9.06 | 234.62 ± 13.60 | 290.07 ± 13.48 | 295.87 ± 11.30 |
| 10/600 | 208.92 ± 4.07 | 203.35 ± 7.70 | 208.66 ± 7.03 | 217.36 ± 12.38 |
| 20/400 | 246.07 ± 4.89 | 249.70 ± 7.96 | 300.83 ± 8.93 | 316.73 ± 19.22 |
| 20/600 | 223.24 ± 6.59 | 210.74 ± 7.92 | 207.51 ± 12.04 | 210.81 ± 6.93 |
| 30/400 | 296.14 ±13.09 | 289.47 ± 8.85 | 336.08 ± 8.33 | 336.87 ± 15.69 |
| 30/600 | 217.43 ± 5.87 | 207.01 ± 6.85 | 215.62 ± 4.13 | 202.58 ± 5.70 |

Figure 56 shows the relationship of the hardness value (Hv) and % reduction of 50.7Ni:49.3Ti (at%) and 45.2Ni:49.8Ti:5.0Cu (at%) in the longitudinal section.

For 50.7Ni:49.3Ti (at%) heat-treated at 400°C, the hardness values increased when the percent reduction increased. At 600°C heat treatment temperature, the hardness value declined and no significant differences was found between the percent reductions.

For 45.2Ni:49.8Ti:5.0Cu (at%) heat-treated at 400°C, the hardness values increased when the percent reduction increased. At 600°C heat treatment temperature, the hardness values extensively decreased and no significant difference between the percent reductions. The 45.2Ni:49.8Ti:5.0Cu (at%) had higher hardness values than the 50.7Ni:49.3Ti (at%) when heat treated at 400°C. On the other hand, at 600°C heat

treatment temperature, the hardness values of both 50.7Ni:49.3Ti (at%) and 45.2Ni:49.8Ti:5.0Cu (at%) were in the same range.

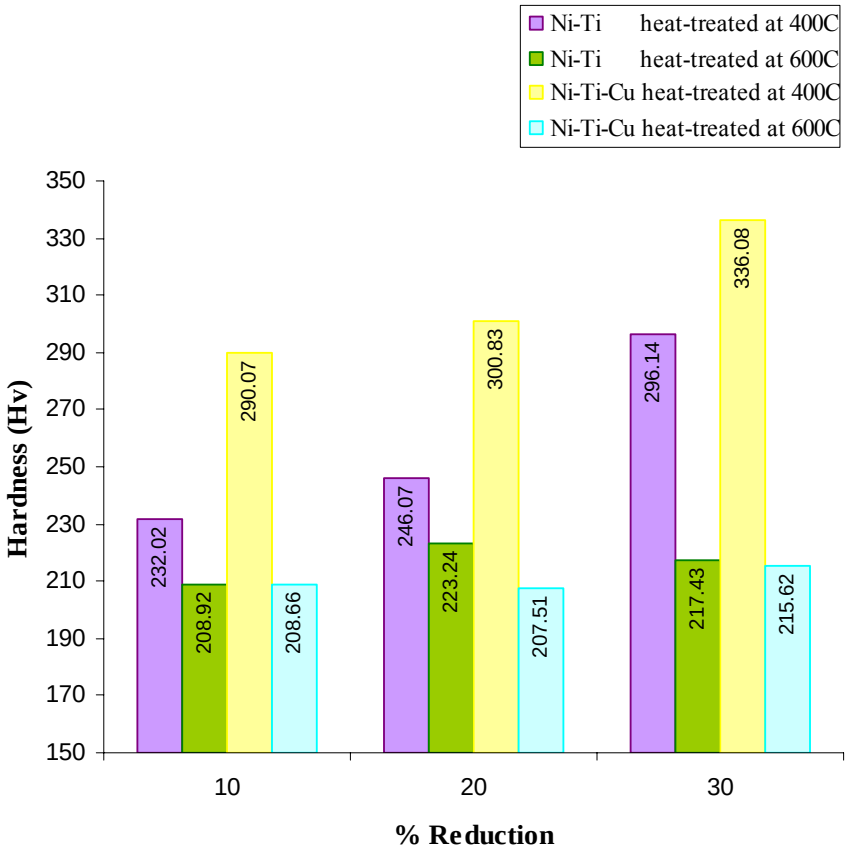


**Figure 56** Hardness values of NiTi alloys in longitudinal section

Figure 57 shows the relationship of the hardness value (Hv) and percent reduction of 50.7Ni:49.3Ti (at%) and 45.2Ni:49.8Ti:5.0Cu (at%) in cross-section.

For 50.7Ni:49.3Ti (at%) heat-treated at 400°C, the hardness values increased when the percent reduction increased. At 600°C heat treatment temperature, the hardness value decreased and there was no significant difference between the percent reductions.

For 45.2Ni:49.8Ti:5.0Cu (at%) heat-treated at 400°C, the hardness values increased when the % reduction increased. At 600°C heat treatment temperature, the hardness values were extensively dropped down and there was no significant difference between the % reductions.

Comparing the two alloys, the 45.2Ni:49.8Ti:5.0Cu (at%) had higher hardness value than the 50.7Ni:49.3Ti (at%) when heat-treated at 400°C. On the other hand, at 600°C heat treatment temperature, the hardness values of both alloys were in the same range.

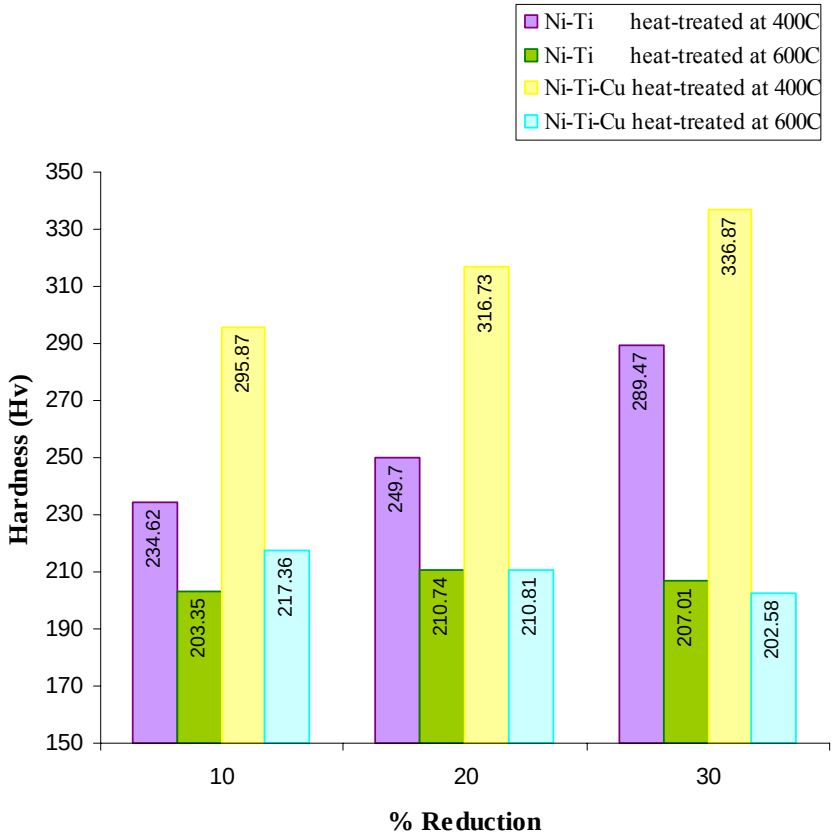


**Figure 57** Hardness values of NiTi alloys in cross section

**Grain Structure**

The grain structure of the specimens was examined under optical microscope using Motic MC 1000 and Motic Image Plus 2.0 ML programmes. For longitudinal section, the grain structures were examined in shape and direction of the grains effected by cool rolling. For cross section, 10 grains of each specimens were randomly chosen for grain size measurement listed in table 7.

**Table 7** The average grain sizes of all alloy specimens. (Average ± SD. in μm.)

| Alloys | %reduction | Heat treatment temperature (°C) | Grain size (μm) |
|---|---|---|---|
| Ni:Ti (50.7:49.3 at%) | 10 | 400 | 70.57 ± 7.89 |
| | | 600 | 74.94 ± 9.22 |
| | 20 | 400 | 61.61 ± 11.74 |
| | | 600 | 77.97 ± 11.74 |
| | 30 | 400 | - |
| | | 600 | - |
| Ni:Ti:Cu (45.2:49.8:5.0 at%) | 10 | 400 | 61.92 ± 9.14 |
| | | 600 | 56.07 ± 6.31 |
| | 20 | 400 | 69.86 ± 9.98 |
| | | 600 | 80.48 ± 7.59 |
| | 30 | 400 | - |
| | | 600 | - |

For longitudinal areas, elongated grains were parallel to the direction of the cold-rolling. The grain sizes of two Ni-Ti alloy systems measured on the cross-sectional area were typically 55-80 μm. No significant difference of the grain sizes was found between the reduction of 10%, 20% and 30%. For the longitudinal area, grains were elongated parallel to the cold-rolling direction and expressed the texture of the alloys. Figure 58-73 shows the microstructure of longitudinal and cross-sectional areas of 50.7Ni:49.3Ti (at%) and 45.2Ni:49.8Ti:5.0Cu (at%) specimens.

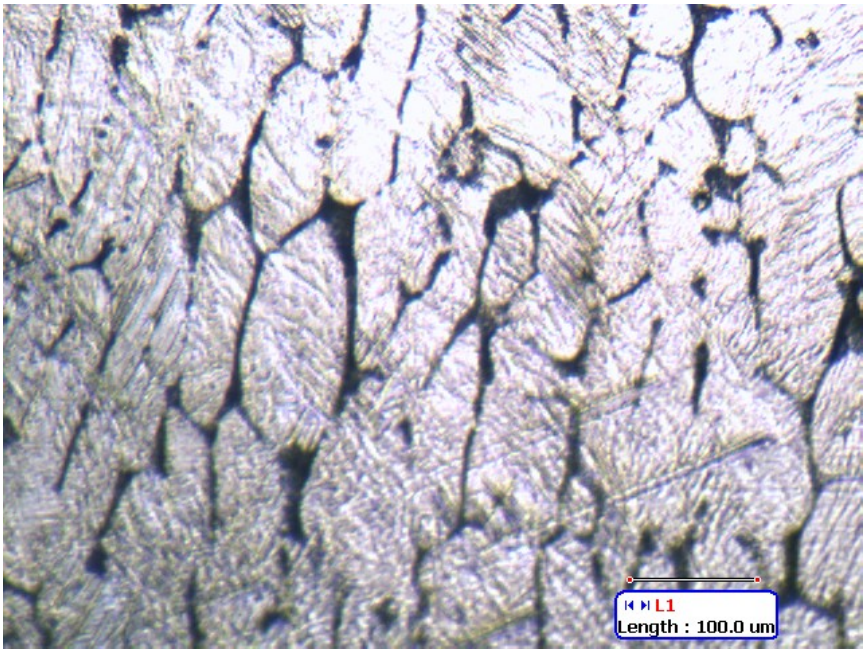


**Figure 58** Optical micrograph showing grain structure of Ni-Ti alloy with 10% reduction by cold-rolling and 400°C heat treatment (Longitudinal area at 20x)

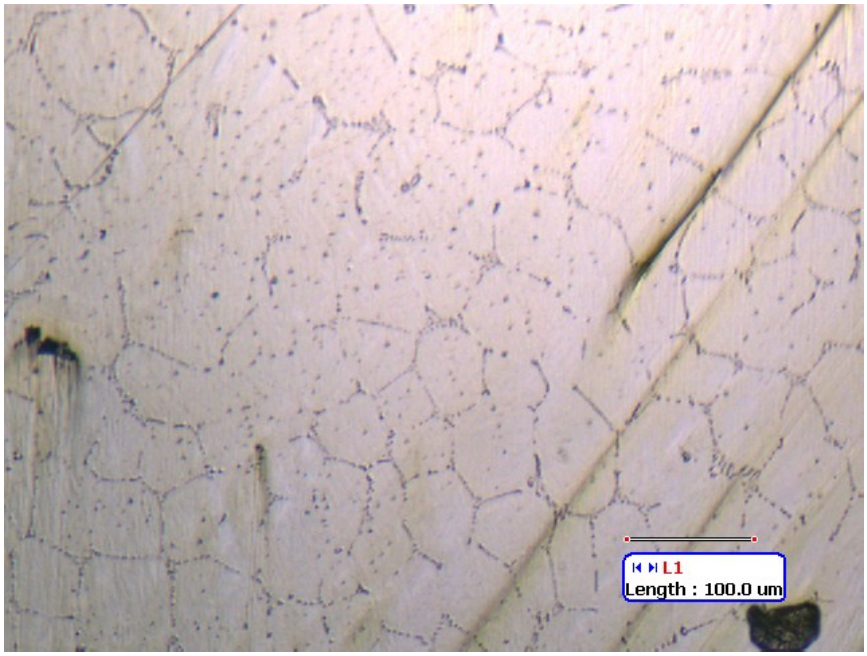


**Figure 59** Optical micrograph showing grain structure of Ni-Ti alloy with 10% reduction by cold-rolling and 400°C heat treatment (Cross-sectional area at 20x)

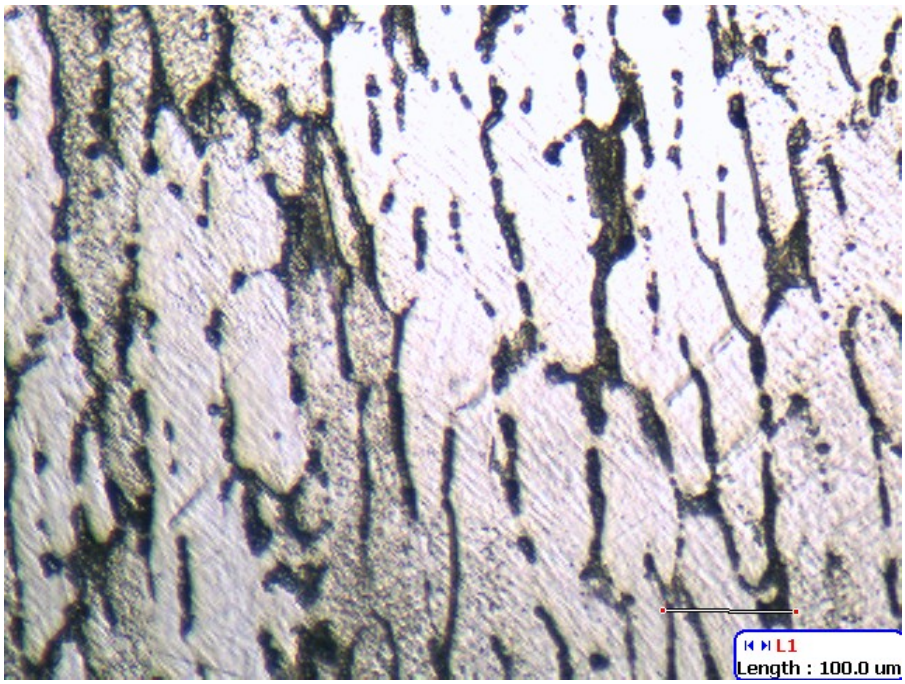


**Figure 60** Optical micrograph showing grain structure of Ni-Ti alloy with 10% reduction by cold-rolling and 600°C heat treatment (Longitudinal area at 20x)

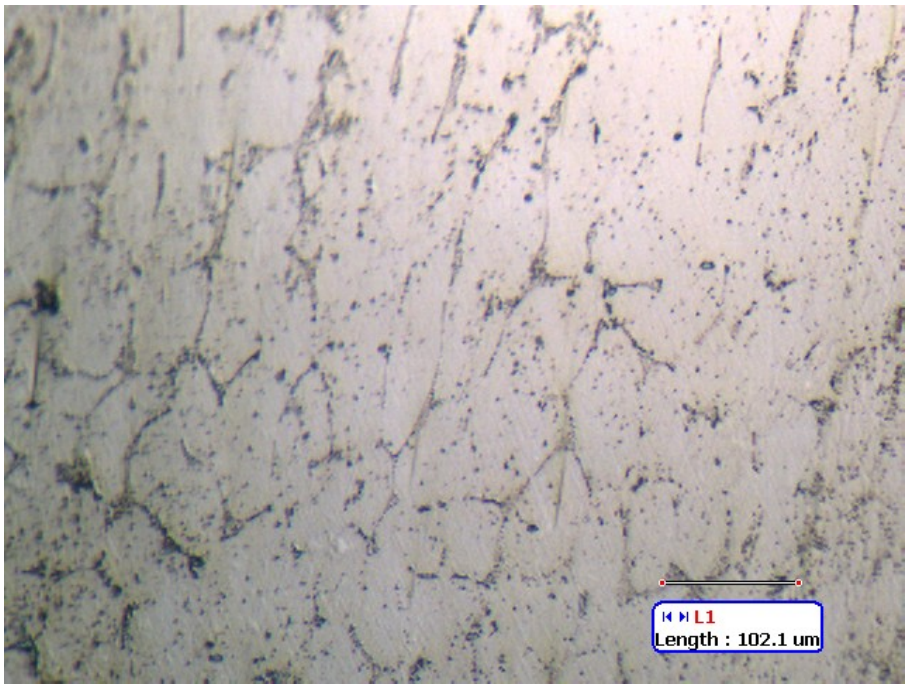


**Figure 61** Optical micrograph showing grain structure of Ni-Ti alloy with 10% reduction by cold-rolling and 600°C heat treatment (Cross-sectional area at 20x)

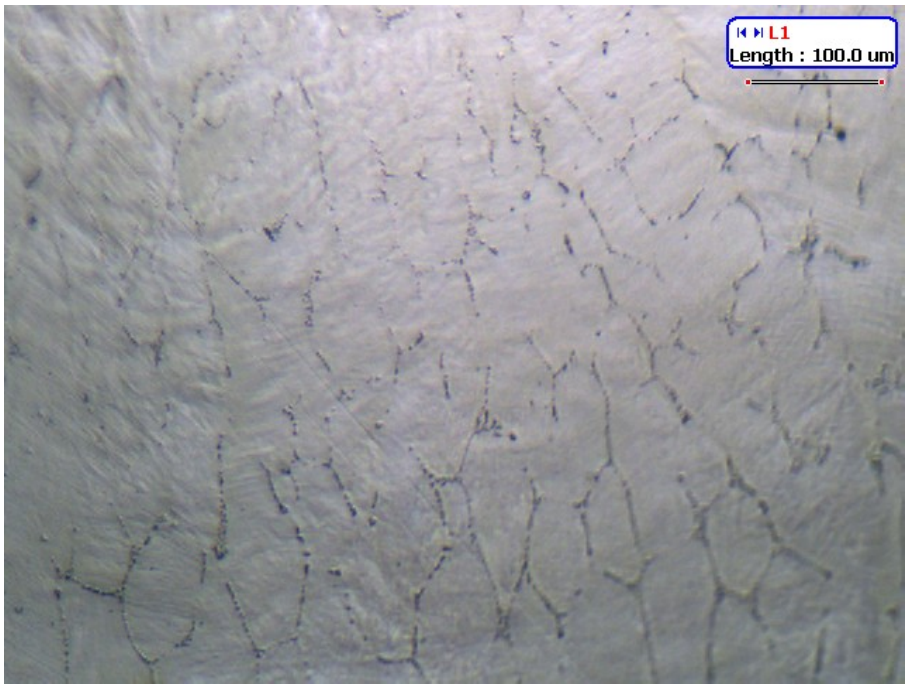


**Figure 62** Optical micrograph showing grain structure of Ni-Ti alloy with 20% reduction by cold-rolling and 400°C heat treatment (Longitudinal area at 20x)

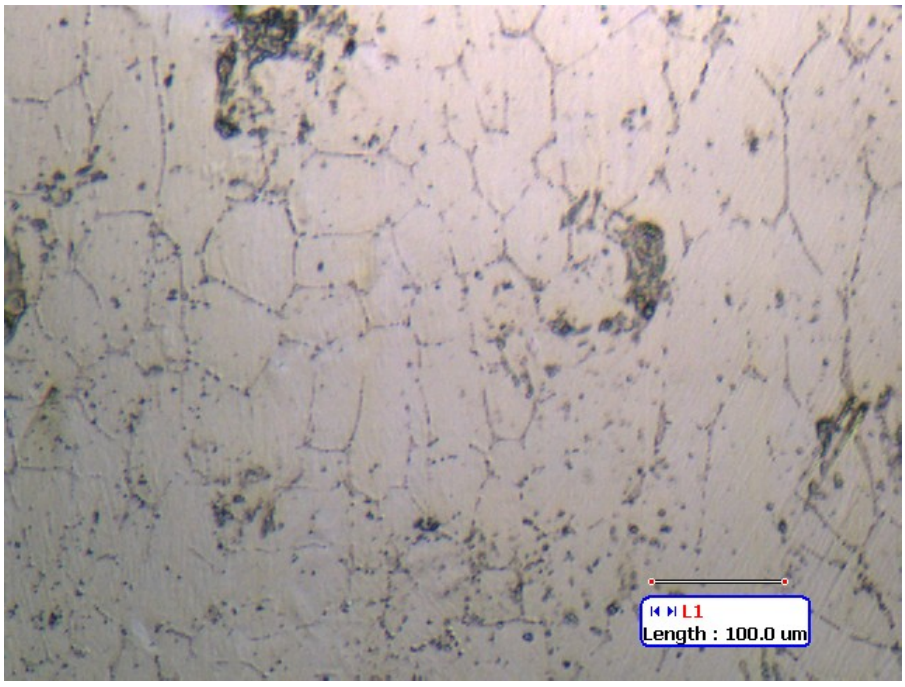


**Figure 63** Optical micrograph showing grain structure of Ni-Ti alloy with 20% reduction by cold-rolling and 400°C heat treatment (Cross-sectional area at 20x)

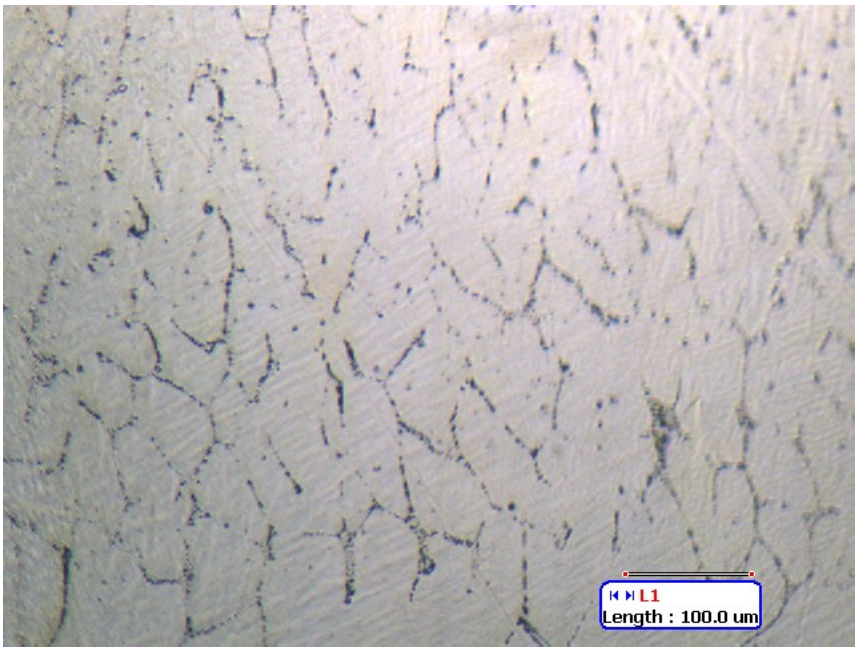


**Figure 64** Optical micrograph showing grain structure of Ni-Ti alloy with 20% reduction by cold-rolling and 600°C heat treatment (Longitudinal area at 20x)

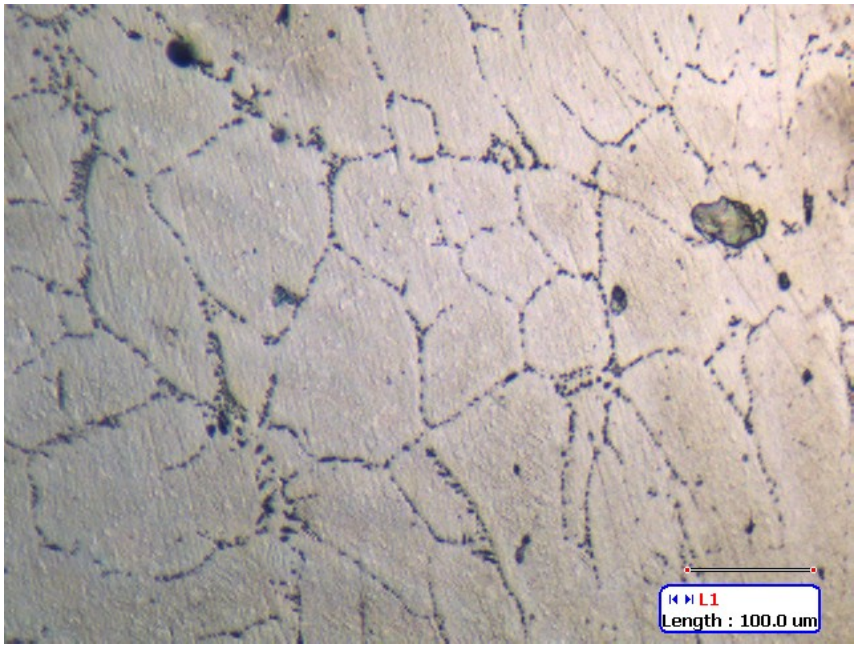


**Figure 65** Optical micrograph showing grain structure of Ni-Ti alloy with 20% reduction by cold-rolling and 600°C heat treatment (Cross-sectional area at 20x)

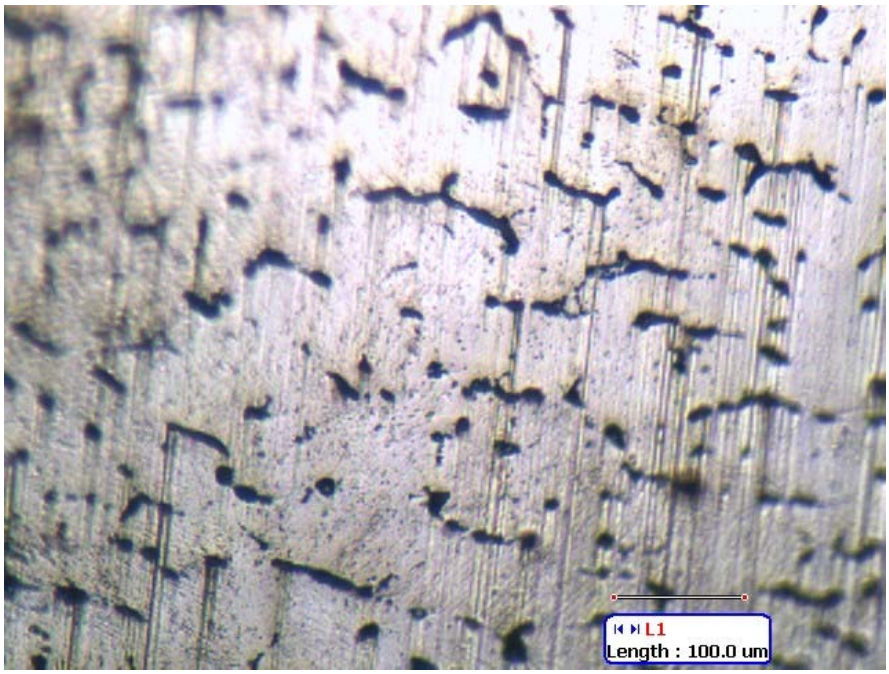


**Figure 66** Optical micrograph showing grain structure of Ni-Ti-Cu alloy with 10% reduction by cold-rolling and 400°C heat treatment (Longitudinal area at 20x)

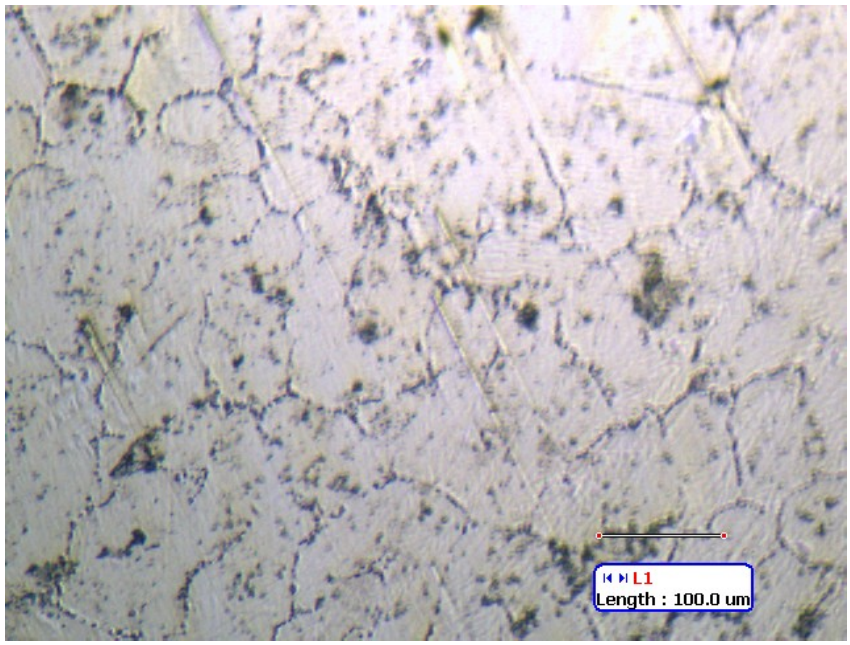


**Figure 67** Optical micrograph showing grain structure of Ni-Ti-Cu alloy with 10% reduction by cold-rolling and 400°C heat treatment (Cross-sectional area at 20x)

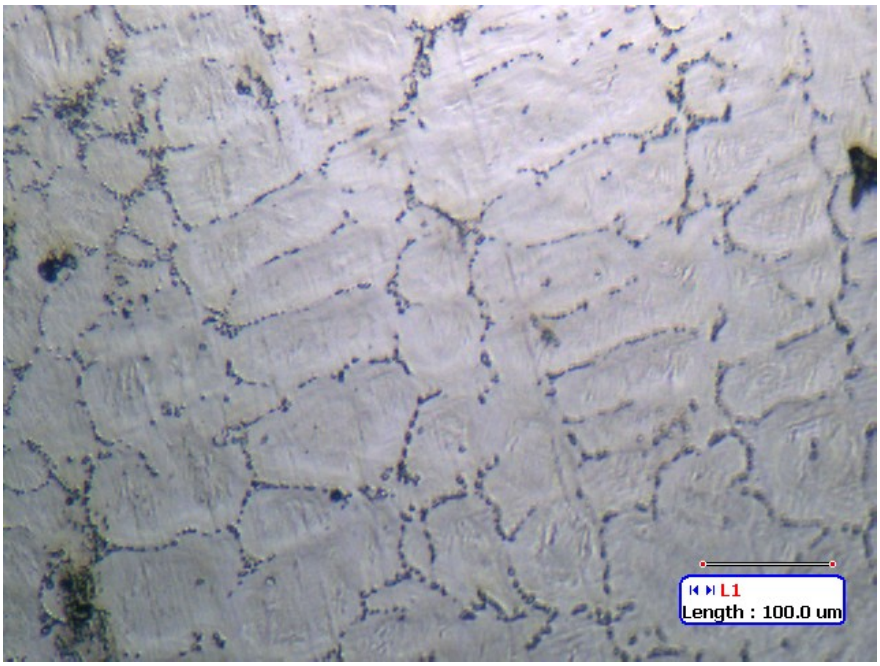


**Figure 68** Optical micrograph showing grain structure of Ni-Ti-Cu alloy with 10% reduction by cold-rolling and 600°C heat treatment (Longitudinal area at 20x)

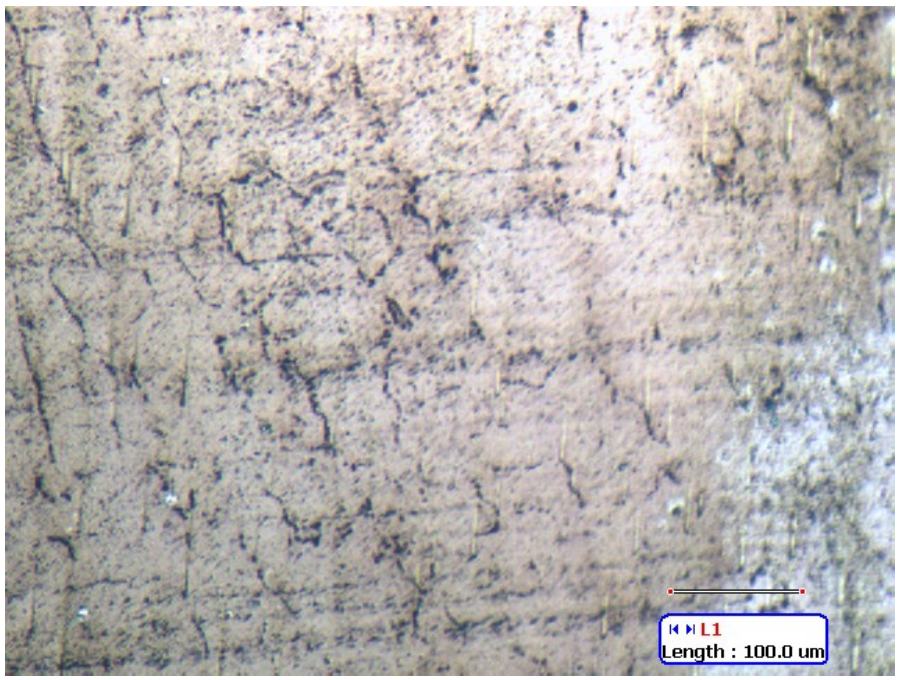


**Figure 69** Optical micrograph showing grain structure of Ni-Ti-Cu alloy with 10% reduction by cold-rolling and 600°C heat treatment (Cross-sectional area at 20x)

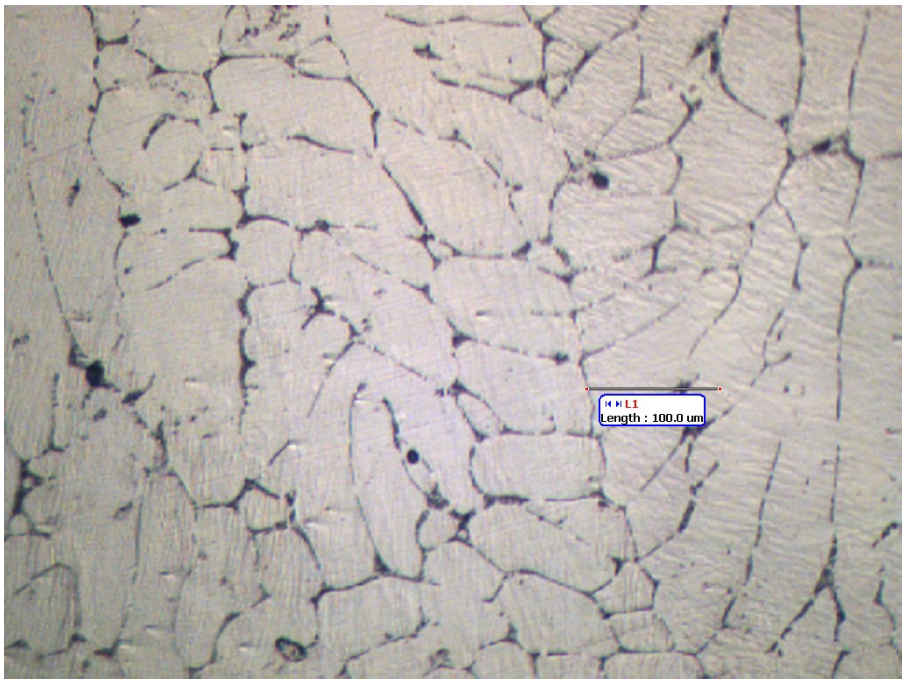


**Figure 70** Optical micrograph showing grain structure of Ni-Ti-Cu alloy with 20% reduction by cold-rolling and 400°C heat treatment (Longitudinal area at 20x)

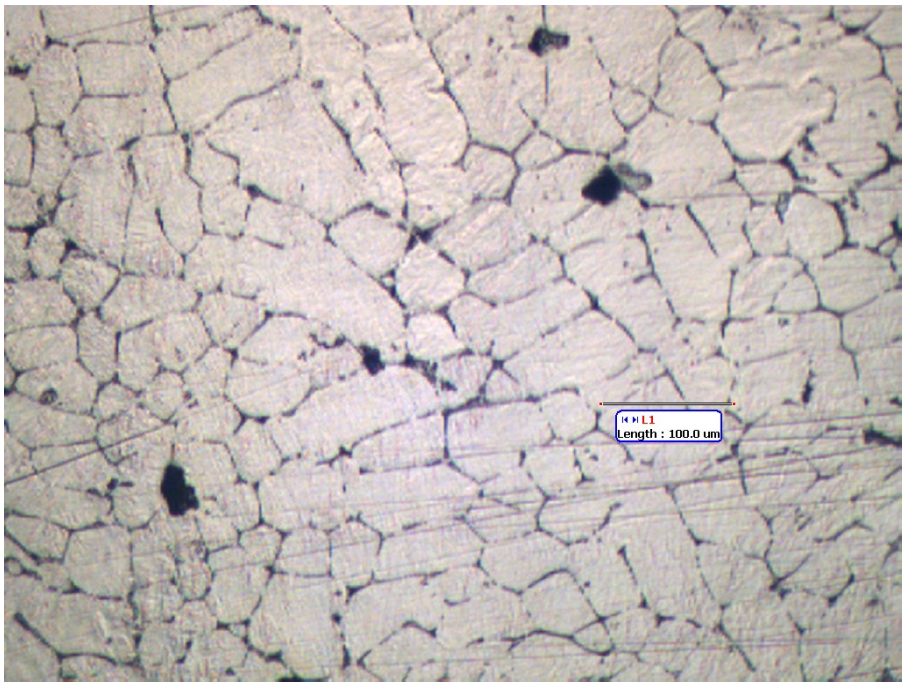


**Figure 71** Optical micrograph showing grain structure of Ni-Ti-Cu alloy with 20% reduction by cold-rolling and 400°C heat treatment (Cross-sectional area at 20x)

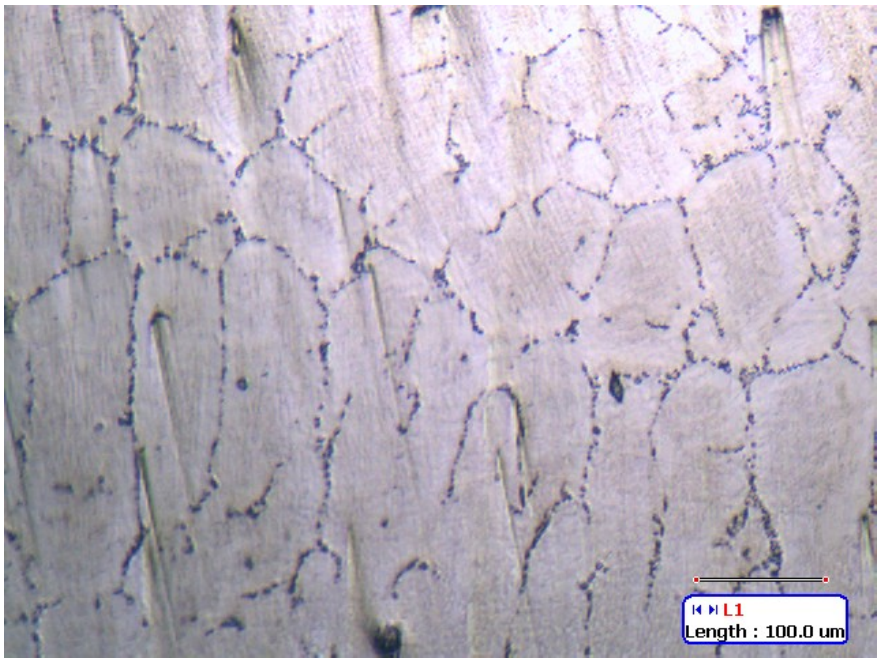


**Figure 72** Optical micrograph showing grain structure of Ni-Ti-Cu alloy with 20% reduction by cold-rolling and 600°C heat treatment (Longitudinal area at 20x)

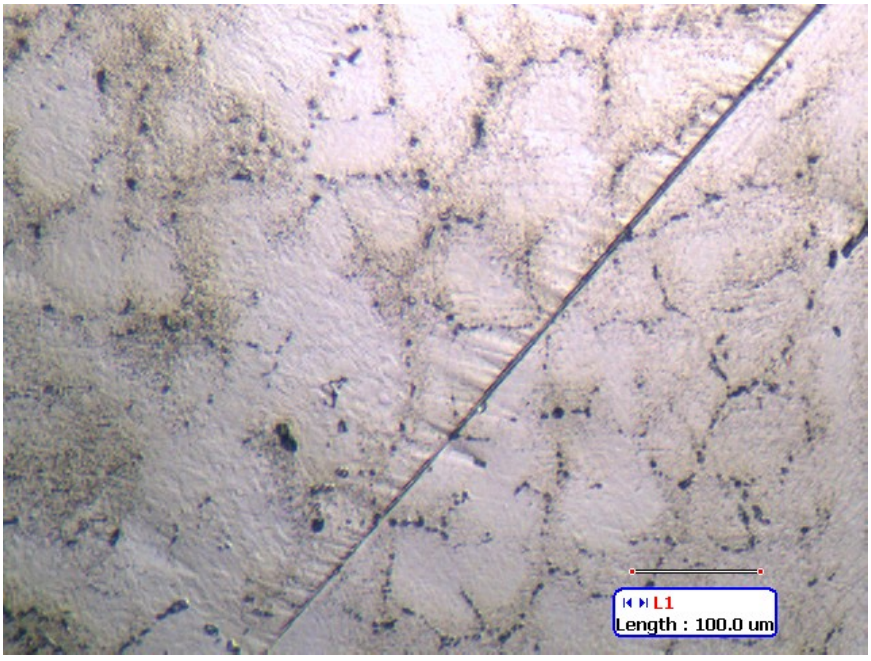


**Figure 73** Optical micrograph showing grain structure of Ni-Ti-Cu alloy with 20% reduction by cold-rolling and 600°C heat treatment (Cross-sectional area at 20x)

**Crystallographic structure**

The diffractogram represented the relationship between the intensities of diffracted x-ray beams and the reflected angles of c-ray beams (2θ) for each phase. The peaks were compared to standard data of The International Center for Diffraction Data (ICDD) of Swartmore, PA, USA in order to identify crystallographic structure of the alloys. The test was conducted at the room temperature (25°C). The results were used to confirm the phase of the specimens in room temperature.

Figure 74 shows the diffractograms of the 50.7Ni:49.3Ti (at%) specimens that received various percent reductions (10%, 20% and 30% reduction) and heat-treated at 400°C. No significant difference of the peak position in all percent reductions were found.

Comparing the diffractogram to the standard data of ICDD, the highest peaks were located at 42.35°2θ, which can be classified as Ni-Ti in 110 preferred orientation of the austenitic NiTi in cubic structure. For the second height of the peak at 39.7° 2θ - 39.8° 2θ, it represents the $Ti_6O$ and $Ti_3O$ in hexagonal structure. At the peak position of 41.39° 2θ – 41.59° 2θ and 45.14° 2θ – 45.41° 2θ, the Ni-Ti in 111 preferred orientation of martensitic NiTi as monoclinic structure was detected.

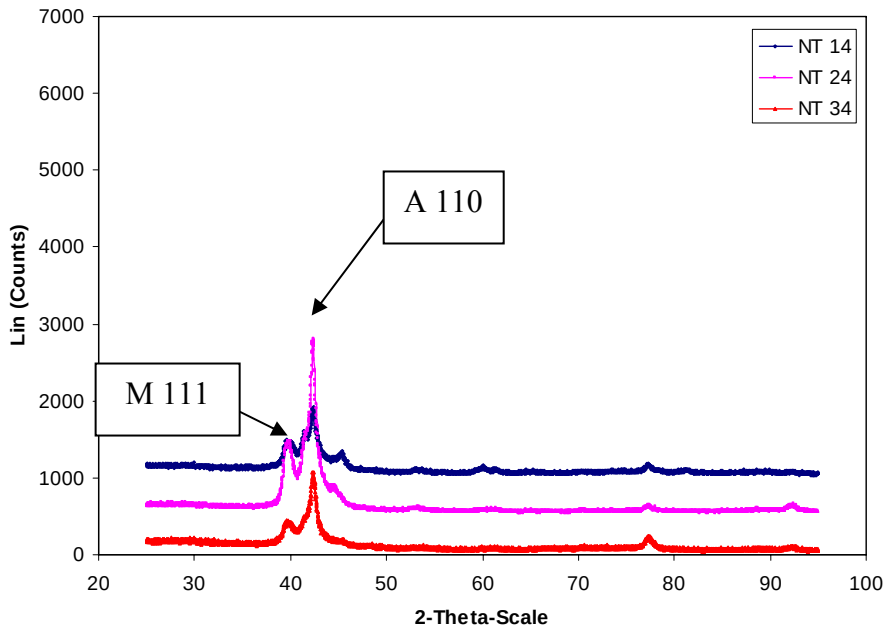


**Figure 74** The diffractograms of 50.7Ni:49.3Ti (at%) with 10, 20 and 30% reductions followed by heat treatment at 400°C for 1 hour

Figure 75 showed the diffractograms of the 50.7Ni:49.3Ti (at%) specimens received various percent reductions (10%, 20% and 30% reductions) and heat-treated at 600°C. No significant difference of the peak position in all % reduction.

Comparing the diffractogram with the standard data of ICDD, the highest peaks were located at 41.26° 2θ – 41.35° 2θ which can be classified as NiTi in monoclinic structure (Martensite in 111 reflecting plane). The other peaks, they represented the 020, 022, 021 and 101 reflecting planes of the martensitic NiTi in monoclinic structure.

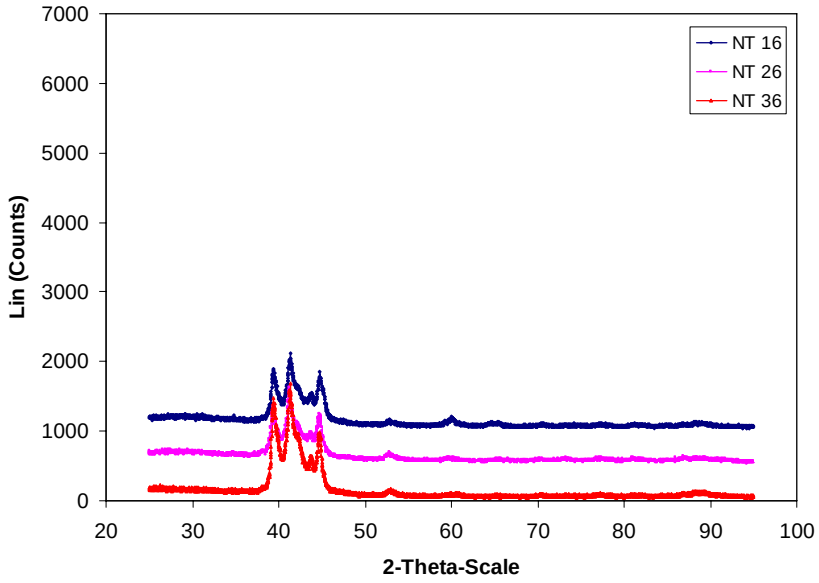


**Figure 75** The diffractograms of 50.7Ni:49.3Ti (at%) with 10%, 20% and 30% reductions followed by heat treatment at 600°C for 1 hour

Figure 76 shows the diffractograms of the 45.2Ni:49.8Ti:Cu5.0 (at%) specimens that received various percent reductions (10%, 20% and 30% reductions) and heat-treated at 400°C. No significant difference of the peak position in all percent reductions.

Comparing the diffractogram with the standard data of ICDD, the highest peaks located at 42.23° 2θ - 42.28° 2θ, which can be classified as Ni-Ti in cubic structure (Austenite). For the peak at 77.60° 2θ - 77.84° 2θ, it represents the Ni-Ti in

cubic structure (Austenite). At the peak position of 39.62° 2θ – 39.80° 2θ, the $CuTi_2$ and $Cuti_3$ in tetragonal structure is detected.

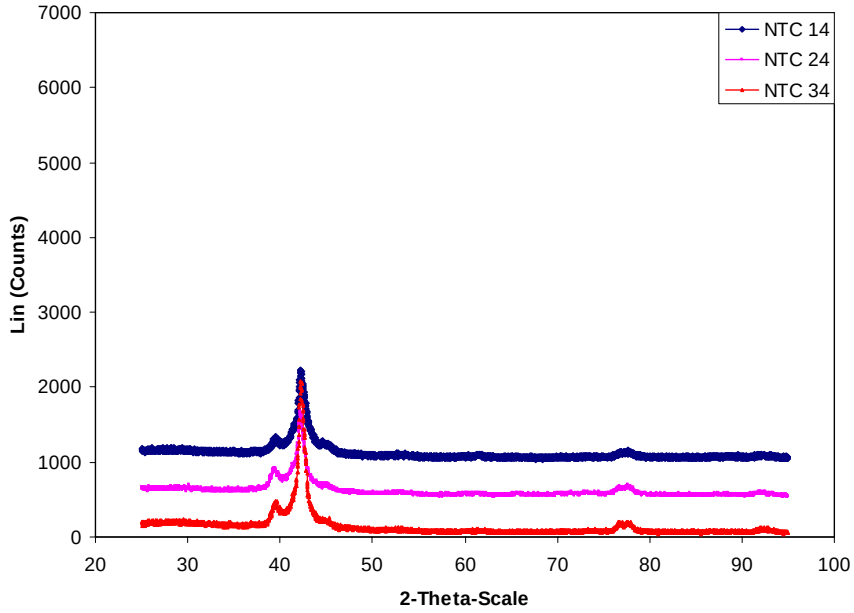


**Figure 76** The diffractogram of 45.2Ni:49.8Ti:Cu5.0 (at%) with 10%, 20% and 30% reductions followed by heat treatment at 400°C for 1 hour

Figure 77 shows the diffractograms of the 45.2Ni:49.8Ti:Cu5.0 (at%) specimens received various percent reductions (10%, 20% and 30 % reduction) and heat-treated at 600°C. no significant difference of the peak position in all % reductions.

Comparing the diffractogram with the standard data of ICDD, the highest peaks were located at 42.40° 2θ which can be classified as Ni-Ti in cubic structure (Austenite). For the peak at 77.53° 2θ, it also represented the Ni-Ti in cubic structure (Austenite). At the peak position of 39.60° 2θ – 39.70° 2θ, the $Ti_6O$ and $Ti_3O$in hexagonal structure was detected.

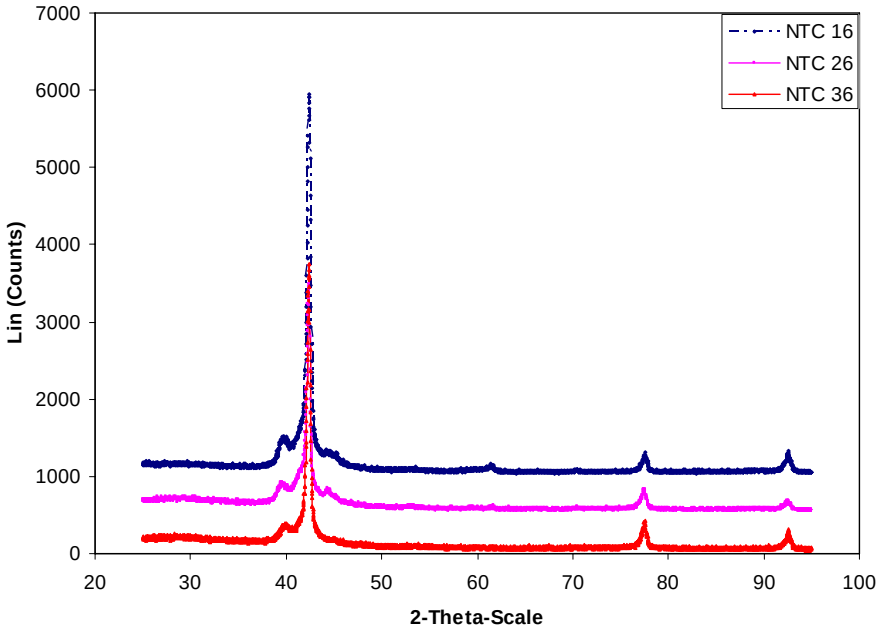


**Figure 77** The diffractogram of 45.2Ni:49.8Ti:Cu5.0 (at%) with 10%, 20% and 30% reductions followed by heat treatment at 600°C for 1 hour

# CHAPTER VI
# DISCUSSION

This study was undertaken to assess the transformation behavior and mechanical properties of two systems of nickel-titanium alloys undergoing different degrees of work-hardening by cold-rolling and followed by different degrees of heat treatment temperature, 400°C and 600°C, respectively.

Factors affecting the transformation temperatures of the Ni-Ti alloys were the chemical composition [10, 2, 39, 49, 60, 66], working history and heat treatment (thermo-mechanical treatment) [10, 53].

For the aspect of the chemical composition, Ni-Ti alloys are extremely sensitive to the precise Ni-to-Ti ratio. Hahn et al reported that at equiatomic composition, if the nickel contents are increased by 1%, the transformation temperature is decreased by 100°C [60]. Ni contents exceeding 50.5 at% are sensitive to heat treatment at temperatures between 300°C and 500°C due to the resulting precipitation of $Ti_3Ni_4$. On the other hand, Ni contents between 50.0-50.5 at% are insensitive to heat treatment because no precipitation of the $Ti_3Ni_4$ occurs in these alloys. However, thermomechanical treatments (annealing at a temperature below 500°C after cold-working) affect their properties greatly, considerably.

Ternary alloying additions affect the transformation temperatures, and thus shape recovery temperatures of Ti-Ni alloys. Copper addition reduces the transformation hysteresis related to the ease of interface movement during the transformation. Moreover, Cu addition is effective for avoiding aging effects: it prevents $Ti_3Ni_4$ precipitation and thus it is effective for avoiding Ms temperature change due to differences in cooling speed. Moreover, Cu addition can also reduce the composition sensitivity of Ms [2, 10, 50, 52].

For the aspect of working history, work-hardening such as cold-rolling increases the dislocation density. Cold work has been reported to decrease Af and Ms. In addition, the cold-rolling method also has a substantial impact on the critical stress

for slip in NiTi alloy [67]. Kurita et al [53], reported that the temperature range of the transformation of cold-worked NiTi alloys was expanded and the DSC peak was small.

For the aspect of heat treatment, annealing in the thermo-mechanical treatment has to be done at an appropriate temperature below the recrystallization temperature for the high dislocation-density introduced by cold-working to be maintained [10].

**Chemical composition**

The chemical composition of each ingot was determined by an X-ray Energy-Dispersive Spectroscope installed in a Scanning Electron Microscope (SEM-EDS: JSM-5410LV JEOL LTD). The result showed that the chemical composition of ingots were slightly different from the nominal composition. The alloy contained less Ni but more Ti and Cu content than nominal composition (Figures 30-32). The cause may result from the technique of alloy fabrication. In the process of melting by an electrolytic arc furnace in argon atmosphere, some amount of Ni may be spattered out of the crucible by the excessive power of the electrode. The second reason was that the heat generated from the electrode may exceed and cause the evaporation of some element. Thus, the transformation temperature range may become higher than expectation because of the reduction of the Ni content.

The shape memory properties of NiTi can be modified by adding ternary elements. For example, a small amount of Co, Fe or Cr (1-3 at%) can depress the martensitic transformation temperature such that the shape memory effect occurs well below ambient. Cu addition can reduce the sensitivity of Ni content dependent on transformation behavior. Miyazaki et al [50] reported that Cu-content can increase fatigue life of drawn Ti-Ni wires because stress hysteresis and transformation strain decrease with increasing Cu-content. Cu has been shown to dissolve in the B2 (austenite) phase in a concentration up to 30 at%. However, NiTi-Cu solid solutions containing more than 10 at% are characterized by poor formability so that alloys of technical interest usually contain Cu in the range from 5 to 10 at% [10,52]. For this reason, Cu addition in this study was 5 at%.

**Transformation temperature range**

For 49.3Ti:50.7Ni (at%) with 10, 20 and 30% reductions followed by 400°C heat treatment for 1 hour (Figure 33), the more the percent reduction, the lower and shorter the transformation temperature range of both heating and cooling paths. This signified that percent reduction has an impact on phase transformation. It can be explained that transformation was suppressed by internal stress due to cold work. In other words, the internal structure of the work-hardened material was composed of multiple dislocations hindering the phase transformation. This result was similar to the study of Kurita et al. [53], which reported that cold-worked Ni-Ti alloys had an expanded transformation temperature range and the peak height was small. The broadening of the peak was enhanced by increasing the cold-working reduction percent.

Actually, we intended to make a superelastic NiTi alloy which has a transitional temperature range below the oral temperature. This can be achieved by increasing Ni content to over 50 at%. Thus, the Ni-Ti alloy used in this study was prepared from the nominal composition of Ni 50.7 at% and Ti 49.3 at%. The chemical composition of each ingot determined by X-ray Energy-Dispersive Spectroscope installed in a Scanning Electron Microscope (SEM-EDS: JSM-5410LV JEOL LTD) showed that there was less Ni content than nominal composition, shown in Figure 30. Thus, the transformation temperature range may become higher than expectation. The deviation of the nominal composition may result from the technique of alloy fabrication. In the process of melting the composition by an electrolytic arc furnace in argon atmosphere, some amount of Ni may spatter out of the crucible.

For 49.3Ti:50.7Ni (at%) with 10%, 20% and 30% reductions followed by 600°C heat treatment (Figure 34), the peaks of transformation showed no difference between different degrees of reductions, because 600°C is higher than the recrystalization temperature (Conventional recrystalization temperature of Ni-Ti alloy was set around 526°C). Thus the dislocation introduced into the microstructure by cold work was eliminated. Besides, transformation temperature ranges in all % reductions of 600°C were higher than that of 400°C, approximately 20°C-30°C. This phenomenon confirmed that the dislocation obstructing the phase transformation disappeared. This result conformed to the study of Saburi et al. [10] which reported

that the recrystalization temperature of the near-equiatomic Ni-Ti alloys lies between 500°C to 600c. Annealing the cold-rolled specimens at 600°C represented partial strain recovery on load-deflection curves. This indicated that annealing in the thermomechanical treatment has to be done at an appropriate temperature below the recrystallization temperature for the high dislocation-density introduced by cold-working to be maintained. In addition, shifted transformation temperature range was over the oral temperature more than that of Ni-Ti alloy heat-treated at 400°C. Thus, this alloy was not superelastic in oral temperature. In clinical use, this alloy is not practical because of martensitic stabilization.

For 45.2Ni:49.8Ti:5.0Cu (at%) with 10%, 20% and 30% reductions followed by 400°C heat treatment, the R-phase transformation or the intermediate phase occurred. The R-phase, a rhombohedral phase between the martensite and austenite can occurr in nickel-rich Ti-Ni alloys aged at an appropriate temperature and in ternary Ti-Ni-Fe and Ti-Ni-Al alloys. [10, 12] Kurita et al, 2004 [53] studied the transformation behavior of the equiatomic rolled NiTi alloy using a differential scanning calorimeter (DSC) in order to reveal the effects of inner stress and defects. They found the intermediate phase appeared after cold-working and subsequent annealing at a temperature of 500°C. Furthermore, the thermal hysteresis of the phase transformation between high and intermediate phases was narrow. Iijima et al. [65] reported that the interposition of an R-phase could be detected in Ni-Ti-Cu alloy and the martensitic transformation temperatures were lower than that of the Ni-Ti alloy. The R-phase is thought to be due to the introduction of dislocation and precipitations and also provided very small stress hysteresis. On the other hand, another possible phase occurring in this transformation was orthorhombic phase (O). This phase occurred by Cu addition or it was a unique phase of NiTiCu. The O-phase presents a narrow transformation temperature hysteresis and low recovery strain on load-deflection curve.

For 45.2Ni:49.8Ti:5.0Cu (at%) specimens with 10%, 20% and 30% reductions followed by 600°C heat treatment, the internal stress induced from cold rolling was diminished by recrystalization at the 600°C heat treatment. Thus, R-phase disappeared and the martensitic transformation was shifted to the higher temperature. Interestingly, the $A_f$ of this specimen set between 26°C-30°C, which was still lower

than the oral temperature (37°C). Therefore, the superelasticity should occur at the oral temperature. On the other hand, clinical use was not a stress-free condition. In applying stress to the alloys, the transformation temperature range had a tendency to shift higher according to **the Clausius-Clapeyron model** [65], which gives the relationships of shape memory and superelastic behavior to stress and temperature. From this theory, the transformation temperature ranges especially Af may shifted over the oral temperature and caused the reverse transformation disappear or partially occur. Thus, transformation temperature range especially $A_f$ should be set lower than this range.

**Mechanical properties**

**Three-point bending test**

For the 50.7Ni:49.3Ti (at%) with 10% and 20% reductions followed by heat treatment at 400°C for 1 hour (Figure 49), the load-deflection curves represented an incomplete reverse transformation more than that of 30% reduction. This signified that the stress-induced martensite was stabilized and induced the transformation temperature range to shift higher by stress applied from the three-point bending process. Thus, the reverse transformation could not occur at the oral temperature. When the percent reduction was increased to 30%, the recovery stress could be noticed on the unloading curve. Moreover, the load-deflection curve showed greater superelastic property than that of 10% and 20% reductions. This phenomenon can be described in that increasing the percent reduction or the densely dislocation has an impact on stabilizing the transformation temperature range not to shift higher from stress-induced martensite. In summary, the load-deflection curve of 30% reduction showed complete superelasticity.

For 50.7Ni:49.3Ti with 10%, 20% and 30% reductions followed by heat treatment at 600°C for 1 hour (Figure 50), load-deflection curves indicated that these alloys were martensite and became reoriented martensite after loading at the oral temperature. This phenomenon conformed to the DSC data, which showed that the transformation temperature ranges in all percent reduction of Ni-Ti specimens heat-treated at 600°C were higher than that of Ni-Ti specimens heat-treated at 400°C and also over the oral temperature. Thus, the superelastic curves could not be obtained in

this alloy. The recovery cannot be detected during unloading curves. Instead, the recovery cannot be detected during unloading surves. recover after the specimen is heat-treated over the $A_f$ temperature. Therefore, this alloy presented the shape memory effect.

For the 45.2Ni:49.8Ti:5.0Cu (at%) specimen with 10%, 20% and 30% reductions, followed by heat treatment at 400°C for 1 hour (Figure 51), the load-deflection curves showed the superelastic curves and the stress hysteresis was smaller than that of Ni-Ti alloys. This result corresponded with thermogram of DSC, which presented the R-phase or O-phase transformation near the oral temperature. Thus, this alloy can present the property of superelasticity at the oral temperature. This can result from Cu addition which can reduce the stress hysteresis in superelastic curve.[10,52]

For the 45.2Ni:49.8Ti:5.0Cu (at%) specimen with 10%, 20% and 30% reductions, followed by heat treatment at 600°C for 1 hour (Figure 52), the load-deflection curves showed incomplete superelastic curves. Compared with the DSC, transformation temperature range of this alloy was below the oral temperature range, so that this alloy should present complete superelasticity in the oral temperature**.** Interestingly, the transformation temperature range especially Af was nearly at the oral temperature (26°C -30°C). The applied stress from the three-point bending test may induce the transformation temperature to shift over the oral temperature. Thus, the superelasticity cannot be obtained completely as in the result of three-point bending test.

**Tensile strength test**

Generally, the ultimate tensile strength increased when the percent reduction increasing. In contrast, the % elongation decreased with increasing the percent reduction.

However, the heat treatment temperature also had an influence on these properties. At 600°C, recrystalization was induced so that the dislocation from the work hardening was eliminated. Thus, the alloys are free from internal stress and should result in homogeneous ultimate tensile strength and percent elongation. This phenomenon did not conform to the result found in both 50.7Ni:49.3Ti (at%) and 45.2Ni:49.8T0Cu (at%) alloys heat treated at 600°C. From Figures 53-54, at the

600°C heat treatment temperature, the ultimate tensile strength and percent elongation of both alloys increased when the percent reduction increased. This result can be explained by the fact that the texture of the cold worked alloy has an important role on the mechanical properties [68-70]. In addition, alloy heat-treated at 600°C should be elongated better than that of alloy heat-treated at 400°C because the dislocation from cold-working was eliminated. Thus, slip transformation can occur resulting in an increase of percent elongation.

At the oral temperature, the alloy characterized as martensite should be elongated better than the alloy characterized as austenite, because the martensitic structure can be reoriented. Moreover, the martensitic phase had low stiffness. This fact conformed to the result of percent elongation between the 50.7Ni:49.3Ti (at%) alloy heat-treated at 400°C and 600°C.

Unusual results included the ultimate tensile strength of the 50.7Ni:49.3Ti (at%) with 30% reduction and heat-treated at 400°C, which decreased lower the ultimate tensile strength of this alloy with 20% reduction and the ultimate tensile strength of the 50.7Ni:49.3Ti (at%) heat treated at 400°C, which was lower than that of the 600°C can be explained by the fact that the error of the data was caused by inhomogeneous dimension of the test specimen. The stress concentration will accumulate in the weak point of the specimens causing fracture before the expected point. Thus, the received data did not represent the true properties of the alloy.

**Micro-hardness test**

The hardness value should be in accordance with ultimate tensile strength. The hardness value increased when the percent reduction increased. Even though, the heat treatment temperature at 600°C can cause recrystalization and eliminate the influence of work hardening. Thus, the hardness value of the alloy heat-treated at 600°C should be in the same range.

Considering 400°C heat treatment temperature, 50.7Ni:49.3Ti (at%) specimens had lower hardness values than 45.2Ni:49.8Ti5.0Cu (at%) specimens. On the contrary, the ultimate tensile strength of the 50.7Ni:49.3Ti (at%) specimens were higher than 45.2Ni:49.8Ti5.0Cu (at%) specimens.

The Vickers Hardness Tester can provide information about the relative proportions of the martensitic and austenitic phases. The austenitic phase has higher hardness than the martensitic phase [6].

**Grain structure**

For the longitudinal section, the grains were elongated parallel to the cold rolling direction and expressed the texture of the alloy. Saburi et al [10], reported that anisotropy of a Ti-50.8Ni (at%) alloy was developed by rolling process. If a suitable texture can be developed, the shape memory capacity will be improved.

For the cross-sectional areas, the grain sizes of two Ni-Ti alloy systems had no significant difference between 10%, 20% and 30% reduction. The average grain size was typically 50-80 μm, considered relatively large. In order to improve the superelasticity, a smaller grain size was preferred. Kurita et al [10], reported that the reduction of grain size was very effective for improving the pseudoelasticity.

**Crystallographic structure**

The intensity ratio of diffraction peaks obtained in this study agreed with the power diffraction data of ICDD (International Center for Diffraction Data, Swarthmore, PA, USA).

For the 50.7Ni:49.3Ti (at%) specimens heat-treated at 400°C, the highest peaks were located at 42.35°, classified as Ni-Ti in cubic structure (Austenite). The second peak was found at 39.7° - 39.8°, representing $Ti_6O$ and $Ti_3O$ in hexagonal structure. This can result from oxygen contamination from the fabrication processes. The atmosphere used in ingot fabrication may not be a true vacuum and sufficient free from oxygen. At the peak position of 45.14° 2θ - 45.41° 2θ, the Ni-Ti in monoclinic structure (Martensite) was detected. This result was in accordance with the relative mechanical property observed with the three-point bending test at 37°C. The specimen was a mixture of austenite and martensite at the oral temperature.

For the 50.7Ni:49.3Ti (at%) specimens heat-treated at 600°C, the XRD spectra showed the presence of a distinct 111 peak representing the Ni-Ti in monoclinic structure. A previous study using conventional XRD indicated the presence of the 111 peak for martensite at about 41.4°[6]. This result was in

accordance with the relative mechanical property observed with the three-point bending test. The load-deflection curve indicated the martensitic reorientation that indicated the recovery strain instead of recovery stress at all percent reductions.

For the 45.2Ni:49.8Ti:Cu5.0 (at%) specimens heat-treated at 400°C and 600°C, the XRD spectrums were similar. The highest peaks, located at 42.23° - 42.40°, were classified as Ni-Ti in cubic structure (Austenite). The peak at 77.53° - 77.84° represented the Ni-Ti in cubic structure (Austenite). At the peak position of 39.62° – 39.80°, the $CuTi_2$ and $Cuti_3$ in tetragonal structure was detected. This result was in accordance with the DSC, where the transformation temperature range was below the oral temperature. Compared with the relative mechanical property observed with the three-point bending test, the load-deflection curves should recover on the unloading path. As shown in Figure 52, the load-deflection curves of the 45.2Ni:49.8Ti:5.0Cu (at%) specimens heat-treated at 600°C represented incomplete recovery which can be explained by the reason that the stress from the bending test may have an influence on shifting the transformation temperature range over the oral temperature. Therefore, the superelastic properties occurred incompletely.

Significant sharpening of the XRD peaks of 45.2Ni:49.8Ti:Cu5.0 (at%) specimens heat-treated at 600°C compared with specimens heat-treated at 400°C indicated that substantial stress relief had occurred.

X-ray diffraction is inherently a near-surface analytical technique, since the depth of penetration of the x-ray beam is typically no greater than 50 μm and frequently much less for the metals of usual interest. Consequently, caution is necessary when interpreting the results of XRD experiments since the near-surface structure of a material may differ significantly from the bulk structure. While such an experiment is generally difficult to conduct, the safest procedure is to perform a series of XRD analyses on specimens from which known thicknesses of surface layers have been removed [6].

# CHAPTER VII
# CONCLUSION

In this study, two locally-made nickel-titanium alloys, 50.7Ni:49.3Ti (at%) and 45.2Ni:49.8Ti:5.0Cu (at%), were fabricated by a conventional vacuum arc re-melting technique using an electrolytic arc furnace in argon atmosphere. In order to clarify the effect of cold-working and heat treatment temperature, the transformation behavior, mechanical properties and microstructures of these two alloys were investigated. The following conclusions were drawn:

1. The chemical composition of two locally-made nickel-titanium alloys contained Nickel 47.65 at%, Titanium 52.01 at% and Silica 0.24 at% for 50.7Ni:49.3Ti (at%) specimen and Nickel 41.94 at%, Titanium 50.21 at%, Copper 7.56 at% and Silica 0.29 at% for 45.2Ni:49.8Ti:5.0Cu (at%) specimen.
2. The transformation temperature ranges were varied as follows:

- The 50.7Ni:49.3Ti (at%) heat-treated at 400°C represented the mixture of austenitic and martensitic structures at the oral temperature.
  (As = 18°C-26°C, Af = 49°C-55°C, Ms = 29°C-34°C, Mf = 0°C-10°C)
- The 50.7Ni:49.3Ti (at%) heat-treated at 600°C represented the martensitic structures at the oral temperature.
  (As = 54°C-49°C, Af = 70°C-72°C, Ms = 48°C-52°C, Mf = 34°C-40°C)
- The 45.2Ni:49.8Ti:5.0Cu (at%) heat-treated at 400°C represented the mixture of austenitic and rhombohedral structures at the oral temperature.
  (As = 25°C-34°C, Af = 55°C-56°C, Rs = 52°C-53°C, Rf = 23°C-32°C)
- The 45.2Ni:49.8Ti:5.0Cu (at%) heat treated at 600°C represented the austenitic structure at the oral temperature.
  (As = -2°C-11°C, Af = 26°C-30°C, Ms = 0°C-3°C, Mf = -31°C- -16°C)

3. Mechanical properties:

3.1 Three-point bending test:

The data conformed to the DSC except the 45.2Ni:49.8Ti:5.0Cu (at%) heat-treated at 600°C, which has TTR below the oral temperature, but the load-deflection curves did not complete recovered. Furthermore, only 45.2Ni:49.8Ti:5.0Cu (at%) heat-treated at 400°C showed the superelastic curve at the oral temperature.

3.2 Tensile test:

- The ultimate tensile stress increased when the percent reduction increased. In contrast, the percent elongation decreased when the percent reduction increased.
- Heat treatment temperature had an influence on the percent elongation.
- Texture of the alloy caused by cold-rolling was another factor affecting the tensile strength.
- According to the inhomogeneous dimension of the test specimens, the unusual result from the tensile strength test appeared not to be the true properties of the alloys.

3.3 Micro-indentation hardness: The hardness value (Hv) increased when the percent reduction increased.

4. The grain sizes of two Ni-Ti alloy systems measured at the cross-sectional area were typically 50-80 μm. For the longitudinal area, the grains were elongated parallel to the cold-rolling direction and expressed the texture of the alloy. No significant difference of the grain sizes between the percent reduction (10%, 20% and 30%) was found. Thus, grain size had no effect on superelasticity of the specimens. On the other hand, grain size had an influence on mechanical properties such as hardness. Hardness value increased when grain size decreased In order to improve the superelasticity, smaller grain size was preferred.

5. Regarding crystallographic structure, the spectra showed peaks that indicated the phase of the alloy, which was conformed to the DSC and three-point bending test.

6. In order to produce the Ni-Ti shape memory alloy used in orthodontics, three principle factors affecting the transformation behavior and mechanical properties of Ni-Ti must be: Chemical compositions, working history such as cold rolling

At the 400°C heat treatment, effect of the percent reduction had an influence on the transformation behavior and mechanical properties of this alloys. Increasing the cold rolling over 30% reduction may improve the superelastic property.

At the 600°C heat treatment, effect of the % reduction was diminished by recrystalization. In order to improve the superelastic property or to reduce the transformation temperature range, adding a small amount of nickel and/or copper to the used nominal composition should be effective.

The results of this study show that locally-made nickel-titanium alloys had various transformation behaviors and mechanical properties dependent on three principal factors as mentioned above. In order to fabricate the Ni-Ti alloy used in orthodontics, these three factors should be carefully monitored and used as a specific recipe. This information is valuable as baseline data for further development of locally-made nickel-titanium alloy used in orthodontics.

# REFERENCES

1. Proffit W, Fields., Jr H. Mechanical principles in orthodontic force control. In: Contemporary orthodontics. 3rd ed. ed. St.Louis: Mosby; 2000.
2. Kusy RP. A review of contemporary archwires: their properties and characteristics. Angle Orthod 1997;67(3):197-207.
3. Gil FJ, Solano E, Pena J, Engel E, Mendoza A, Planell JA. Microstructural, mechanical and citotoxicity evaluation of different NiTi and NiTiCu shape memory alloys. J Mater Sci Mater Med 2004;15(11):1181-5.
4. Iijima M, Ohno H, Kawashima I, Endo K, Mizoguchi I. Mechanical behavior at different temperatures and stresses for superelastic nickel-titanium orthodontic wires having different transformation temperatures. Dent Mater 2002;18(1):88-93.
5. Bishara SE. Fixed Edgewise Orthodontic Appliances and Bonding Techniques. In Textbook of Orthodontics: Saynder Company; 2001.
6. Brantley WA, Eliades G. Orthodontic Material: Scientific and Clinical Aspects Orthodontic Wires. New York: Thieme Stuttgart; 2001.
7. Kusy RP, Greenberg AR. Comparison of the elastic properties of nickel titanium and beta titanium wires. Am J Orthod 1982;82:199-205.
8. Kusy RP, Greenberg AR. Effects of Composition and Cross Section on the Elastic Properties of Orthodontic Wires. The Angle Orthodontist 1981;51(4):325-341.
9. Buehler WH, Gilfrich JV, Wiley RC. Effect of low temperature phase changes on the mechanical properties of alloys near composition TiNI. Journal of Applied Physics 1963;34:1475-7.
10. Otsuka K, Wayman. Shape memory materials. United Kingdom: Cambridge University Press; 1998.
11. Kim JI, Liu Y, Miyazaki S. Ageing-induced two-stage R-phase transformation in Ti - 50.9at.%Ni. Acta Materialia 2004;52(2):487-499.
12. Su PC, Wu SK. Acta Materialia 2004;52:1117.

13. Khalil-Allafi J, Dlouhy A, Eggeler G. Acta Materialia 2002;50:4255.

14. Chang SH, Wu SK, Chang GH. Grain size effect on multiple-stage transformations of a cold-rolled and annealed equiatomic TiNi alloy. Scripta Metall. 2005; 52:1341-1346.

15. Andreasen GF, Morrow RE. Laboratory and clinical analyses of nitinol wire. Am J Orthod 1978;73:142-51.

16. Meling TR, Odegaard J. Short-term temperature changes influence the force exerted by superelastic nickel-titanium archwires activated in orthodontic bending. Am J Orthod Dentofacial Orthop 1998;114:503-9.

17. Tonner RI, Waters NE. The characteristics of superelastic Ni-Ti wires in the three-point bending. Part I: the effect of temperature. European Journal of Orthodontics 1994;16:409-19.

18. Rock WP, Wilson HJ. Forces exerted by orthodontic aligning archwires. British Journal of Orthodontics 1988;15:255-9.

19. Andreasen GF, Bigelow, Andrews JG. 55 Nitinol wire: Force developed as a function of "elastic memory". Aust Dent J 1979;24(146-49).

20. Water NE. Orthodontic products update: Superelastic nickel-titanium wires. British Journal of Orthodontics 1992;19:319-322.

21. O'Brien WJ. Dental Materials and Their Selection. 3rd edition Chicago: Quintessence Publishing co. Inc.; 2002.

22. Santoro M, Nicolay OF, Cangialosi TJ. Pseudoelasticity and thermoelasticity of nickel-titanium alloys: A clinically oriented review. Part I: Temperature transitional ranges. Am J Orthod Dentofacial Orthop 2001;119:587-93.

23. Burstone CJ, Qin B, Morton JY. Chinese NiTi wire--a new orthodontic alloy. Am J Orthod 1985;87(6):445-52.

24. Miura F, Mogi M, Ohura Y, Hamanaka H. The super-elastic property of the Japanese NiTi alloy wire for use in orthodontics. Am J Orthod Dentofacial Orthop 1986;90(1):1-10.

25. Hurst CL, Duncanson MG, Nanda RS, Angolkar PV. An evaluation of the shape memory phenomenon of nickel-titanium orthodontic wires. American Journal of Orthodontics and Dentofacial Orthopedics 1990;98:72-76.

26. Khier SE, Brantley WA, Fournelle RA. Bending properties of superelastic and nonsuperelastic nickel-titanium orthodontic wires. Am J Orthod Dentofacial Orthop 1991;99(4):310-8.

27. Mohlin B, Muller H, Odman J, Thilander B. Examination of Chinese NiTi a combined clinical and laboratory approach. Eur J Orthod 1991;13(5):386-91.

28. Chen R, Zhi YF, Arvystas MG. Advanced Chinese NiTi alloy wire and clinical observations. Angle Orthod 1992;62(1):59-66.

29. Husmann P, Bourauel C, Wessinger M, Jager A. The frictional behavior of coated guiding archwires. J Orofac Orthop 2002;63(3):199-211.

30. Jia W, Beatty MW, Reinhardt RA, Petro TM, Cohen DM, Maze CR, et al. Nickel release from orthodontic arch wires and cellular immune response to various nickel concentrations. J Biomed Mater Res 1999;48(4):488-95.

31. Meling TR, Odegaard J. The effect of short-term temperature changes on superelastic nickel-titanium archwires activated in orthodontic bending. American Journal of Orthodontics and Dentofacial Orthopedics 2001;119(3):263-273.

32. Otsubo K. Development of the superelastic Ti-Ni alloy wire appropriate to the oral environment. The Journal of Japan Orthodontic Society 1994;53:641- 650.

33. Evan TJW, Durning P. Orthodontic Products Update: Aligning Archwires, The Shape of Things To Come? - A Fourth and Fifth Phase of Force Delivery. British Journal of Orthodontics 1996;23(3):269-275.

34. Andreasen GF. Treatment advantages using nitinol wire instead of 18-8 stainless steel wire with the edgewise bracket. Quint Int 1980;4:43.

35. Andreasen GF. A clinical trial of alignment of teeth using a 0.019 inch thermal nitinol wire with a transition temperature range between 31$^{o}$C and 45$^{o}$C. Am J Orthod 1980;78:528-537.

36. Andresen G, Zhilleman T. An evaluation of 55-cobalt substituted wire for orthodontics. J Am Dent Assoc 1971;81:1373-5.

37. Kusy RP. Nitinol alloys: So, who's on first?. Am J Orthod Dentofac Orthop 1991; 100:25A-6A.

38. Sachdeva RCL, Miyazaki S. Engineering Aspects of Shape Memory Alloys: Superelastic Ni-Ti Alloys in Orthodontics.
39. Thompson SA. An overview of nickel-titanium alloys used in dentistry. International Endodontic Journal 2000;33:297-310.
40. Khantachawana A. Characterization of Transformation and Shape Memory Behavior of Ti-Ni and Ti-Ni-Cu Melt-Spun Ribbons.: University of Tsukuba; 2003.
41. Kalpakjian S, Schmid SR. Manufacturing Engineering and Technology. Fourth edition ed: Prentice Hall International; 2000.
42. ASTM Standard Specification F2063-00: American Society for Testing and Materials. 2000.
43. Wu MH. Fabrication of Nitinol Materials and Components. Proceedings of the International Conference on Shape Memory and Superelastic Technologies, Kunming, China 2001:285-292.
44. Tang GH, Liu K, Cao HJ, Lu J, Zhang CW. [Orthodontic wires in a simulated oral environment:change in mechanical properties]. Shanghai Kou Qiang Yi Xue 1997;6(3):159-62.
45. Wu SK, Lin HC, Yen YC. Materials Science&Engineering A 1996;215(1-2):113.
46. Miyazaki S, Kimura S, Takei F, Miura T, Otsuka K, Suzuki Y. Scripta Metall. 1983;17:1057.
47. Shabalovskaya SA, Anderegg J, Laab F, Thiel PA, Rondelli G. Surface Conditions of Nitinol Wires, Tubing, and As-Cast Alloys. The Effect of Chemical Etching, Aging in Boiling Water, and Heat Treatment. J Biomed Mater Res Part B: Appl Biometer 2003;65B:193-203.
48. Miller D, Lagoudas D. Influence of cold work and heat treatment on the shape memory effect and plastic strain development of NiTi. Materials Science & Engineering A 2001;308:161-175.
49. Gall K, Tyber J, Brice V, Frick CP, Maier HJ, Morgan N. Tensile deformation of NiTi wires. J Biomed Mater Res 2005;75A:810-823.
50. Miyazaki S, Mizukoshi K, Ueki T, Sakuma T, Liu Y. Fatigue life of Ti-50 at.% Ni and Ti-40Ni-10Cu (at.%) shape memory alloy wires. Materials Science & Engineering A 1999(273-275):685-663.

51. Parvizi F, Rock WP. The load/deflection characteristics of thermally activated orthodontic archwires. Eur J Orthod 2003;25:417-421.

52. Gil FJ, Planell JA. Effect of copper addition on the superelastic behavior of Ni-Ti shape memory alloys for orthodontic applications. J Biomed Mater Res 1999;48(5):682-8.

53. Kurita T, Matsumoto H, Abe H. Transformation behavior in rolled NiTi (Article in press). Journal of Alloy and Compounds 2004.

54. Thayer TA, Bagby MD, Moore RN, DeAngelis RJ. X-ray diffraction of nitinol orthodontic arch wires. Am J Orthod Dentofacial Orthop 1995;107:604-12.

55. Bradley TG, Brantley WA, Culbertson BM. Differential scanning calorimetry (DSC) analyses of superelastic and nonsuperelastic nickel-titanium orthodontic wires. Am J Orthod Dentofacial Orthop 1996;109(6):589-97.

56. Champagne M. The NiTi Distalizer. A non-compliance maxillary molar distalizer. Int J Orthod Milwaukee 2002;13(3):21-4.

57. Crone WC, Yahya AN, Perepezko JH. Influence of Grain Refinement on Superelasticity in NiTi. Proceedings of the SME Annual Conference on Experimental Mechanics 2001:510-513.

58. Patino PVDDSMP, Biedma BMDDSMP, Liebana CRM, Cantatore GDDSMP, Bahillo JGDDSMP. The Influence of a Manual Glide Path on the Separation Rate of NiTi Rotary Instruments.114-116.

59. ASTM international. Standard Test Method for Microindentation Hardness of Materials.E384-05a:444-476.

60. Oh KT, Joo UH, Park GH, Hwang CJ, Kim KN. Effect of silver addition on the properties of nickel-titanium alloys for dental application. J Biomed Mater Res B Appl Biomater 2006;76(2):306-14.

61. Yokoyama K, Kanebo K, Ogawa T, Moriyama K, Asaoka K, Sakai J. Hydrongen embrittlement of work-hardened N-Ti alloy in fluoride solutions. Biomaterials 2005;26:101-108.

62. International Organization for Standardization. Metallic materials-Bending test. International Standard ISO 7438-1985-07-01.

63. ASTM International standard test methods for bend testing of metallic flat materials for spring applications involving static loading: E 855-90 (Reapproved 2000).734-741.

64. Miura F, Mogi M, Ohura Y, Karibe M. The super-elastic Japanese NiTi alloy wire for use in orthodontics. Part III. Studies on the Japanese NiTi alloy coil springs. Am J Orthod Dentofacial Orthop 1988;94(2):89-96.

65. Iijima M, Ohno H, Kawashima I, Endo K, Brantley WA, Mizoguchi I. Micro X-ray diffraction study of superelastic nickel-titanium orthodontic wires at different temperatures and stresses. Biomaterials 2002;23(8):1769-74.

66. Hitoshi Matsumoto. Characterization of transformation behavior in NiTi(Si). Journal of Alloys and Compounds 2004;366:182-186.

67. Crone W.C., Wu D., Perepezko J.H. Pseudoelstic behavior of nickel-titanium melt spun ribbon. Material Science and Engineering A 2004;375-377:1177-1181.

68. Gao S., Yi S. Experimental study on the anisotropy behavior of textured NiTi pseudoelastic shape memory alloys. Materials Science and Engineering A 2003;362:107-111.

69. Khantachawana A., Miyazaki S., Iwai H., Kohl M. Effect of heat-treatment on the texture and anisotropy of transformation strain in Ti-Ni-Fe rolled thin plates.

70. Kohl M., Allen D.M., Chen T.T., Miyazaki S., Schworer M. Anisotrophy in microdevices produced by micromachining of cold-rolled NiTi sheets.

# APPENDIX

## Chemical composition of the Ni-Ti alloys.

| Alloys | Location | Ni | | Ti | | Cu | | Si | |
|---|---|---|---|---|---|---|---|---|---|
| | | At% | Wt% | At% | Wt% | At% | Wt% | At% | Wt% |
| Ti-Ni (49.3:50.7at%) | 1 | 47.46 | 52.48 | 52.13 | 47.03 | - | - | 0.25* | 0.13* |
| | 2 | 47.83 | 52.97 | 51.63 | 46.66 | - | - | 0.5 | 0.27 |
| | 3 | 47.76 | 52.91 | 51.92 | 46.92 | - | - | 0.32* | 0.17* |
| | 4 | 47.32 | 52.45 | 52.45 | 47.43 | - | - | 0.23 | 0.12 |
| | 5 | 47.87 | 52.96 | 51.83 | 46.79 | - | - | 0.24 | 0.13 |
| | 6 | 47.67 | 52.74 | 52.1 | 47.03 | - | - | 0.16* | 0.09* |
| | Average | 47.65 | 52.75 | 52.01 | 46.98 | - | - | 0.235 | 0.13 |
| | SD. | 0.22 | 0.24 | 0.28 | 0.26 | - | - | 0.15 | 0.08 |
| Ti-Ni-Cu (50:45:5 at%) | 1 | 40.55 | 44.58 | 51.52 | 46.22 | 7.58 | 9.01 | 0.35 | 0.19 |
| | 2 | 40.62 | 44.64 | 51.28 | 45.98 | 7.71 | 9.17 | 0.39 | 0.2 |
| | 3 | 40.42 | 44.43 | 51.66 | 46.34 | 7.63 | 9.08 | 0.28 | 0.15 |
| | 4 | 40.54 | 44.6 | 51.58 | 46.3 | 7.46 | 8.88 | 0.42 | 0.22 |
| | 5 | 40.46 | 44.48 | 51.38 | 46.08 | 7.76 | 9.23 | 0.41 | 0.21 |
| | 6 | 41.06 | 45.09 | 50.85 | 45.56 | 7.69 | 9.14 | 0.4 | 0.21 |
| | Average | 40.61 | 44.64 | 51.38 | 46.08 | 7.64 | 9.09 | 0.38 | 0.20 |
| | SD. | 0.23 | 0.24 | 0.29 | 0.29 | 0.11 | 0.13 | 0.05 | 0.03 |
| Ti-Ni-Cu (49.8:45.2:5.0at%) | 1 | 41.85 | 45.89 | 50.36 | 45.06 | 7.5 | 8.9 | 0.29 | 0.15 |
| | 2 | 42.01 | 46.13 | 50.54 | 45.28 | 7.06 | 8.39 | 0.4 | 0.21 |
| | 3 | 41.78 | 45.89 | 50.36 | 45.13 | 7.31 | 8.69 | 0.55 | 0.29 |
| | 4 | 42.08 | 46.09 | 49.95 | 44.64 | 7.7 | 9.13 | 0.27 | 0.14 |
| | 5 | 42.04 | 46.04 | 50.22 | 44.88 | 7.6 | 9.01 | 0.15 | 0.08 |
| | 6 | 41.9 | 45.81 | 49.84 | 44.46 | 8.19 | 9.69 | 0.06 | 0.03 |
| | Average | 41.94 | 45.98 | 50.21 | 44.91 | 7.56 | 8.97 | 0.29 | 0.15 |
| | SD. | 0.12 | 0.13 | 0.28 | 0.31 | 0.383 | 0.44 | 0.17 | 0.09 |

**Transformation Temperature Range from Differential Scanning Calorimetry of Twelve Ni-Ti and Ni-Ti-Cu Alloy Specimens**

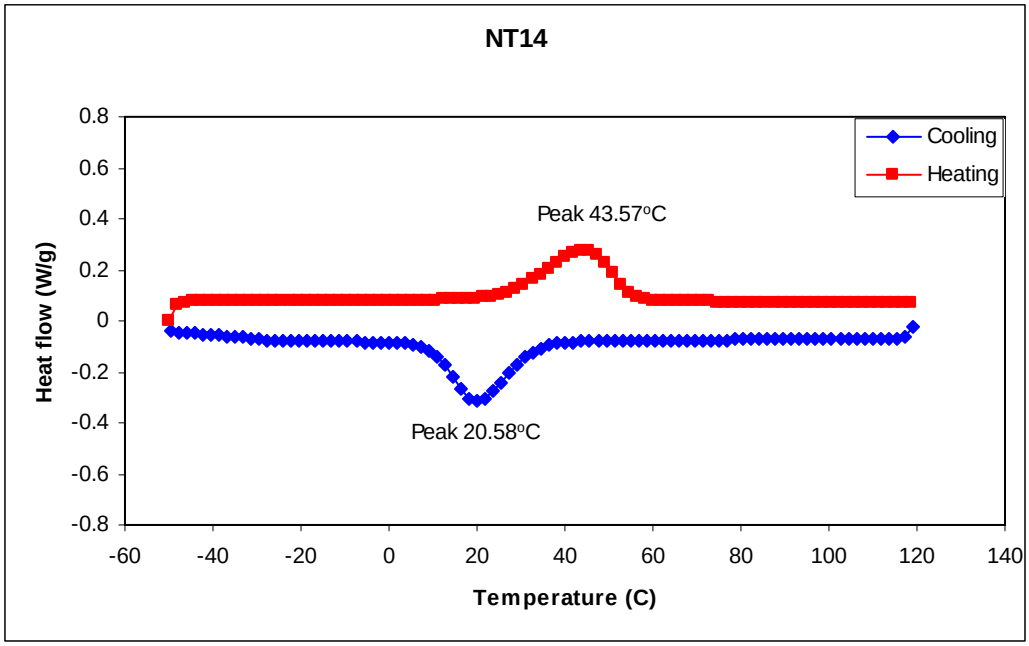


Thermogram of Ni:Ti (50.7:49.3 at%) with 10% reduction and 400°C heat treatment

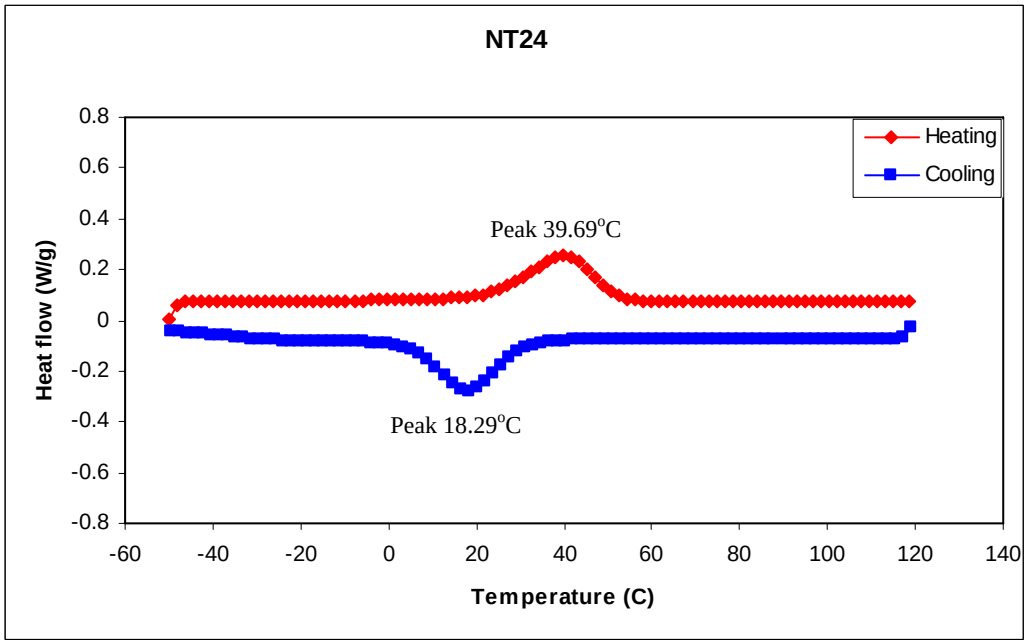


Thermogram of Ni:Ti (50.7:49.3 at%) with 20% reduction and 400°C heat treatment

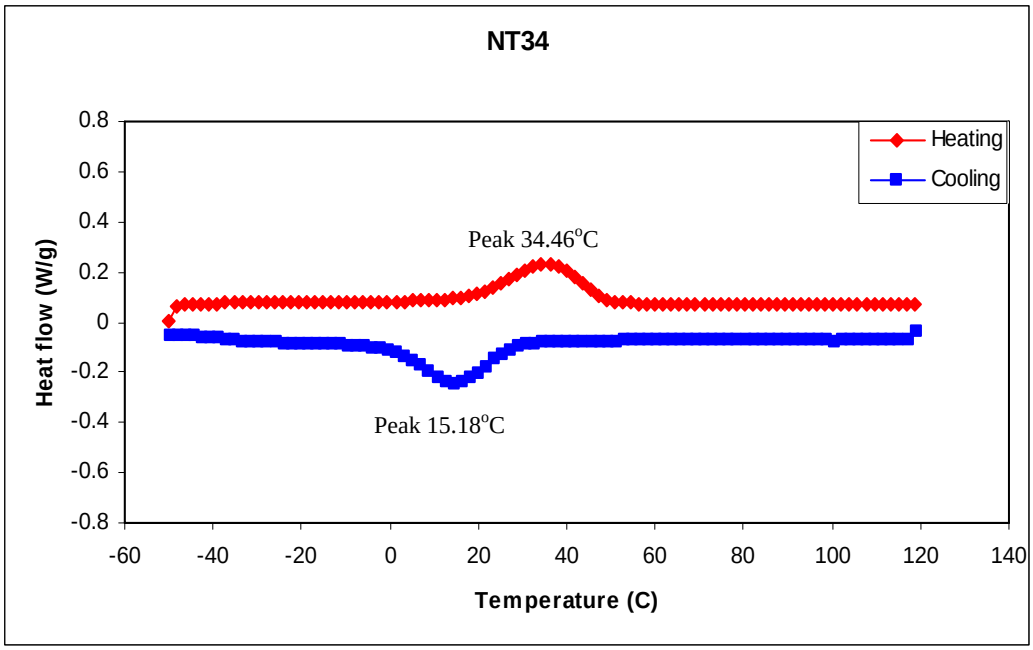


Thermogram of Ni:Ti (50.7:49.3 at%) with 30% reduction and 400°C heat treatment

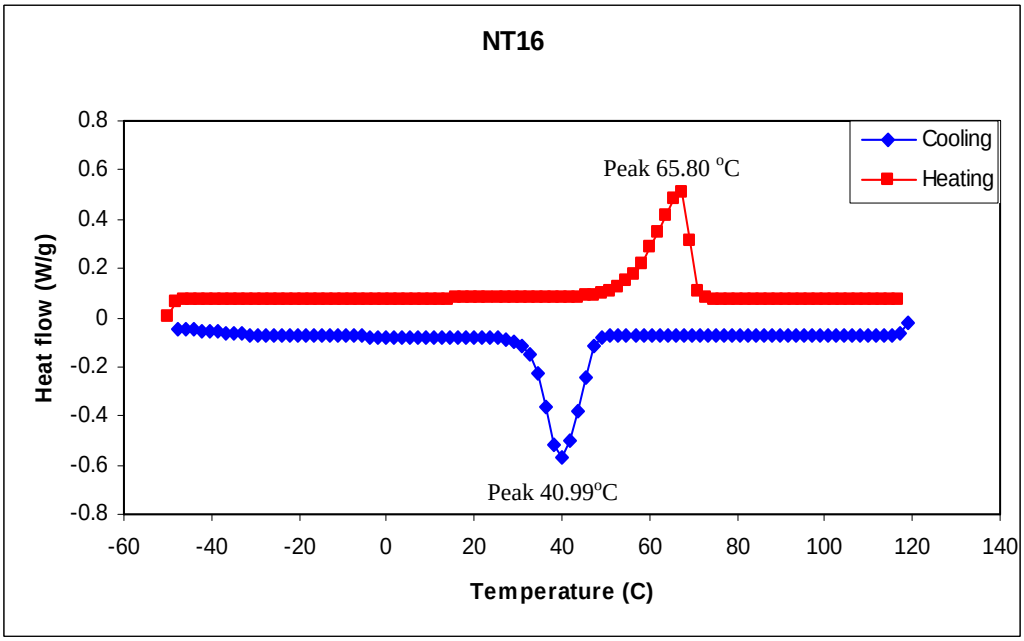


Thermogram of Ni:Ti (50.7:49.3 at%) with 10% reduction and 600°C heat treatment

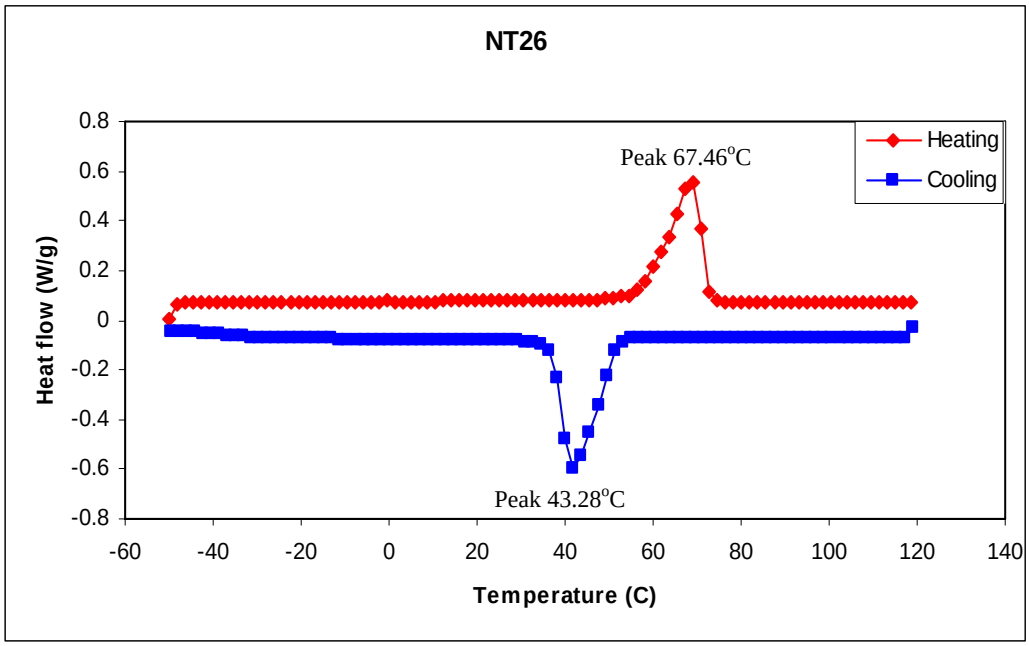


Thermogram of Ni:Ti (50.7:49.3 at%) with 20% reduction and 600°C heat treatment

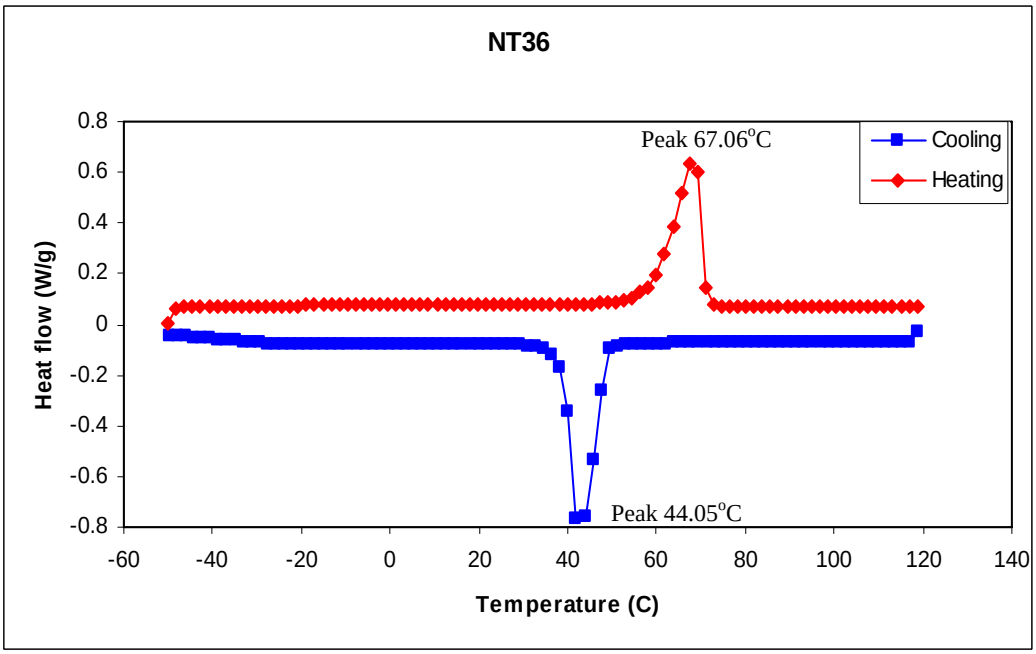


Thermogram of Ni:Ti (50.7:49.3 at%) with 30% reduction and 600°C heat treatment

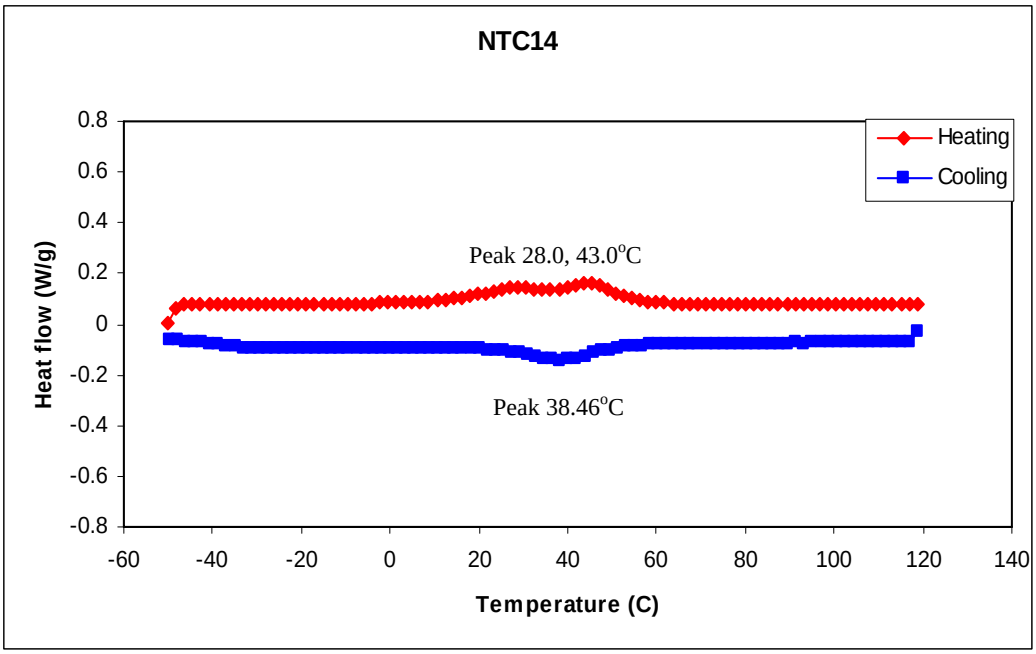


Thermogram of Ni:Ti:Cu (45.2:49.8:5.0 at%) with 10% reduction and 400°C heat treatment

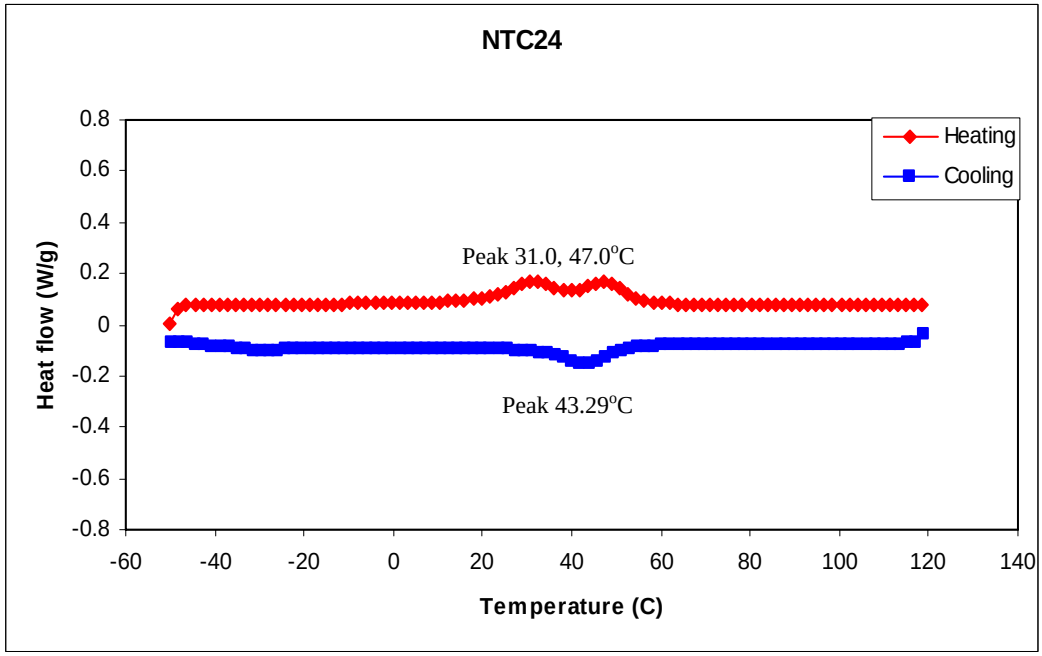


Thermogram of Ni:Ti:Cu (45.2:49.8:5.0 at%) with 20% reduction and 400°C heat treatment

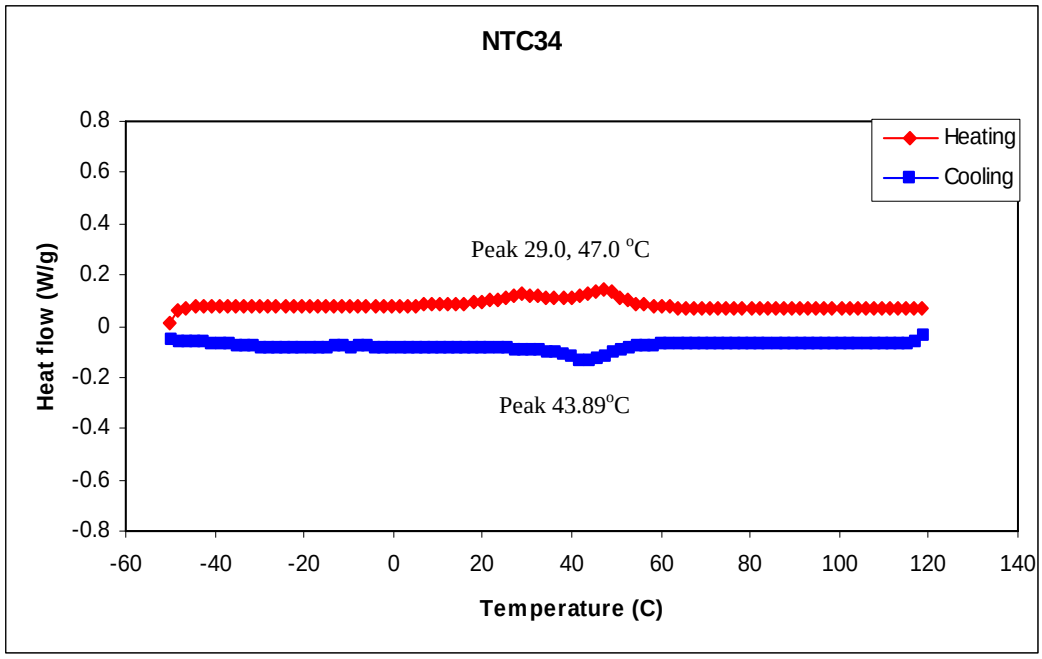


Thermogram of Ni:Ti:Cu (45.2:49.8:5.0 at%) with 30% reduction and 400°C heat treatment

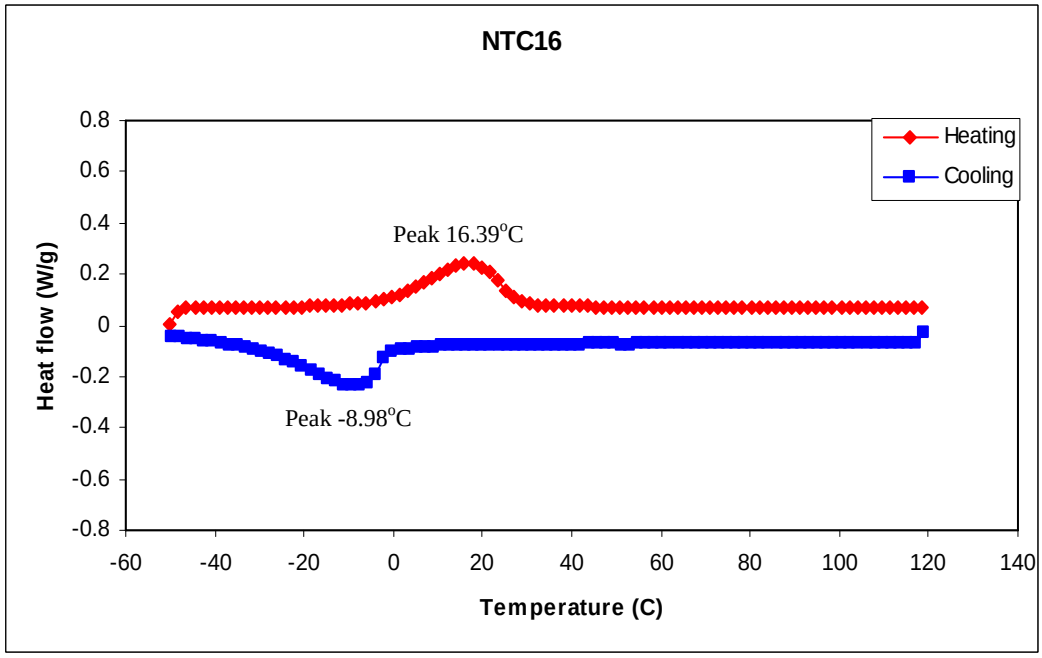


Thermogram of Ni:Ti:Cu (45.2:49.8:5.0 at%) with 10% reduction and 600°C heat treatment

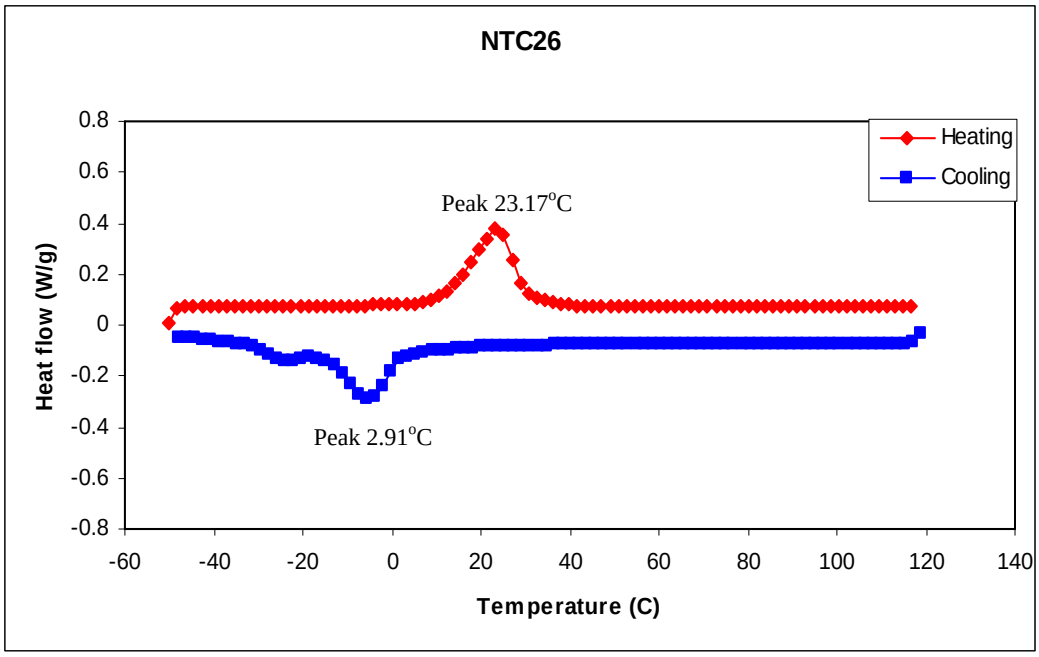


Thermogram of Ni:Ti:Cu (45.2:49.8:5.0 at%) with 20% reduction and 600°C heat treatment

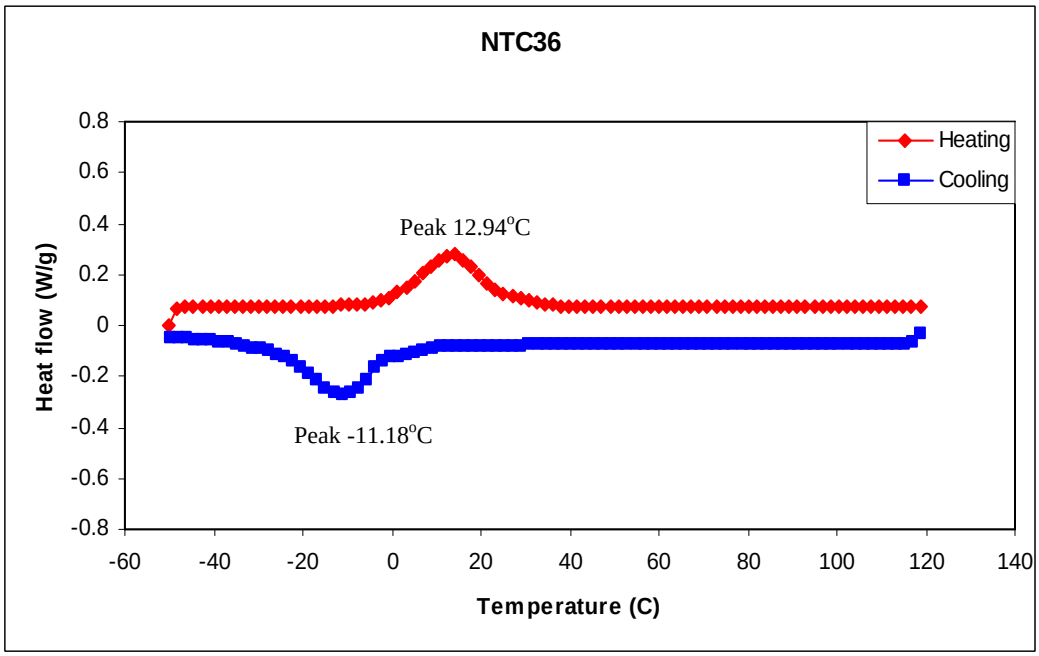


Thermogram of Ni:Ti:Cu (45.2:49.8:5.0 at%) with 30% reduction and 600°C heat treatment

# BIOGRAPHY

| | |
|---|---|
| **NAME** | Miss Nattiree Chiranavanit |
| **DATE OF BIRTH** | 18 May 1979 |
| **PLACE OF BIRTH** | Bangkok, Thailand |
| **INSTITUTIONS ATTENDED** | Chulalongkorn University, 2001:<br>Doctor of Dental Surgery (DDS)<br>Mahidol University, 2008:<br>Master of Science (Orthodontics) |
| **SCHOLARSHIP** | Faculty of Dentistry, Mahidol University |
| **HOME ADDRESS** | 6 Soi Huamark 7, Huamark, Bangkapi,<br>Bangkok, Thailand<br>Tel. 02-3751222 |